

Deciphering How the Germline Inhibits Longevity

by

T. Richard Parenteau

DISSERTATION

Submitted in partial satisfaction of the requirements for the degree of

DOCTOR OF PHILOSOPHY

in

Biomedical Sciences

in the

GRADUATE DIVISION

of the

UNIVERSITY OF CALIFORNIA, SAN FRANCISCO

To my grandfather and grandmother, Sabas and Consuela Reyna

PREFACE

Earning a PhD is definitely the most intense, exciting, challenging and rewarding experience I have ever had, and there is no way I would have gotten through it without the help and support of some amazing people. First and foremost, I have to thank my adviser Cynthia Kenyon for her guidance throughout this entire process. Her unwavering enthusiasm for aging research and deep scientific curiosity are traits I hope to emulate throughout the rest of my career. Cynthia is the very definition of a big-picture thinker, and I am truly lucky to have trained under the visionary pioneer of our field.

I would like to thank Kaveh Ashrafi, Aimee Kao, and Dena Dubal, the brilliant scientists who served double-duty as my qualifying exam and thesis committee members. Kaveh taught me *C. elegans* genetics 10 years ago, when I was just a summer student in his lab, and continues to better me as a scientist to this day. He is the most exact, sharp, and uncompromising thinker I have ever meet, and his fair criticisms and questions on my science were invaluable to my success. I am so fortunate to have had Aimee chair my thesis committee, as she is a perfect example of the kind of physician-scientist that I want to be. Her passion, perseverance and unique perspective make her an amazing mentor and an amazing friend. Dena, I believe, is single-handedly responsibly for helping me to preserve my love of science and medicine throughout this whole process. She continuously made sure that I could see the importance of my work and the questions I was asking, and never let me lose sight of myself and my motivations.

Though I am grateful to the whole Kenyon Lab for all of their help and support, there are three people who have truly impacted my science and life. Hildegard Mack is the hardest worker I have ever meet, and I could not have asked for a better collaborator. I would not have survived our lab's transition without her. Whether we were washing dishes or doing high-level biochemistry, we leaned on each other and soldiered on together. Nina Riehs and I have been teammates throughout our entire tenures in the Kenyon Lab. We trust each other so much that we shared all of our strains and reagents and we respect each other so much that we've always looked to each other's opinion and guidance on projects. We couldn't have asked for a better last "lab baby" than Peter Chisnell, who was really the heart and soul of our lab. Peter has also become one of my closest friends. He kept me healthy by being the best workout partner anyone could ask for, and kept me sane by being a caring confidant. I know that he will achieve great things in his career, and I feel very honored to have been able to play a role in his development as an outstanding scientist.

There are many other UCSF people I would like to thank. Hao Li and the entire Li lab were very gracious to adopt me in when Cynthia left UCSF, and I am incredibly grateful to them. Jennifer Thompson, Mayra Melville, Rigo Roman-Albarran and Loan Doan helped ensure I had the supplies I needed to actually do my work. The UCSF MSTP has been incredibly supportive, especially Mark Anderson, Jana Toutolmin, Catherine Norton and Geri Ehle. Geri has been such an incredible advocate and ally for my success and for the program's success. I am very grateful to Lisa Magargal, Demian Sainz and the rest of the BMS program administration for their help along the way. Also thank you to all of my colleagues in the BMS program, medical school, and

MSTP. Special thanks to the brilliant friends who I've meet in SACNAS, S4D and GQA; your dedication to diversity in science is going to help change the world for the better!

Of course, a big thank you to my family. My parents for their love. Christina and Robert, my brother and sister, for being my best friends and for always believing in me. Danny Vega, my brother from another mother, who has been through so much with me, but has always stayed by my side. I dedicated this thesis to my grandparents because their love of learning allowed them to come up from humble beginnings to make a good life for themselves and their family, and I thank them for inspiring me.

I also have a family of friends in the Bay Area who I am forever grateful to. Thank you to my med school brother and sister, Mark Dela Cruz and Bogdana Schmidt for always inspiring me with their strength and compassion. Thank you to Jonathan Snyder and Paul Mittermiller, for being the best allies and modern men I know. Marky Jeng, my little brother, is the only true genius I've ever meet, and the only one who can constantly keep me on my toes. Conor Madigan and Tommy Tran are both different from me in so many ways, and I believe these differences have made our friendships and bonds over the years all the more interesting and complex. I love that Derrick Djang and Matt Buchanan have hearts so big and passions so strong that they could swallow the earth if they wanted to; I want to live with that zeal. Mike "Donny" Kenney and Adam "Admiral" Moore never cease to make me crack-up; they are sources of so much laughter and joy in my life. Ning Zhou and Raad Shebib, thank you for making Monday my favorite night of the week and for all of the adventures and great conversations. Mike McCoy, Mikey Zilberleyb and Teak Sowapruux, you sweet, sweet angels, thank you for shining your light on me. Laronne Faulkner thank you for being our MVP. Gregoire Camus, thank you for always

knowing who's on fi'ah. Robyn Fenty, thank you for inspiring me to work. Abbie Dillon, my sister, soul-mate, crying-partner and fellow social-justice-warrior princess, you have changed me life in unquantifiable ways and I will always strive to live up to your example of empathy and sincerity.

Lastly, but certainly not least, thank you to my partner Sai-Wing Chan, who is the most kind, hilarious, generous, fun-loving, and dedicated friend I've ever had. He kept me company in lab late-at-night and on the weekends, helped with experiments when I needed a second pair of hands, and listened to all of my scientific hopes, questions, big-ideas and petty complaints, with unwavering grace and love. Sai is my heart and my rock, and my life is so much richer because of him.

Deciphering How the Germline Inhibits Longevity

T. Richard Parenteau

ABSTRACT

Understanding the evolutionary links between an animal's reproductive state and its rate of aging has been of interest to scientists since the field of aging research first began. Contrary to the "Disposable Soma Theory" on the evolution of aging, which proposes that the greedy germline poses an unavoidable cost to the rest of the body, studies exploring germline-less *C. elegans* have revealed that the longevity afforded these animals is due to complex and highly regulated molecular mechanisms, rather than just a change in resource allocation from progeny production to somatic tissue maintenance. The fact that lifespan benefits are seen when the germline tissues are disrupted in worms, flies, grasshoppers, rats and humans excitingly suggests an evolutionarily conserved pathway linking reproductive tissues to aging. This study aimed to uncover the upstream effectors of this longevity pathway, in order to determine how the germline functions to prevent life extension in normal intact *C. elegans*. Unbiased genetic and biochemical screens were performed to find genes and proteins involved in the KRI-1-mediated activation of DAF-16, which occurs upon germline-ablation and is integral to the resulting longevity. Many overlapping factors were found using these complimentary techniques, validating the combined genetic/biochemical approach. One particular gene of interest found to promote DAF-16 activity in germline-less worms was *itr-1*, a gene encoding the worm's only IP3-responsive Ca²⁺ channel. However, RNAi knockdown of *itr-1* not only

decreased the lifespan of germline(-) worms, but did so in germline(+) worms as well, suggesting ITR-1 plays more broad role in lifespan regulation. Consistent with this, *itr-1(RNAi)* was found to impair DAF-16 activity in the intestine of two *daf-2* mutants (*e1370* and *e1368*), and also greatly inhibit the lifespan of these long-lived strains. Thus, ITR-1 appears to act as a more general longevity promoting factor in *C. elegans*, possibly working through regulation of intestinal DAF-16. Interestingly though, ITR-1 was also shown to regulate activity of several other components of germline-less longevity, specifically SKN-1, DAF-12 and the MitoUPR. Thus, ITR-1 may actually control lifespan through regulation of multiple downstream pathways. Understanding these pathways, as well as those upstream of ITR-1 in lifespan regulation, will be of great interest for future research.

TABLE OF CONTENTS

Introduction

Overview and general motivation	1
Background on the mechanisms of germline-less longevity in <i>C. elegans</i>	2
Hypothesis	4
Outline of approach and rationale	4
Reverse genetic screening for genes that regulate DAF-16 function	5
Biochemical screening for KRI-1 binding partners	7
ITR-1, an IP3-regulated calcium channel capable of regulating lifespan	8
ITR-1 converts receptor signals into Ca ²⁺ signals	9
Physiological functions of ITR-1	9
Specific regulation of ITR-1 signaling	10
ITR-1 can regulate longevity	11

Results

Optimization of RNAi procedures	12
Optimization of liquid culture RNAi for 96-well screening	12
Optimization of solid agar RNAi for efficiency and strength	13
Dual whole-genome RNAi screens unveil many potential DAF-16 regulators	14
Surprising and significant overlap in hits between the two screens	15
Significant overlap in GO Term enrichment between the two screens	16
Further analysis of screen hits	16

DAF-16 dependency and impact on health and fertility	17
Tissue autonomy in regulation of intestinal DAF-16	17
Modulation of other markers of germline-less longevity	18
ITR-1 is a positive effector of DAF-16 activity in germline-ablated worms	18
<i>itr-1(RNAi)</i> tissue-autonomously inhibits <i>sod-3</i> reporter expression	19
<i>itr-1(RNAi)</i> also inhibits the TCER-1 co-regulated <i>dod-8</i> reporter	19
Worms treated with <i>itr-1(RNAi)</i> do not have nuclear localized DAF-16	20
<i>itr-1(RNAi)</i> inhibits longevity of germline(+) and germline(-) worms	20
Effect of <i>itr-1(RNAi)</i> on two different <i>daf-2(lf)</i> mutants	21
Effect of <i>itr-1(RNAi)</i> on SKN-1 and MitoUPR activity	21
<i>itr-1(RNAi)</i> surprisingly lowers somatic gonad signaling	22
Initiation of <i>itr-1(RNAi)</i> after L2 is insufficient to inhibit DAF-16 activation	22
Analysis of upstream regulators of ITR-1	23
A C-terminally FLAG-tagged KRI-1 construct rescues <i>kri-1(null)</i> worms	23
Rescue of development and appearance	23
Rescue of DAF-16 activation	24
Rescue of lifespan	24
KRI-1 Co-Immunoprecipitations reveal novel binding partners	25
KRI-1a::FLAG can be efficiently pulled down	25
KRI-1 Co-IPs uncover many interaction partners	25
KRI-1 is preferentially bound in the germline(+) state	26
Significant overlap between genetic and biochemical screens	26

Discussion

Overview and general reflections	27
The importance of stringent liquid and solid culture RNAi protocols	28
Generating a mutant library that is otherwise genetically homogenous	29
RNAi screening in 96-well liquid culture	31
Dual genome-wide RNAi screens unveil many potential DAF-16 regulators	32
GO Term enrichment	32
Significant gene set overlap between screens	32
Our DAF-16 effecters are enriched for SKN-1 and MitoUPR modulators	33
Top hits that we not explored further	34
ITR-1 is an upstream regulator of the germline-less longevity pathway	35
ITR-1 may be a universal regulator of intestinal DAF-16 activity	36
Analysis of pathway members upstream and downstream of ITR-1	37
Biochemical identification of pathway members	37
PLCs, receptors and the elusive germline signal	37
Calcium responsive genes and pathways	37
KRI-1 Co-IPs discovery both known and new regulators of DAF-16 activity	38
C-terminally FLAG tagged KRI-1 is functional	38
KRI-1 interacts constitutively with many proteins	38
Several KRI-1 binding partners also found in genetic screens	39
Final Thoughts	40

Methods

Strains	42
Cloning	42
Generation of transgenic worms	43
Injections	43
Integrations	44
Solid culture RNAi	44
Liquid culture RNAi	45
Genome-wide RNAi screens	46
Aringer Library Replication	46
Initial round of screening	47
Validation of hits	47
Sequencing of hits	48
Characterization of RNAi Screen Hits	48
DAF-16, SKN-1 and MitoUPR activity	49
DAF-16 dependency	49
Fertility	49
Health	50
Tissue autonomy	50
Analysis of Gene Ontology (GO) Enrichment	51
Quantification of Fluorescent Markers	52
Lifespans	53

Co-Immunoprecipitations	54
Preparation of worm samples	54
KRI-1 pulldowns	55
Western blotting	56
Scientific Contributors	58
Citations	59
Figures	64
Tables	92

LIST OF TABLES

Table 1: Dual whole-genome RNAi screens unveil many DAF-16 regulators	64
Table 2: Identity and function of the 25 genes that were found in both genetic screens	65
Table 3: Significant overlap in enriched GO Terms between the two screens	66
Table 4. Characterization of sequence-verified hits from the screen for negative effectors of DAF-16 activity	67
Table 5: Characterization of sequence-verified hits from the screen for positive effectors of DAF-16 activity	72
Table 6. List of all high-confidence KRI-1 interacting proteins identified from the Co-IPs	76

LIST OF FIGURES

Figure 1: Molecular activity in the absence of the germline	77
Figure 2: Two potential models for germline inhibition of KRI-1-mediated DAF-16 nuclear localization	78
Figure 3: Dual whole genome-wide RNAi screens to find DAF-16 regulators	79
Figure 4: Two protein complex based models for germline inhibition of KRI-1-mediated DAF-16 translocation	80
Figure 5: Dual biochemical screens to find KRI-1 binding partners	81
Figure 6: Initial optimization of solid agar RNAi protocol	82
Figure 7: Further optimization of solid agar RNAi protocol	83
Figure 8: Significant overlap between the two genetic screens	84
Figure 9: KRI-1 promotes the activation of multiple components of the germline-less longevity pathway	85
Figure 10: The list of DAF-16 effectors found in both genetic screens is enriched for modulators of SKN-1 and MitoUPR activity	86
Figure 11: <i>itr-1(RNAi)</i> inhibits DAF-16 activity in germline-ablated worms	87
Figure 12: <i>itr-1(RNAi)</i> tissue-autonomously inhibits intestinal DAF-16 activity in germline-ablated worms	88
Figure 13: Expression of <i>dod-8</i> , a TCER-1 co-regulated DAF-16 target gene, is also reduce by <i>itr-1(RNAi)</i>	89
Figure 14: Germline-ablated worms treated with <i>itr-1(RNAi)</i> do not display	

a pattern of nuclear localized DAF-16	90
Figure 15: <i>itr-1(RNAi)</i> inhibits longevity of germline(+) and germline(-) worms	91
Figure 16: Knocking down <i>itr-1</i> lowers DAF-16 activity in insulin signaling mutants	92
Figure 17: The longevity of insulin signaling mutants is partially ITR-1 dependent	93
Figure 18: The increased SKN-1 and MitoUPR activity seen in germline-ablated worms is ITR-1 dependent	94
Figure 19: ITR-1 also regulates DAF-12 activity in germline-ablated <i>C. elegans</i>	95
Figure 20: Initiation of <i>itr-1(RNAi)</i> after L2 is insufficient to inhibit DAF-16 activity	96
Figure 21: Individual knockdown of the five worm phospholipase C enzymes fails to phenocopy <i>itr-1(RNAi)</i>	97
Figure 22: Schematic of the C-terminally FLAG-tagged KRI-1 construct	98
Figure 23: The C-terminally FLAG-tagged KRI-1 construct rescues DAF-16 activity in <i>kri-1(null)</i> worms	99
Figure 24: The C-terminally FLAG-tagged KRI-1 construct rescues germline-less longevity in <i>kri-1(null)</i> worms	100
Figure 25: Western blot of pilot KRI-1a::FLAG pulldown	101
Figure 26: Schematic of both KRI-1 Co-IP experiments	102
Figure 27: KRI-1 is preferentially bound in the germline(+) state	103
Figure 28. Significant overlap between genetic and biochemical screens	104

INTRODUCTION

Overview and general motivation:

Though it is well established that aging is a systemic process affecting the entirety of an organism, many studies have revealed that genetic modulations in just a single organ or tissue can drastically alter lifespan (1-4). These modulations are often accompanied by other phenotypic changes associated with aging and longevity, such as alterations in stress resistance, metabolism and healthspan. Thus, it appears that there must exist networks of communication between organs and tissues that function to coordinate aging as a unified, whole-organism trait.

One well-studied example of a single tissue that controls the aging rate of the entire organism is the *C. elegans* germline. Several years ago, our lab discovered that laser ablation of the germline stem cell (GSC) precursors in these worms is able to lead to a lifespan extension of up to 60% (5). Additionally, other phenotypes, such as changes in metabolism, stress resistance and body size, have also been reported in *C. elegans* that have undergone germ cell removal, suggesting multiple large-scale and systemic changes are occurring (6-8). Excitingly, germline ablation in flies and ovariectomy in grasshoppers have also been shown to extend lifespan, and castration has been linked to increased longevity in both male rodents and human men (9-12). These studies suggest an evolutionarily conserved link between the germline and aging, one that could potentially be targeted in humans to treat age-related conditions. Thus, gaining greater understanding of how the germline normally inhibits longevity in lower-level organisms may provide therapeutic targets to treat human aging and age-related diseases.

Background on the mechanisms of germline-less longevity in *C. elegans*

Though at first glance these results would seem to suggest the undesirable dilemma of choosing longer life over reproductive capacity, it is worth noting that the positive lifespan effects of removing the germline are not due to sterility alone. For example, many infertile *C. elegans* mutants have been identified that have completely normal lifespans (13-14). Even more convincing is that additional removal of the somatic gonad, the tissue that normally houses and supports the germline, fully reverses the lifespan extension seen upon GSC ablation (5). These results suggest the longevity benefits germline-less animals enjoy are part of a specific and coordinated response, and not just due to a more favorable allocation of resources to offset the stochastic damage of age.

Indeed, continuing research has revealed that this longevity is tightly controlled by a number of converging, yet distinct, pathways that are activated in the absence of the germline. The complexity of the downstream mechanisms regulating germline-less longevity continues to build, and our understanding of these positive effectors has grown dramatically over the last few years. So far, insulin/IGF signaling, microRNA signaling, TOR signaling, autophagy, lipid metabolism, steroid signaling and several nuclear factors have been shown to contribute to this multifaceted longevity effect (15-20, 31-33).

One unifying aspect of germline-less longevity is that the intestine appears to be the eventual tissue of action in all of these distinct downstream pathways (30, 15-20). As shown in Figure 1, the five main branches of this longevity network are as follows: 1) Removal of the germline allows intestinal DAF-16 to enter the nucleus through the action of KRI-1, FTT-2 and

PHI-62, where it interacts with the transcriptional elongation factor TCER-1 to promote specific gene expression; 2) Using substrate derived from DAF-36 in the intestine, the somatic gonad produces dafachronic acid via the cytochrome-P450 DAF-9, which signals back to the intestine by binding to DAF-12 and promoting expression of microRNA's that also help promote DAF-16 nuclear localization; 3) NHR-80, NHR-49 and SBP-1 regulate a host of changes in lipid metabolism, including inducing the production of oleic acid in the intestine through positive transcriptional regulation of the delta-9 desaturases FAT-6 and FAT-7, which signals to activate SKN-1; 4) TOR signaling is reduced in the intestine upon germline ablation, resulting in increased activity of the PHA-4 transcription factor, which promotes autophagy in concert with the pro-autophagy factor HLH-30; and 5) increased mitochondrial ROS activates the mitochondrial unfolded protein response (MitoUPR), and also leads to increased cytosolic ROS which acts as a longevity promoting signal (Y. Wei and C. Kenyon, unpublished).

One important and promising fact to note is that the germline-less longevity pathway works in an adult specific manner. This is evidenced by the observation that nuclear localization of DAF-16, a transcription factor fully required for this longevity, is further decreased in intact worms midway through Day 1 of adulthood, which is the same time at which it is increased in germline ablated animals (8, 19, 20, 27). This has lead researchers to postulate that the germline provides its own repression of DAF-16, in adulthood, that is distinct from the repression provided by insulin signaling. Also, stopping GSC proliferation even at the beginning of adulthood provides some lifespan benefit (14). With these results in mind, it seems wholly possible that the benefits of the germline-less longevity pathway could be obtained without

compromising development or fertility, which is an absolutely necessary condition to be met for any potential human intervention.

Still, despite years of research on this longevity pathway, to this day we have absolutely no idea how the intact germline normally serves to inhibit lifespan in *C. elegans*. That is, how does the presence of the germline suppress DAF-16 nuclear localization, somatic gonad production of dafachronic acid, NHR-80 mediated production of oleic acid, and mitochondrial ROS production, while positively regulating TOR activity? The purpose of this study is to begin to define these upstream mechanisms.

Hypothesis:

I hypothesize that, rather than acting as a detrimental nutrient sink, the germline decreases lifespan through the use of specific signaling molecules that communicate with the somatic tissues, and that it will be possible to block these lifespan reducing signals while still maintaining fertility in worms.

Outline of approach and rationale:

It is also important to point out that before this study we had zero clues to how the germline represses longevity. The putative germline signal may be anything from a hormone, to a cell-cell contact protein, to a secreted metabolite. Because of this, it made sense to take an unbiased, whole-genome approach to try to identify these upstream signaling mechanisms.

However, as described above, there are many known downstream factors that are modulated when the germline is removed. These different pathways may be controlled by

multiple signals from the germline, or by a single signal that eventually branches apart.

Interrogating all of these pathways at once using genome-wide methodology would cripple the power of this study, as it would introduce many additional false-positives and negatives, as well as require an insurmountable amount of work. Thus, I instead decided to focus on a single pathway that is absolutely integral to germline-less longevity: KRI-1-mediated activation of DAF-16.

Uniquely, I decided to use a combined genetic and biochemical approach to search for regulators of this pathway. Specifically, I performed dual-genome-wide RNAi screens for genes that effect intestinal DAF-16 activity in the presence and absence of the germline, and paired this with dual-KRI-1 co-immunoprecipitations (Co-IPs), also in the presence and absence of the germline. There are currently no publications in which unbiased genetic screens and unbiased biochemical screens were simultaneously performed in *C. elegans*. Furthermore, though there have been thousands of publications on aging in worms, to my knowledge, only two of these have utilized a biochemical Co-IP approach (35, 36). Therefore, the design of this study is quite novel, and represents a new way to investigate this established longevity pathway.

Genetic screening for genes that regulate DAF-16 function:

The DAF-16/FOXO forkhead transcription factor is absolutely required for germline-less longevity, and mediates its effects on lifespan through transcriptional control of genes related to development, stress-resistance, metabolism and innate immunity (5, 13). In germline-ablated Day 1 adults, intestinal DAF-16 translocates from the cytosol into the nucleus. Unlike lifespan, which can be modified by a number of downstream pathways, DAF-16 nuclear

localization acts as a binary switch in germline-ablated animals; always staying mostly out of the nucleus (“off”) in the presence of the germline and always entering the nucleus (“on”), to a majority degree, in the absence of the germline (5,8,19).

The only factor specific to germline-less longevity shown to be fully necessary for the DAF-16 nuclear localization switch is KRI-1 (21). KRI-1, a plasma membrane-associated adaptor protein, is the most upstream factor so far identified in this pathway, and its ability to promote DAF-16 nuclear accumulation is negatively regulated by the germline. This germline inhibition of KRI-1-mediated DAF-16 nuclear localization could take two different forms. As shown in Figure 2, one possibility is that the germline produces a signal (S) that activates a set of negative effecters (N) of DAF-16 localization and function. The other possibility, is that the germline signal instead inhibits a set of positive effecters (P). Thus, any complete screen for upstream members of this pathway must take both potential mechanisms into account.

To address both models for germline regulation of DAF-16, I performed two separate genome-wide RNAi screens, one aimed at finding negative effecters of DAF-16 activity and the other aimed at finding positive effecters. Both screens took advantage of *Psod-3::gfp*, a robust fluorescence reporter of DAF-16 activity, which is much easier to screen than assaying DAF-16 nuclear localization. *sod-3* (superoxide dismutase) is a direct and canonical target of DAF-16 transcriptional activation, and the *Psod-3::gfp* reporter turns on in all cases of DAF-16 activation so far reported, becoming very bright in the intestine of germline-less animals.

In the screen for negative effecters of DAF-16 activity, I searched for RNAi clones that could induce intestinal expression of the *Psod-3::gfp* reporter, in worms that should produce an intact germline (Figure 3). This screen was performed in an *rrf-1(-)* background. RRF-1 is an

RNA-dependent RNA polymerase needed for efficient RNAi activity in somatic tissues, and *rrf-1(-)* mutants fortuitously only perform RNAi knockdown in the two tissues I was interested in, the germline and the intestine (22). Looking for RNAi clones that turn on *Psod-3::gfp* in this strain should allow us to identify elements normally inhibitory to the DAF-16 nuclear switch, such as the theoretical germline signal or an intestinal receptor and signaling cascade with inhibitory activity.

In the screen for positive effectors of DAF-16 activity, I searched for RNAi clones that could repress intestinal expression of the *Psod-3::gfp* reporter in germline-ablated worms (Figure 3). This screen was performed in a *glp-1(ts)* background. When raised at 25°C, instead of 20°C, the GSCs of these mutants fail to propagate and they become long-lived germline-less adults. Looking for RNAi clones that turn off *Psod-3::gfp* in these animals should allow us to identify an intestinal receptor and signaling cascade with activating activity, or other positive regulators of DAF-16 function.

Biochemical screening for KRI-1 binding partners:

KRIT1, the mammalian homolog of KRI-1, is known to act in a number of protein complexes, and KRI-1 contains all of the conserved domains necessary to make very similar interactions. Even though proteins that theoretically work with KRI-1, or just downstream of KRI-1, will be identified using the genetic screening method outlined above, these genetic techniques will miss any factors with functional redundancy, and will not themselves indicate whether or not these newly identified factors actually interact physically with KRI-1. Protein-

protein interaction is extremely informative in extending our knowledge of a pathway beyond genetic interaction, towards explicit molecular mechanisms.

When considering the regulation of KRI-1 through interacting proteins, two potential models arise. As shown in Figure 4, one possibility is that a germline signal (S) promotes the formation of an inhibitory complex (I), which sequesters KRI-1 and interferes with its function. The other possibility is that the germline signal instead prevents the formation of an activating complex (A), which would otherwise help to assist KRI-1 in its function. Thus, to fully understand the regulation of KRI-1, both potential mechanisms must be taken into account.

To assay both models of KRI-1 regulation, we performed two separate biochemical screens, via KRI-1 co-immunoprecipitation (Figure 5). To screen for potential inhibitory-complex members, we performed KRI-1 Co-IPs in germline(+) worms, when KRI-1 is functionally inhibited. To screen for potential activating complex members, we performed KRI-1 Co-IPs in germline(-) worms, when KRI-1 is functionally active. Both of these Co-IPs were performed using a FLAG-tagged version of KRI-1a, an isoform capable of rescuing the lifespan of germline-ablated *kri-1(-)* mutants (21). The Co-IPs were all performed with Dr. Hildegard Mack, a talented worm biochemist from the Kenyon lab.

ITR-1, an IP3-regulated calcium channel capable of regulating lifespan:

The genetic and biochemical screens described above ended up revealing many genes that can influence DAF-16 activity, and many proteins that associate physically with KRI-1, respectively. One gene that came out of my genetic screen for positive effectors of DAF-16 was *itr-1*. I choose to follow-up on the role of this gene in germline-less longevity, as well as more

general regulation of DAF-16 function, neither of which have been previously associated with this gene. A lot is known about ITR-1, and it has even been previously linked to a different longevity paradigm. What follows is some key background information about this protein and its functions, focusing on aspects relevant to how it may fit into the germline-less longevity pathway.

ITR-1 converts receptor signals into Ca^{2+} signals

Inositol-triphosphate receptor-1 (ITR-1) is a calcium channel present in the ER, which opens in response to the modified signaling lipid inositol-triphosphate (IP3) (38). IP3 is produced at the cell membrane by phospholipase C (PLC) enzymes, of which the worm has five. In response to membrane-bound receptor signaling, PLCs cleave the membrane lipid phosphatidylinositol-bisphosphate (PIP2) to produce diacylglycerol (DAG) and IP3. DAG stays with the membrane and signals to protein kinase C (PKC). IP3, on the other hand, diffuses into the cytosol, where it eventually makes its way to activate the IP3 receptor (IP3R), ITR-1, at the ER. Ca^{2+} released from ITR-1 can then signal to a whole cascade of calcium-responsive proteins and pathways (38).

Physiological functions of ITR-1

Homologs of ITR-1 in higher organisms have been shown to be involved in many important and diverse physiologic processes, and the same holds true in worms. Signaling through *C. elegans* ITR-1 helps control embryogenesis, gonadogenesis, feeding, defecation, fertilization, mating, exogenous RNAi, touch response, neuronal reprogramming and necrotic cell death (39-46).

One of the most well studied roles of *C. elegans*' ITR-1 is in the defecation motor program (DMP) (47-51). In short, intestinal ITR-1 regulates the oscillations of a rhythmic Ca^{2+} wave that in turn causes precise body-wall muscle contractions, which mechanically force feces out of the worm's anus. These cycles proceed approximately every 50 seconds in wild-type worms and will continue at the same rate even if the intestine is removed from the animal, making them ultradian rhythms (self-starting, self-sustaining). A whole host of other proteins have been shown to assist ITR-1 in this function, including: 1) intestinal plasma membrane Ca^{2+} channels (GLT-1, GON-2), 2) intestinal phospholipase Cs (EGL-8, PLC-3), 3) muscle CAMKII (UNC-43), and several others (47-51).

Specific regulation of ITR-1 signaling

ITR-1 and its Ca^{2+} signals are used in many distinct processes, yet these processes often overlap within the same cell and tissue type. Thus, there must be mechanisms in place to prevent every possible Ca^{2+} responsive pathway from being activated each time IP3 is produced and Ca^{2+} is released. The specificity of this signaling is thought to be achieved in several ways (38-44). The first is that specific PLCs are used to control specific physiological processes, and the receptors that signal to these PLCs likely produce other signals that help couple IP3 production to the desired response. The second is that ITR-1 is known to bind to co-regulatory proteins which can help divert the released Ca^{2+} signal into certain pathways and responses (53). The third is that ITR-1 exists in several tissue-specific and timing-specific isoforms, and these isoforms are thought to bind different sets of co-regulatory proteins (52). In these ways, the general diffuse IP3 and Ca^{2+} signals can actually be earmarked for specific physiologic responses.

ITR-1 can regulate longevity

One of the physiological traits ITR-1 signaling regulates is lifespan (54). Monica Driscoll's group found that increased EGF signaling promotes longevity by activating PLC-3, which in turn activates ITR-1. Convincingly, this study showed that a loss-of-function mutation in *itr-1* decreases worm lifespan, whereas a gain-of-function mutation in *itr-1* increases worm lifespan. Furthermore, it was found that adult-only reduction in ITR-1 activity is sufficient to decrease lifespan, meaning that in the adult ITR-1 has a specific longevity promoting role. Unfortunately, the authors did not try to determine any of the genetic dependencies of *itr-1(gf)* longevity, nor did they attempt to place ITR-1 into any known longevity pathways. Thus, understanding the upstream and downstream mechanisms of ITR-1 lifespan regulation is a promising avenue of study, with much to be discovered.

RESULTS

Optimization of RNAi procedures:

Before beginning the genome-wide screens and their follow-up, I optimized my RNAi protocols for both liquid and solid agar culture, in order to achieve strong and reliable knockdown, both within a single experiment as well as between sequential experiments.

Optimization of liquid culture RNAi for 96-well screening

For liquid culture, I based my initial protocol on a previous study that established RNAi screening for worms in 96-well liquid format (68). Based on the needs of my study, I further optimized this base protocol by growing varying amounts of worms, in varying amounts of food, for varying durations, to see when I could time both the germline(+) and germline(-) worms to be assayable back-to-back in time. This was done using *Psod-3::gfp* reporter strains, to determine when changes in the marker could be visualized. It became apparent that three variables were critical to the success of this culture technique: 1) growing the bacteria overnight while shaking at 37°C, which standardized the amount of bacteria per well in spite of initial differences in inoculation strength, and provided enough bacteria to culture 25-30 worms through adulthood without starving; 2) proper gas exchange, which was achieved by keeping the smallest possible amount of liquid per well, venting the plates every 24 hours, and adding kanamycin at the W-stage of L4 to halt further bacterial growth; and 3) treatment of germline(+) worms with FUdR at the W-stage of L4, which prevented progeny overgrowth and adult bagging, yet was still a late enough stage in development that the entire germline had been produced and was functional.

Optimization of solid agar RNAi for efficiency and strength

For solid culture, there was a large impetus to optimize the procedure our lab was using because our lab members were only able to achieve very low knockdown strength, with a large variability in efficiency. Our previous protocol was to take overnight cultures of RNAi bacteria and plate them directly onto NG + CARB + IPTG plates that had been stored a week or more at room temperature, and then let these spotted plates dry two or more days at room temperature. As a trained microbiologist, many of these conditions seemed wrong to me. I instead decided to base my protocol on the one originally used by Andy Fire's lab (60). This introduced four critical steps: 1) diluting the overnight culture, 2) adding IPTG directly to the liquid culture, 3) spotting on fresh plates (stored at 4°C, not room temperature), and 4) using the plates the next day after spotting.

I further optimized a number of these variables, and discovered that the density of the bacterial lawn could be increase by growing the diluted bacteria for 2 hours before plating, and that regular NG plates (without CARB or IPTG) could also be used efficiently to grow thicker lawns (Figure 6). I decided that the best and easiest protocol would be to dilute the overnight culture 1:10 into fresh LB + CARB, grow for two hours at 37°C/200rpm, add IPTG and plate onto fresh NG + CARB + ITPG plates that had been pre-warmed for an hour at 37°C. I then optimized the amount of IPTG added to the liquid culture before plating, and found that adding 2X ITPG (final concentration of 2mM) was ideal, and would also work well on regular NG plates if these were ever desired (Figure 7). I then tested the effect that the time post-spotting had on efficiency and found that plates left 14-20 hours post-spotting were all relatively efficient, though plates left for less time were slightly stronger (Figure 7). Lastly, I found that strength of

RNAi was equally robust when the plates were dried at 30°C, which ensured that 150uL of spotted bacteria would be dry by the next day, so this condition was also adopted into my protocol.

Dual whole-genome RNAi screens unveil many potential DAF-16 regulators:

In order to address the previously mentioned possibility that the putative germline signal regulates intestinal DAF-16 through negative or positive effecters, we designed a two-headed approach that would allow us to uncover potential upstream regulators fitting either scenario.

To discover potential negative effecters of this pathway, we screened for RNAi clones that were able to induce intestinal *Psod-3::gfp* expression in germline-intact animals (i.e. clones that could mimic germline ablation) (Figure 3). This screen was done in an *rrf-1(-)* null background, which fortuitously performs RNAi knockdown only in our two tissues of interest, the germline and intestine. This permitted us to assay many gene knockdowns that may have lethal effects in other tissues. This screen allowed us to identify elements normally inhibitory to DAF-16, such as a theoretical signal from the germline or an intestinal receptor with inhibitory activity (Figure 2).

To discover potential positive effecters of this pathway, we screened for RNAi clones that were able to reduce intestinal *Psod-3::gfp* expression in germline-ablated animals (i.e. clones that could mimic an intact germline) (Figure 3). This screen was done in a *glp-1(ts)* background, which prevents germline stem cell division at 25°C, thereby genetically ablating the germline. This screen allowed us to identify elements that normally activate DAF-16, such as

an intestinal receptor with activating activity, or other cytosolic or nuclear factors that promote DAF-16 function (Figure 2).

As shown in Table 1, both screens uncovered a large number of potential regulators of DAF16 function. All preliminary hits were subjected to three rounds of validation, which eliminated a substantial number of false positives. Sequencing was performed on all validated hits, which revealed that 20+ clones from both screens were either duplicate clones or were different clones but targeting the same gene. In the end, the screen for negative effectors and the screen for positive effectors uncovered 210 and 149 unique gene knockdowns, respectively.

Surprising and significant overlap in hits between the two screens:

Though the screens were designed to hunt for genes with opposite effects on DAF-16 activity, surprisingly there was a large amount of overlap between both hit lists. In all, 25 genes were shared between the two screens (Figure 8). The identity of these overlapping genes is shown in Table 2.

Interestingly, two of these overlapping hits, *dlt-1* and *ogdh-1*, are components of the three-member oxoglutarate dehydrogenase complex (OGDC), which plays important roles in the citric acid cycle, lysine degradation and tryptophan metabolism. The third member of this complex, *dld-1*, was also identified in the screen for negative effectors of DAF-16 nuclear localization. Furthermore, out of the 42 genes listed on Wormbase as predicted or verified interactors with this complex, 13 were identified across my two screens (*atp-2*, *atp-5*, *B0491.5*, *ima-3*, *imb-3*, *npp-10*, *sams-1*, *hrp-1*, *qars-1*, *spg-7*, *tba-1*, *tbb-2*, and *ucr-1*). Two more

overlapping hits of interest are *let-92* and *paa-1*, which represent the catalytic and structural subunits of the protein phosphatase 2A complex (PP2A).

Significant overlap in GO Term enrichment between the two screens:

Each set of genes from the two screens was individually analyzed for gene ontology (GO) enrichment using the GOrilla platform. These lists of GO terms were then trimmed using REVIGO, removing terms with a similarity/dispensability score > 0.5. As shown in Table 3, there is a significant amount of overlap in the top 20 GO terms from each screen. For both screens, terms related to reproduction and development were the most enriched. More interesting, however, is that both GO term lists contained the same two provocative term doublets: 1) “endocytosis” and “vesicle-mediated transport”, and 2) “apoptotic process” and “death”. It is also worth noting that “determination of adult lifespan” was enriched in both the negative regulator screen (log10 P-value = -7.5575), as well as the positive regulator screen (log10 P-value = -3.6904).

Further analysis of screen hits:

In order to determine which hits were the most promising for follow-up, I analyzed DAF-16 dependency, tissue autonomy, impact on general health and fertility and ability to modulate other markers of germline-less longevity. This was done in liquid culture, under the same conditions used for screening. All metrics were analyzed at least three times, each time assigning a qualitative score from 0 to 3, with zero meaning no change and 3 meaning total change from control RNAi. These scores were averaged and are reported in Table 4 and Table 5, respectively, for the screens for negative and positive effectors.

DAF-16 dependency and impact on health and fertility

For hits from the screen for negative effecters, I assayed each for its DAF-16 dependency and impact on fertility, as I was most interested in hits that induce the *Psod-3::gfp* marker in a DAF-16-dependent manner, without ablating the germline. The fertility measure was done in the original *rrf-1(-)* screening background, whereas the DAF-16 dependency was done in a *rrf-1(-) daf-16(-)* background.

For the hits from the screen for positive effecters, I assayed each for its impact on overall health, as I was most interested in hits that are not turning off the reporter simply by making the worms sick. This was done in the original *glp-1(ts)* background.

Tissue autonomy in regulation of intestinal DAF-16

For hits from both screens, I assayed whether they were impacting intestinal DAF-16 activity tissue-autonomously or non-autonomously. For the negative effector hits, I compared the ability of the RNAi clones to induce reporter expression in the original *rrf-1(-)* background versus a *ppw-1(-) rrf-1(-)* background, as the former performs knockdown in the intestine and germline, but the latter only performs knockdown in the intestine. Those that could still induce the report in the latter strain were considered to be working tissue-autonomously in the intestine.

For the positive effector hits, I compared the ability of the RNAi clones to induce reporter expression in the original *glp-1(ts)* background versus a *rrf-1(-); glp-1(ts)* background, as the former performs knockdown in the whole body, except neurons, but the latter only performs knockdown in the intestine of these germline-ablated worms. Those that could still

induce the reporter in the latter strain were considered to be working tissue autonomously in the intestine.

Modulation of other markers of germline-less longevity

For hits from both screens, I tested each for its ability to modulate the activities of SKN-1 and the MitoUPR, using the *Pgst-4::gfp* and *Phsp-6::gfp* markers, respectively. This was done because a post-doc in our lab, Yuehua Wei, has recently shown that both of these pathways are activated in germline-ablated animals, are dependent on KRI-1 for this induction, and contribute to the longevity of these animals (unpublished, Figure 9). To test the ability of the negative and positive effectors to modulate these markers, I crossed each into *rrf-1(-)* or *glp-1(ts)* backgrounds, respectively, and assayed them as was done for *Psod-3::gfp*.

When considering both screens together, 85% of all screen hits were also able to modulate SKN-1 activity, and 49% were able to also modulate MitoUPR activity (Figure 10). This is striking when we consider that previous genome-wide RNAi screens showed hit rates from 0.08% to 2.2% for SKN-1 reporters, and 0.48% to 0.83% for MitoUPR reporters (61-65). Thus, by looking for modulators for DAF-16 activity we have significantly enriched for modulators of SKN-1 and MitoUPR activity.

ITR-1 is a positive effector of DAF-16 activity in germline-ablated worms:

When ranking all of our screen hits for the metrics assayed, two non-overlapping RNAi clones targeting *itr-1* clustered together, very high in our list for positive effectors. In addition, two cDNA-targeting RNAi clones obtained from Howard Baylis' lab were also tested and shown to have high efficiency. Because four distinct and separate RNAi clones of *itr-1* were able to

robustly inhibit *Psod-3::gfp* expression robustly in germline ablated animals, we concluded that off-target knockdown is unlikely to explain this shared effect. ITR-1 is an IP3-regulated calcium channel on the ER, and many genes upstream and downstream of it are well defined, so we chose to move forward analyzing the relationship of this protein to germline-less longevity.

As shown in Figure 11, *itr-1 RNAi* preferentially decreases reporter expression in the intestine, leaving the background expression in the pharynx and vulva relatively untouched. It can also be seen in these photographs that *itr-1 RNAi* makes the worms smaller than control treated worms, though it should be noted that they are not developmentally delayed, and appear healthy as adults.

itr-1 RNAi tissue-autonomously inhibits *sod-3* reporter expression:

Knockdown of *itr-1* only in the intestine of germline-ablated animals was equally efficient at reducing intestinal DAF-16 activity as whole body knockdown (Figure 12). Isolating knockdown to the intestine also partially reversed the smaller size of *itr-1 RNAi* treated worms (data not shown).

itr-1(RNAi) also inhibits the TCER-1 co-regulated *dod-8* reporter:

In germline-ablated worms, DAF-16 activity is co-regulated by the transcription elongation regulator TCER-1, such that expression of a subset of DAF-16 target genes is fully dependent on the presence of TCER-1. One of these DAF-16/TCER-1 co-regulated genes is *dod-8*. This co-regulation is specific to the germline-less state, unlike *sod-3* expression, and thus serves as an output for germline-ablation-specific DAF-16 activity. Encouragingly, we found that

itr-1 RNAi also inhibits expression of a *Pdod-8::gfp* reporter (Figure 13). Therefore, two differentially regulated reporters of DAF-16 activity are dependent on ITR-1 for their induction upon germline-ablation.

Worms treated with *itr-1(RNAi)* do not have nuclear localized DAF-16:

Interestingly, worms grown on solid culture RNAi have a dramatically decreased expression of the *Pdaf-16::GFP::DAF-16* fusion construct, as compared to worms grown on OP50. This made analysis of DAF-16 nuclear-localization using RNAi very difficult, as nuclear DAF-16 puncta become almost impossible to see under these conditions. Still, as can be seen in Figure 14, *itr-1 RNAi* treated worms show a diffuse/cytosolic GFP::DAF-16 pattern, rather than the typical nuclear pattern seen upon germline-ablation. However, because nuclear localization in the control treated worms is so difficult to measure, conclusions from this experiment are suggestive at best.

itr-1 RNAi inhibits longevity of germline(+) and germline(-) worms:

Worms treated with *itr-1(RNAi)* had a decrease in lifespan, regardless of germline status (Figure 15). This was not surprising given that *itr-1(lf)* mutants were previously reported to have a shorter lifespan than WT. Interestingly, worms on *itr-1(RNAi)* have a pronounced intestinal explosion phenotype, which is relieved in germline-ablated animals. As both germline(+) and germline(-) worms depend on DAF-16 for their longevity, it is possible that *itr-1(RNAi)* is decreasing lifespan in both contexts through DAF-16 inhibition and, thus, that ITR-1 is a more general regulator of DAF-16 activity and lifespan.

Effect of *itr-1 RNAi* on two different *daf-2(lf)* mutants:

To test the hypothesis that ITR-1 is a general regulator of DAF-16 activity, we assayed the effect *itr-1 RNAi* has on other paradigms of DAF-16-dependent longevity, namely *daf-2* mutants. *daf-2* encodes the worm Insulin/IGF-1 receptor, which normally activates a signaling cascade that inhibits DAF-16 nuclear localization. Mutations in *daf-2*, activate DAF-16 by relieving this repression, and confer exceptional longevity.

We tested representatives of two different classes of *daf-2(lf)* mutations, *e1370* and *e1368*, and found that *itr-1 RNAi* decreases *Psod-3::gfp* reporter expression in both mutant backgrounds (Figure 16). Though the overall decrease in expression is not as dramatic as that seen in germline-ablated animals, it is worth noting that intestinal expression appears to be greatly impacted. Thus, even though most tissues maintain a high level of DAF-16 activity in *daf-2* mutants, the intestine may be specifically dependent on ITR-1 for the function of this transcription factor.

Consistent with this, and with previous data suggesting intestinal DAF-16 is responsible for the majority of *daf-2(lf)* mutant lifespan, *itr-1 RNAi* profoundly suppressed the longevity of both *daf-2* mutants (Figure 17). In fact, the effect on longevity of *itr-1(RNAi)* appears to be even more pronounced in these strains than in WT or germline(-) worms.

Effect of *itr-1(RNAi)* on SKN-1 and MitoUPR activity:

Though our results are consistent with the idea that *itr-1 RNAi* is preventing proper activation of DAF-16 in multiple contexts, it is also possible that knocking down *itr-1* decreases

lifespan through shared pathways. As seen in Figure 18, *itr-1 RNAi* significantly lowers expression of the SKN-1 reporter *Pgst-4::gfp*, and the MitoUPR reporter *Phsp-6::gfp*. Repression of these reporters appears even stronger than repression of *Psod-3::gfp*. It is therefore possible that knocking down *itr-1* decreases lifespan through its effects on either of these two pathways or, even more likely, through modulation of these pathways combined.

itr-1 RNAi surprisingly lowers somatic gonad signaling:

In germline-ablated worms, the spermatheca of the somatic gonad produces dafachronic acid, a steroid hormone, which diffuses into the intestine and activates the nuclear hormone receptor DAF-12. This increase in ligand-bound DAF-12 activity can be measured using the *Pcdr-6::gfp* reporter. I integrated an extra-chromosomal array line carrying *Pcdr-6::gfp*, thereby creating a stable transgenic line with consistent reporter expression between individual worms. This line was then fully outcrossed to remove background mutations, and crossed to *glp-1(ts)*. Upon examination, we were surprised to find that *itr-1 RNAi* is able to suppress the *Pcdr-6::gfp* induction seen in germline(-) worms (Figure 19). This potentially puts dafachronic acid/DAF-12 signaling downstream of, or in parallel to, *itr-1*.

Initiation of *itr-1 RNAi* after L2 is insufficient to inhibit DAF-16 activation:

To determine when in the worm's life cycle ITR-1 activity is needed for DAF-16 activation, we performed time-course experiments placing worms on *itr-1 RNAi* at various developmental stages. Moving worms from control to *irt-1 RNAi* at L1 and L2 significantly reduced *Psod-3::gfp* expression, as compared to worms raised their entire lives on control; yet

moving them at L3 or later was unable to do the same (Figure 20). Unfortunately, as RNAi may not have its full knockdown effect until 12-24 hours post-initiation, and stable proteins may not actually be decreased in level until even later, this analysis does not allow us to perfectly pinpoint when ITR-1 activity is needed.

Analysis of upstream regulators of ITR-1:

ITR-1 releases Ca^{2+} from the ER in response to the modified lipid IP3. This IP3 signal is generated at the plasma membrane by phospholipase C (PLC) enzymes which cleave PIP2 into DAG and IP3, in response to receptor kinase and G-protein coupled signals. The worm has 5 PLCs and one catalytically dead PLC-like enzyme (*pll-1*). We used RNAi against all 5 of these PLCs to determine which is producing the IP3 signal needed for ITR-1 activation, using RNAi against *pll-1* as a negative control. Unfortunately, none of these RNAi clones caused a significant difference in DAF-16 reporter expression in germline(-) worms, as compared to control (Figure 21). This was even repeated with double generation RNAi to achieve stronger knockdown to no avail. Most analyses of PLC function take advantage of null or near null mutations in these enzymes, with very few studies ever using RNAi; moreover, it is possible that *itr-1* is regulated redundantly by multiple PLCs.

A C-terminally FLAG-tagged KRI-1 construct rescues *kri-1(null)* worms:

All following experiments were done in collaboration with Dr. Hildegard Mack.

Rescue of development and appearance

Because there are no commercially available antibodies for KRI-1, we needed to epitope-tag it for co-immunoprecipitation. We decided to use a dual 3XFLAG-6XHIS tag for strength and methodological flexibility. A previous post-doc in our lab was unable to obtain phenotypic rescue using a N-terminally TAP-tagged version of KRI-1, which could be due to the terminus where it was tagged or the size of that tag. We decided to put our much smaller 3XFLAG-6XHIS tag on both ends of the protein to address these possibilities. After obtaining transgenic worm lines expressing both tagged versions of KRI-1, it was quickly apparent that the C-terminally-tagged transgene (Figure 22) could rescue the slow development and pale appearance of *kri-1(-)* worms, whereas the N-terminally-tagged version could not (data not shown).

Rescue of DAF-16 activation

When tested in germline(-) worms, the C-terminally-tagged KRI-1 protein was able to robustly rescue the increased *Psod-3::gfp* expression that would otherwise be prevented by *kri-1(-)* mutation (Figure 23). In fact, overexpression of this tagged KRI-1 actually caused a huge induction of the reporter beyond what is seen in otherwise wild-type worms, but only in the germline(-) state. This data supports the previous hypothesis that KRI-1 helps promote DAF-16 activity, but can only do so in the permissive state of germline absence.

Rescue of lifespan

When tested in germline(-) worms, the C-terminally-tagged KRI-1 protein was able to fully rescue the longevity that would otherwise be prevented by *kri-1(-)* mutation (Figure 24). Interestingly, though the results from the *Psod-3::gfp* reporter experiments suggest that DAF-16 is hyper activated (or hyper-nuclear) in the tagged overexpression line, lifespan of this strain

upon germline-ablation was the same as that for regular germline(-) worms. That is, increased KRI-1-mediated activation of DAF-16, over the levels already found in germline(-) worms, does not seem to confer an added lifespan benefit.

KRI-1 Co-Immunoprecipitations potentially reveal novel binding partners:

As mentioned previously, it is equally likely that the germline regulates KRI-1 via formation of inhibitory complexes or via repression of activating complexes (Figure 4). To address both of these scenarios we used a two-headed biochemical approach (Figure 5). To enrich for potential inhibitory binding partners, we performed KRI-1 Co-IPs in the presence of the germline. To enrich for potential activating binding partners, we performed KRI-1 Co-IPs in the absence of the germline.

KRI-1a::FLAG can be pulled down efficiently

Before beginning our large Co-IP experiments, we wanted to ensure that we could efficiently pull-down our tagged KRI-1 protein from worm lysates. Using germline(-) worms, we performed several smaller-scale pull-down experiments. As can be seen in the Western Blot in Figure 25, we are able to pull down an ~80KD protein that cross reacts with an anti-FLAG-antibody, which is what we would expect for our tagged KRI-1. Its also important to note that this protein was pulled down only when IP'd with anti-FLAG antibodies and not when IP'd with non-specific antibodies (mixed mouse IgG1).

KRI-1 Co-IPs uncover many potential interaction partners

As can be seen in Figure 26, protein extracts from both the germline(+) and germline(-) worms were subjected to magnetic-agarose bead precipitation using the M2 anti-FLAG

antibody, to find KRI-1 interaction partners. A control Co-IP was also performed on both samples using the same type of bead and antibody, but instead having affinity for Hemagglutinin A (HA), which is not present in the worms. After mass spec analysis, proteins found in both the HA and M2 lists were considered to be non-specifically binding to the beads/antibodies and were removed from analysis, unless they were statistically significantly enriched in the M2 experimental sample as compared to the HA control. These lists of high confidence KRI-1 interacting proteins are available in Table 6.

KRI-1 is preferentially bound in the germline(+) state

Analysis of our lists of interacting proteins reveal that only a single protein, F37C4.5, is bound preferentially in the germline(-) state (Figure 27). The majority of proteins seem to be constitutively bound, as they were found at similar spectral counts in both Co-IPs. There are, however, a significant number of proteins that are enriched in the germline(+) state, perhaps supporting the model that these specific interacting proteins are acting as inhibitory complex members.

Significant overlap between genetic and biochemical screens

Though the combined hits from our genetic screens only comprised 1.7% of the entire worm genome, they make up 23% of the proteins identified in our biochemical Co-IP experiments. Specifically, 15 out of our 65 high-confidence binding proteins were previously shown to have functional effects on DAF-16 activity in one of the two RNAi screens. The identity of these proteins is shown in Figure 28.

DISCUSSION

Overview and general reflections:

The purpose of this study was to identify potential upstream regulators of germline-less longevity through unbiased genetic and biochemical approaches. I specifically focused on uncovering factors that influence KRI-1 mediated DAF-16 activation, as this pathway is not only integral to the longevity of germline(-) worms, but is also consistently activated upon germline-ablation, even when other mechanisms of germline-less longevity are perturbed. In this way, DAF-16 activation acts as a reliable binary switch; “off” in the presence of the germline, “on” in its absence (as long as KRI-1 is also present).

I took advantage of this DAF-16 switch to screen the entire genome twice over: in one case looking for genes that could mimic germline-ablation in worms that should be germline(+), and in the other case looking for genes that could mimic an intact-germline in worms that are germline(-). This was performed using a high throughput 96-well liquid screening technique, which made this dual whole genome approach tractable in terms of time, space and supplies needed. Also integral to success was the use of the *Psod-3::gfp* reporter, which served as a robust proxy for DAF-16 activity. Though the initial set-up and optimization time was not insignificant, the actual screens themselves ran impressively quickly, highlighting this methodology as a promising avenue to interrogate the whole genome in a timely manner.

In addition to these reverse genetic techniques, my collaborator Hildegard Mack and I also performed unbiased biochemical screening for proteins that bind to KRI-1, both in the presence and absence of the germline. This is rare for studies in *C. elegans* biology and the field of aging research, which both have a strong foundation and history in genetic and molecular

analysis, but very infrequently delve into biochemical techniques. While I was undertaking this study, it became known that KRI-1 is upstream of several other important pathways related to germline-less longevity, specifically SKN-1 signaling, the mitochondrial unfolded protein response and increased cytosolic reactive oxygen species (Y. Wei and Kenyon, unpublished). This places KRI-1 as a central, upstream, master-regulator of germline-less longevity, and greatly expands the relevance of its binding partners.

When performing multiple screens on the same pathway, it was encouraging to see overlapping pathways and mechanisms emerge, as this helps validate that all screens are uncovering factors that are likely to be biologically relevant. With this in mind, I was very pleased to see the significant amount of overlap in 1) enriched GO Terms between my genetic screens, 2) binding partners between both conditions of my biochemical screens, and 3) genes identified in my genetic screens and proteins identified in my biochemical screens.

What follows is a reflection on my results, which of course includes discussion of ITR-1 signaling, but also highlights some pathways and genes I did not have time to follow-up on, yet I still find to be of great interest. I generated a large set of genes and proteins that may be involved in germline-less signaling, and I hope that this list proves to be a valuable resource for the field.

The importance of stringent liquid and solid culture RNAi protocols:

When I first joined our lab, all members I talked to were having very frustrating difficulties obtaining strong and consistent knockdown on solid culture RNAi. Phenotypes that can be mediated via low-level chronic RNAi exposure, such as the lifespan effects of *daf-2 RNAi*

or *daf-16 RNAi*, were still able to be seen; however, certain phenotypes that required intense knockdown, such as certain adult phenotypes that need to be initiated in larvae, were almost unattainable. Comparing our RNAi protocol to what I knew from my years as a microbiologist, I quickly found a number of factors that were likely reducing knockdown efficiency. These hunches were proven correct when I searched the literature and found a number of protocols from leading RNAi labs (Fire lab, Aringer lab, Hunter lab) that differed from our lab's protocol in all the ways I expected. Changing these factors, and then further optimizing them and several others, led to a new lab RNAi protocol that yields vigorous and reliable knockdown.

This experience provided a foundation for me to create an additional protocol for liquid RNAi, for which there are far fewer methodological resources. In the end, I designed a method for liquid culture RNAi that also yields strong and consistent knockdown. In fact, I dependably observed more intense knock down in liquid culture than on solid culture, which I speculate may be due either to the fact that worms in liquid are feed the RNAi bacteria much sooner after induction, or to liquid bacterial RNAi's acting as hybrid between feeding and soaking RNAi.

In all, I recommend maintaining a vigilant level of fidelity to RNAi methods between experiments. RNAi even at its best can produce a large amount of intra-experiment variability, which already complicates experimental repeatability, so it is paramount to reduce inter-experiment variability by adhering zealously to one's protocol.

Generating a mutant library that is otherwise genetically homogenous:

Between the time I rotated in and actually joined Cynthia's lab, a number of scientists in the aging field wrote a letter to *Nature* rejecting the claims from Lenny Guarente and Heidi

Tissenbaum that overexpression of SIR-2.1 increases lifespan (67). They instead identified a background mutation in the original overexpression strain that provides the actual lifespan benefit. The authors concluded that all alleles, not just new EMS derived alleles should be outcrossed at least 10 times to ensure isogenic lines for comparison. This controversy exposed the fact that for a very long time worm researches often compared mutant strains raised in different backgrounds with very little or even no backcrossing, something that would never have been accepted in other model organisms such as mice.

I decided that I wanted to do better than the worm researchers before me, and that every strain I would use and publish would be outcrossed 12 times into a single genetic background, N2E. This level of outcrossing meant that all of my strains would be isogenic except for the corresponding mutations they held, and made the possibility of non-tightly-linked background mutations statistically negligible. All mutations were outcrossed individually first before building multi-mutant strains, and all outcrosses were done using a double cross protocol that alternated between crossing against N2E males and N2E hermaphrodites.

Though this may come off as “overkill”, I have high confidence in comparisons between my mutant lines, and would trust my data over that obtained in previous studies where outcrossing was not sufficient. I have generated a large personal library of single and multi-mutant strains in the N2E background, and hope that this set of strains will also be a resource for my future lab mates. I believe that one day we may see labs that outcross all new alleles fully before storing these strains, which will make it much faster to begin experiments with reliable and trustworthy results.

RNAi screening in 96-well liquid culture:

The tactic of performing whole genome-wide RNAi screens in 96-well liquid culture proved to be incredibly efficient once I had developed and optimized my protocol. I strongly believe that another researcher could easily take my techniques and now perform a single-whole genome RNAi screen in approximately 3-4 months, with validation and sequencing finished in under 6 months. Another benefit to this technique is that, once hit libraries are built, the initial screening strain can be easily swapped out for many other mutants, in order to test the effects of the hits on those new strains.

Still, one drawback to this technique is that it definitely relies on using a very robust reporter or phenotypic readout, in order to reduce the number of false negatives. Large scale screening where each gene is only tested once, in one well, before being considered a “miss” also increases the chance of having false negatives. Lastly, there is large amount of edge effect in these plates, where the outer wells have more exposure to air, less humidity and potentially larger temperature fluctuations.

Some of these drawbacks may be combated using a plate reader to assay which clones are “hits” and which are not. After my screen was already fully completed, a program was written for GE Healthcare Life Sciences’ IN Cell Analyzer, allowing it to read 96-well plates, find worms in each well, and measure each worm for a number of metrics, including fluorescence. This would have saved me countless hours at the microscope, and sped up my research immensely. I believe coupling my protocol to this new technology will allow truly high-throughput screening for genes affecting a number of markers and phenotypes.

Dual genome-wide RNAi screens unveil many potential DAF-16 regulators

GO Term enrichment

I was initially surprised to uncover so many DAF-16 effecters from my screens. However, I was encouraged to see that my two lists of hits, generated in different strains and looking for opposite (but related) effects, had such a profound amount of overlap in GO Term enrichment. In fact, the top terms from both screens involved reproduction and development, which is unsurprising given the pathway I was analyzing. What was surprising, however, was that the two term doublets “endocytosis” & “vesicle-mediated transport” and “apoptotic process” & “death” also came up independently from both screen lists, and all at almost the same ranking.

These are actually very exciting terms to find, as both could be related to germline-to-intestine signaling. It has been shown that gamma-irradiation-induced germline apoptosis is dependent on intestinal KRI-1, so it is possible that the other genes associated with these terms help to promote this tissue-tissue signaling. Endocytic processes are capable of importing, exporting and processing many secreted or membrane bound signals. They may even be used to control or sense yolk proteins that have been noted to accumulate in the pseudocoelomic cavity of germline(-) worms (33). Could endocytosis of this extra yolk lead to activation of DAF-16, a known repressor of yolk gene transcription? It will be interesting to investigate these possibilities.

Significant gene set overlap between screens

The most initially curious and surprising finding of my study was the large number of genes I found to be shared between screens. In total, 25 genes showed up in both the negative effector and positive effector screen. This was unexpected because these screens were

theoretically designed to pick-up genes with opposite effects on DAF-16 activity and, thus, having opposite roles in the germline-less longevity pathway. Though purely speculative, there are a number of potential explanations for this finding. First, is that there is a dosage effect of these genes, such that some level of knockdown causes a beneficial feed-back or hormetic response, but too much knockdown is detrimental (supporting this: the germline-intact screening strain has weaker intestinal RNAi function than the germline-ablated screening strain). Second, is that these clones are having effects in different tissues to cause their disparate effects, such that knockdown in the germline/intestine activate the pathway but knockdown in another tissue represses it (supporting this: the germline-intact screening strain I used only performs germline and intestinal RNAi, whereas the germline-ablated screening strain performs RNAi in the whole body). Third, is the general possibility that germline(+) animals respond to some RNAi clones oppositely than germline(-) worms.

Our DAF-16 effectors are enriched for SKN-1 and MitoUPR modulators

Yuehua Wei, a post-doc in our lab, has a paper in revision at PNAS showing that germline-ablation increases SKN-1 activation, the MitoUPR and cytosolic ROS, all in a KRI-1 dependent manner, which subsequently links the regulation of these other pathways with the regulation of DAF-16. As shown previously, 85% and 49% of my DAF-16 effectors also effect reporters of SKN-1 and MitoUPR activity, respectively. This is a huge enrichment over what would be expected from random sampling of the genome (based on previous genome-wide screens for these reporters). The fact that many of my hits strongly activate or inactivate all three of these markers leads me to believe that I have truly discovered upstream regulators in the germline-less longevity pathway.

Top hits that we not explored further

I ranked my list of genes from my screen for negative effectors based on their ability to induce *Psod-3::gfp* expression in a DAF-16 dependent manner and without impacting fertility. The two genes that came to the top were *C16A3.5* and *T02H6.11*, which are mitochondrial/redox related genes, and both of these RNAi clones were shown to be acting in the germline and not the intestine. A number of other mitochondrial/redox genes were also found in this screen, leading to the possibility that germline mitochondria send out a signal that “all is well” under positive growth conditions, but under negative growth conditions or germline-ablation this signal is absent and the intestine responds accordingly.

I ranked my list of genes from my screen for positive effectors based on their ability to reduce *Psod-3::gfp* expression without making the worms sick. My top hits were three translation elongation factors, *eef-1B.1*, *erfa-3* and *eef-1G* (my fourth best hit was actually another distinct clone targeting *erfa-3*). We already know that germline(-) animals utilize a special transcription elongation factor (TCER-1), so its possible they recruit special translation elongation factors as well.

The fifth best hit from my positive effector screen was *sptl-1*, a gene involved in sphingolipid metabolism. This was interesting to me as TORC1 activation can be positively regulated by *elo-5*, *sptl-1*, *cgt-3* and *rheb-1*, which were all found in this screen (58). Additionally, TORC1 can positively regulate lifespan in the intestine through ROS-mediated activation of RHEB, which in turn activates another top hit of mine, *ELT-2* (59). This perhaps ties a number of genes and already known germline-ablated phenotypes into one pathway. To speculate: perhaps *elo-5*, *sptl-1*, and *cgt-3* promote TORC1 through sphingolipid regulation of

RHEB-1, allowing it to respond to the increase in ROS seen upon germline ablation, which in turn leads to increased ELT-2 activation and lifespan extension.

ITR-1 is an upstream regulator of the germline-less longevity pathway:

Four different RNAi clones targeting *itr-1* were shown to similarly decrease *Psod-3::gfp* expression. As two of these clones have 0% overlap, and *itr-1* has no paralogs, it is safe to conclude that this effect is not due to off-target knockdown. *itr-1 RNAi* was also able to reduce SKN-1 and MitoUPR activity, placing it genetically at the level of KRI-1. Interestingly, *itr-1 RNAi* also decreased expression of the *Pcdr-6::gfp* reporter, suggesting that it is also upstream of DAF-12 function. It would be interesting to test whether KRI-1 is also upstream of DAF-12.

One important future question to ask is if whether ITR-1 is actually more active in germline(-) worms. This will be tested using a fluorescent Ca^{2+} reporter expressed exclusively in the intestine. It's possible that Ca^{2+} signaling is up throughout life, only at a critical developmental stage, or only in adulthood, and all of these possibilities will be assessed. It's also possible that Ca^{2+} signaling is increased either in magnitude or periodicity, and both of these possibilities will be tested as well.

Though the exact life stage at which ITR-1 activity is needed for DAF-16 activation in germline(-) worms is not fully clear, due to caveats in RNAi timing experiments, my current results seem to suggest that activity in the later larval stages or young adult stage is critical. Evidence for this is that knockdown starting in L3 or L4 is unable to suppress the *Psod-3::gfp* reporter in Day 2 adults, even though full knockdown should happen 24 hours post initiation. So either ITR-1 activity is needed only to initiate the pathways during late-development/early-

adulthood, and then is dispensable, or the ITR-1 protein is stable enough to circumvent the effects of this later-life knockdown.

ITR-1 may be a universal regulator of intestinal DAF-16 activity:

Not only did *itr-1(RNAi)* decrease the lifespan of germline(-) worms, but it also decreased the lifespan of WT germline(+) worms and two *daf-2* mutants. As reducing DAF-16 activity (via mutation or RNAi) in all four of these strains reduces their lifespan, it is possible that this is how *itr-1 RNAi* is also reducing lifespan under all of these conditions. In support of this idea, *itr-1 RNAi* inhibits the increased intestinal *Psod-3::gfp* expression in germline(-) worms and both *daf-2* mutants. In order to test this hypothesis further, it is critical to test whether *itr-1 RNAi* decreases the lifespan of *daf-16(-)* mutants. If *itr-1 RNAi* fails to further shorten the lifespan of *daf-16(-)* mutants, then we can assume its impact on longevity is likely DAF-16-dependent.

Another important detail that still needs clarification is how exactly ITR-1 promotes DAF-16 function. Decreases in DAF-16 activity may occur due to impaired translocation into the nucleus, but may also occur due to impaired activity once in the nucleus. I've shown that DAF-16 activity is down in worms treated with *itr-1 RNAi*, but my data on DAF-16 nuclear localization is far from convincing. Unfortunately, testing GFP::DAF-16 translocation on RNAi bacteria appears to be impossible. Thus, I will need to take WT and loss-of-function *itr-1* mutants raised on OP50, and determine the relative amount of GFP::DAF-16 nuclear localization each has in the presence and absence of the germline.

Though I was able to convincingly show that ITR-1 controls DAF-16 activity tissue-autonomously in the intestine, it will be interesting to test if intestine-only knockdown of *itr-1* is sufficient to lower lifespan in all of the above strains. It's notable that whole body *itr-1 RNAi* causes a significant number of explosions in germline(+) worms, but not germline(-) worms or worms treated with FUdR, suggesting this effect is due to knockdown in the germline. Perhaps intestine-only RNAi will also prevent these explosions and provided cleaner lifespan analyses.

Analysis of pathway members upstream and downstream of ITR-1:

Biochemical identification of pathway members

Hildegard Mack, an incredibly talented biochemist in our lab, performed Co-IPs of DAF-16 in the presence and absence of the germline. In her list of binding partners, we were very excited to find proteins that could act in the ITR-1 pathway. Excitingly, the highest confidence DAF-16 interacting protein in the germline(-) state was EGL-8, a phospholipase C that can generate IP3 to activate ITR-1. Hildegard also found the Ca^{2+} responsive kinase UNC-43, the worm homolog of calmodulin kinase II (CAMKII), which is known to activate DAF-16 through direct phosphorylation (57). Hildegard is currently outcrossing null mutants of both of these genes, and will test them for their effects on germline-ablated DAF-16 activity and longevity.

PLCs, receptors and the elusive germline signal

We can assume that ITR-1 must be activated by one or more of the PLCs, as non-IP3-mediated activation of this channel has never been reported. Unfortunately, RNAi of the 5 worm PLCs was not enough to phenocopy *itr-1 RNAi*, so we will need to use mutant analysis, which has a stronger effect on activity. It's important to note that there may be redundancy of

PLCs activating ITR-1, so mutant and RNAi combinations will need to be tested if no single mutant shows an effect. Finding the PLC upstream of ITR-1 is paramount because it can lead us to the receptor that is activating it. Finding this receptor can help us to identify its corresponding ligand, which is theoretically the germline signal that normally inhibits longevity.

Calcium responsive genes and pathways

Aside from UNC-43, there are many intestinal factors that are activated by Ca^{2+} . In order to determine which are needed to transmit the signal from ITR-1 to DAF-16, we will test as many of these genes as possible using RNAi. Central hubs for calcium signaling that are especially of interest are calmodulin, CREB, calcineurin and calreticulin.

KRI-1 Co-IPs discovery both known and new potential regulators of DAF-16 activity:

C-terminally FLAG tagged KRI-1 is functional

Della David, a post-doc in our lab, previously tried to TAP tag KRI-1 for pull down, but this protein was unable to rescue the lifespan of germline-less *kri-1(-)* mutants. We decided to employ a much smaller tag, specifically a 3XFLAG-6XHIS tag to avoid interference with normal protein function. We put this tag at the N and C termini of KRI-1a, to also address the possibility that one end of the protein may be more sensitive than the other. In the end we found that only the C-terminally tagged version rescued lifespan and DAF-16 activity in germline-ablated animals, and only this construct was used in our Co-IPs.

KRI-1 interacts constitutively with many proteins

The majority of KRI-1 binding partners were found to interact in both the presence and absence of the germline. There were a large number of proteins, however, that also interact

preferentially in the germline(+) state, which may support the model that KRI-1 is regulated via formation of an inhibitory complex. It will be interesting to analyze the functional contribution of these proteins via RNAi; will knocking them down in germline-intact worms relieve KRI-1 repression, and promote DAF-16 activity?

Strikingly, only one protein interacted with KRI-1 preferentially in the germline(-) state. It should be noted that this protein was also found in the germline(+) Co-IPs, but at a significantly lower spectral count. This protein, F37C4.5, is uncharacterized and has no direct ortholog in higher-level organisms. However, BLAST-search analysis of the protein sequence found that the closest mammalian homolog is an alpha-integrin. This is noteworthy because mammalian KRIT1 is known to bind to beta-integrin in endothelial cells (66). When the germline is not present there is less cell-cell contact between the intestine and the gonad, and this may be sensed via an integrin/KRI-1 signaling mechanism.

Several KRI-1 binding partners also found in genetic screens

A very nice final result for my double-genetic screen and double-biochemical screen study with Hildegard was the discovery of a significant number of genes/proteins that were identified in both approaches. These 15 overlapping proteins are therefore suspected known to physically associate with KRI-1, as well as functionally regulate DAF-16 activity, which makes them especially promising and deserving of further analysis. Though it should be noted that many of these potentially interacting proteins may be false positives.

One set of genes/proteins that was found genetically and biochemically was the T-chaperonin complex. All 8 members were found in the genetic screen for positive effectors, and 6 were found to bind KRI-1 with high confidence. Finding this whole complex using two very

different unbiased approaches is remarkable. Still, as the T-chaperonin complex is thought to assist in folding of hundreds of different proteins, its exact function in the germline-less longevity pathway may not be easy to parse out.

Final Thoughts:

This study has generated large lists of functionally validated and characterized genes that effect DAF-16 activity, as well as proteins that physically interact with KRI-1. Though I was unable to follow-up on most of the genes and proteins identified, I hope that these lists can serve as a resource for other researchers interested in the mechanisms associated with germline-less longevity.

The goal of this study was to decipher how the germline inhibits longevity in intact worms. Though I did not discover the theoretical germline signal that communicates with the intestine, my results suggest that repression of ITR-1 activity may be an important mechanism through which the germline exerts its lifespan repression. I am excited to finish my analysis of ITR-1 activity and function, and publish these results. Ca^{2+} signaling through ITR-1 is an attractive mechanism to explain how removing the germline simultaneously activates so many downstream pathways. It's possible that each downstream mechanism is activated by a different Ca^{2+} responsive protein, which would make cytosolic Ca^{2+} a critical bifurcation point in the germline-less longevity pathway.

I am very proud of the overlap observed between my genetic and mine and Hildegard's biochemical data. I firmly believe that the field of *C. elegans* aging research will benefit from incorporating more biochemical analyses, as it can often be difficult to show direct mechanisms

using genetic association and epistasis alone. Studies of protein-protein interactions and post-translational modifications can help us to more deeply understand known longevity pathways, as well as discover new ones.

Lastly, as society continues to age, and the cost of medical care for our geriatric population continues to increase, it is imperative that we find effective treatments for age-related conditions. This includes both diseases of aging, as well as conditions that we consider “normal” physiological consequences of getting older. Studies of longevity in model organisms, like this one, have provided many potential targets to treat age-associated decline. In the future, I hope to use my position as a physician scientist to help translate these basic science findings into clinical studies and trials. In this way, I hope to achieve the goal I set for myself many years ago, which is to help improve the lives of the elderly through dedicated medical care and scientific research.

METHODS

Strains:

Worms were grown on NGM agar plates using standard nematode husbandry techniques. Before each experiment, the strains to be used were grown at 20°C for at least three generations post starvation or bleaching. Strains were grown in succession for only 4 months before thawing from the original frozen strain. The wild-type isolate used in this study is N2E, and all mutant alleles used in this study were outcrossed 12 times to N2E, using a repeating double-cross strategy, which alternates between crossing to wild-type males and hermaphrodites. Only after an allele was fully outcrossed, were multi-mutant strains constructed. Integrated transgenes were also outcrossed accordingly, as were extra-chromosomal arrays that were injected into a non-N2E background. Extra chromosomal arrays injected into N2E (or a 12X N2E outcrossed mutant strain) were not outcrossed, as the presence of these arrays should not impact the genome.

Cloning:

Synthesis of transgenic constructs was performed using Invitrogen's Gateway Cloning Technology. Either promoter or ORF elements of interest were amplified from the genome of N2E worms using primers from Elim Biopharmaceuticals that were designed to contain flanking *att* integration elements. The PCR reactions were performed using Bio-Rad's iProof high-fidelity DNA polymerase, and a low cycle number (~20), to avoid errors in DNA synthesis.

These amplicons were cleaned using Qiagen's PCR Purification Kit. They were then mixed with the corresponding pDONR plasmid, and subjected to the BP Clonase reaction, so as to generate pENTRY vectors. The product of each BP Clonase reaction was transformed into Thermo Fisher's One Shot TOP10 *E. coli* competent cells. Single colonies were picked, grown and frozen, and plasmid was extracted using Qiagen's Mini Prep Kit. These plasmids were sequenced by Elim Biopharmaceuticals using insert flanking M13F and M13R primers, as well as element specific primers, to achieve full coverage.

Expression vectors were then generated using the LR Clonase reaction. Three element recombination was performed by mixing the pENTRY vectors for the desired promoter and the desired ORF with the Addgene provided plasmids pCM1.36 (*tbb-2* 3'-UTR in pDONRP2RP3) and pCG150 (*unc-119(+)* rescuing pDESTR4R3). The product of these reactions were transformed into TOP10 competent cells and colonies were picked, grown, frozen, mini prepped and sequenced at full coverage.

Generation of transgenic worms:

Injectations

New transgenic worm lines were generated via germline injection of expression vectors and co-injection markers, using a Zeiss Observer A1 AX10 light microscope with the Eppendorf FemtoJet injection system. This technique produces worms that carry extrachromosomal arrays composed of concatamers of all plasmids injected, and leads to overexpression of the injected construct. In this study, newly gravid *unc-119(ed3)* mutant worms were injected, as all Expression vectors contained an *unc-119(+)* rescue element. Each injection was also done using

a *Podr-1::rfp* co-injection marker. The expression vectors were injected at 10ng/uL and the co-injection marker was injected at 50ng/uL, and a total of 100ng of DNA was injected per worm. Progeny that rescued the *unc-119(-)* phenotype were isolated and clonally expanded. Only lines that passed on both the *unc-119(+)* marker and *Podr-1::rfp* marker in complete concert were kept and further analyzed.

Integrations

The *Pcdr-6::gfp* reporter was converted from an extrachromosomal array into a genome integrated line via UV cross-linking. To do this, 50 L4 worms that highly expressed the array were subjected to 0.010 J/cm² of UV-irradiation. These worms were then split onto 5 separate 10cm plates containing OP50, and the population was allowed to grow at 25°C until it starved out. The worms on these plates were then scrapped into the middle of the plate using a spatula, and one chunk of these concentrated worms was transferred to a new 10cm plate. Four more rounds of this serial starvation procedure were performed. Afterwards, all five plates were assayed for worms still expressing the transgene. These worms were isolated and assayed to ensure that 100% of their progeny also carried the transgene. The single line that passed this requirement was then outcrossed 12X to N2E, to remove any potential background mutations from the initial UV exposure.

Solid culture RNAi:

NGM plates (6cm) for RNAi experiments were prepared contained 100ug/mL carbenicillin and 1mM IPTG. They were poured using a peristaltic pump, so as to contain equal amounts of agar, allowed to dry overnight at room temperature and then stored at 4°C. Plates

were seeded with RNAi bacteria the night before needed, as follows: an overnight liquid culture was diluted 10-fold into new LB containing 100ug/mL carbenicillin and these cultures were shaken at 37°C/200rpm for 2 hours, then IPTG was added to 2mM (2X the plate concentration) and 150uL of culture was immediately spotted onto pre-warmed plates, these plates were then dried overnight at 30°C. Worms were egg-prepped the same day the plates were prepared, and hatched overnight while rocking at 20°C in M9. Early the next day, 35-50 arrested L1's were spotted onto each plate, depending on the experimental need.

Liquid culture RNAi:

Experiments using liquid culture were all performed in 96-well black-well plates with clear bottoms. The night before seeding with worms, these plates were filled with 100uL of LB containing 100ug/mL carbenicillin, using a Q-Fil automated machine, and inoculated from a corresponding glycerol-stock master plate using a metal 96-pronged “frogger” that was ethanol sterilized. These plates were shaken at 37°C/200rpm overnight, in order to standardize the amount of bacteria in each well. The next day, 100uL of fresh LB containing carbenicillin was added to each well, and these plates were shaken for two hours at 37°C/175rpm. Then 50uL of pre-warmed fresh media containing carbenicillin and 5mM IPTG was added, such that the final concentration of IPTG in each well was 1mM, and these plates were then shaken for 30 minutes at 37°C/150rpm.

Next, plates were spun-down for 15 minutes at 3500rpm/4°C in a swinging bucket centrifuge, to pellet the bacteria. The supernatant was removed from all wells using a multi-channel aspirator, being careful to not disturb the pellet. Strains to be used were egg-prepped

the previous day, and hatched overnight while rocking at 20°C in M9. L1 worms in S basal liquid media containing carbenicillin and IPTG were added directly to the freshly pelleted bacteria, such that each well contained 15uL and ~25 worms.

These plates were surrounded with moist paper towels and grown at 25°C. Each was vented with fresh air, next to a flame, at 24 hours post-plating. At 40-44 hours post-plating, when the worms were at the W-stage of L4, 15uL of M9 containing 50ug/mL kanamycin (final concentration of 25ug/mL) was added to halt bacterial growth, and the plates were then grown at 20°C. For germline(+) worms, this 15uL of M9 also contained 200uM FUdR (final concentration of 100uM), to halt overgrowth of the progeny.

Genome-wide RNAi screens:

Aringer Library Replication

Before beginning the RNAi screens, it was determined that our laboratory copy of the Aringer Library of *C. elegans* RNAi clones was from ~2003, meaning that it had many wells that would no longer grow and many wells with cross-contamination. In order to perform the best screens possible, two fresh sets of the Aringer Library were made from our original 96-well master set. To do this, 96-well clear-well plates were filled with 100uL of LB containing 100ug/mL carbenicillin and 50ug/mL Tetracycline, using a Q-Fil automated machine, and inoculated from the corresponding glycerol-stock master plate using a fresh, sterile, disposable 96-pronged “frogger”. These plates were grown overnight, unshaken, at 37°C. The next day, one set of plates had 100uL of 50% glycerol mixed into each well and was covered with foil seals to make a “picking” set. The other set had 100uL of 30% glycerol mixed into each well and

was covered with plastic seals to make a “screening” set. Both were then frozen at -80°C. The “screening” set was used for the initial whole-genome wide screens, and the “picking” set was used in the following validation steps.

Initial round of screening

For both genome-wide RNAi screens, worms were seeded in liquid culture as described above. At 68-74 hours post-seeding, plates were scanned by eye for changes in GFP fluorescence, using a Leica MZ16F fluorescent stereomicroscope. In the screen for negative regulators, wells containing worms with brighter fluorescence were recorded. In the screen for positive regulators, wells containing worms with dimmer fluorescence were recorded. All 19000+ clones in the library were evaluated for both screens.

Validation of Hits

For all preliminary hits, a set of validation plates were made as follows. The original identified clone was picked from the RNAi library and streaked onto a Luria agar plate containing 100ug/mL carbenicillin. Two individual colonies from each strain were then picked into two of the internal 60 wells of a 96-well plate, which contained 100uL of LB and 100ug/mL carbenicillin and 50ug/mL tetracycline. The outer 36 wells of these plates (the edges) were inoculated with empty vector RNAi. These plates were then grown overnight, not shaking, at 37°C. The next day they were replica plated to produce working sets. Then 100uL of 50% glycerol was mixed into each well, the plates were sealed with foil seals, and they were frozen and stored as a master set at -80°C. The next day the working sets had 100uL of 30% glycerol added, were sealed with plastic seals and were frozen and stored at -80°C. Using these new plates, the effect each clone had on *Psod-3::gfp* expression was assayed three times, in the

exact same way as the original screen. Only clones that passed all three rounds were labeled as validated hits. The pairs of wells from each preliminary hit were compared, and only the best and most consistent from each was chosen to move forward with for sequencing.

Sequencing of Hits

For all validated hits, a set of sequencing plates was made as described above, except that now the clones were picked directly from the frozen master copy of the validation plates into the internal 60 wells of new 96-well sequencing plates (without a Luria agar intermediate step). This final set of plates was then replica plated into deep-well 96-well plates, grown overnight, sealed and sent for sequencing by Elim Biopharmaceuticals using the M13F primer. Sequences for all wells were blasted using Wormbase to determine their corresponding gene.

Characterization of RNAi Screen Hits:

Further characterization of all hits was performed in liquid culture as before, this time however using additional worm strains to measure other markers of germline-less longevity, specific genetic dependencies, and tissue specificity of action. The only difference in the methodology, compared to the screening/validation rounds, was that visualization was now performed using a Kramer FBS10 fluorescent stereomicroscope, which has enhanced visibility for liquid culture. This allowed us to pick-up more subtle differences between the hits (as opposed to the blunt “yes” or “no” criteria used in the initial round of screening). All metrics assessed were given a qualitative score, and subjected to at least three independent rounds of measurement. The results of these rounds of testing were combined to form an average score for each hit, for that particular metric.

DAF-16, SKN-1 and MitoUPR activity

All hits were assayed three or four times for their ability to impact DAF-16, SKN-1 and MitoUPR activity, using the *Psod-3::gfp*, *Pgst-4::gfp* and *Phsp-6::gfp* reporters, respectively. The hits were scored on a qualitative scale from 0 to 3, with 0 meaning no change from control, and 3 meaning complete change from control. For the hits from the Screen for Negative Effecters, each marker was crossed into an *rrf-1(-)* background, and a score above zero meant that the RNAi clone induced expression. For the hits from the Screen for Positive Effecters, each marker was crossed into a *glp-1(ts)* background, and a score above zero meant that the RNAi clone inhibited expression. It should be noted that the *Pgst-4::gfp* marker was the strongest in general, and the *Phsp-6::gfp* was the weakest.

DAF-16 dependency

For the Screen for Negative Effecters, all hits were assayed three times for their ability to induce the *Psod-3::gfp* reporter in a *rrf-1(-) daf-16(-)* background. If a hit still turned on the reporter in this null background, then it was considered to be working in a *daf-16*-independent manner. If a hit no longer could turn on the reporter, however, it was considered to work in a *daf-16*-dependent manner.

Fertility

For the Screen for Negative Effecters, all hits were assayed four times for their ability to impact the fertility of *rrf-1(-)* worms. The hits were scored on a qualitative scale from 0 to 3 as follows: 0 = infertile (no eggs or progeny), 1 = low fertility (few eggs or progeny), 2 = fully fertile but dead eggs, 3 = fully fertile and viable progeny. Unlike for the fluorescent markers, this was done in clear-well 96-well plates, and was visualized under transmitted white light.

Health

For the Screen for Positive Effectors, all hits were assayed three times for their impact on the health of germline-less worms. The hits were scored on a qualitative scale from 0 to 3 as follows: 0 = larval arrest, 1 = very sick, 2 = pale or small, 3 = superficially normal. This assessment was done in clear-well plates, as fluorescence was not needed. This was done in clear well 96-well plates, and was visualized under transmitted white light.

Tissue autonomy

The two tissues of interest in this study are the intestine and germline. Thus, we wanted to determine the contribution that knockdown in each individual tissue has to the change in intestinal *Psod-3::gfp* expression.

For the hits from the Screen for Negative Effectors, we knew that the clones had to be working in either the intestine or germline, as these are the only tissues that perform RNAi in *rrf-1(-)* single mutants. To distinguish between these two tissues, we performed the same analyses in *rrf-1(-) ppw-1(-)* double mutants. PPW-1 is a PIWI domain-containing Argonaute protein needed for efficient germline RNAi. Therefore, *rrf-1(-) ppw-1(-)* double mutants only perform RNAi in the intestine, and do so at the same strength as *rrf-1(-)* single mutants (i.e. ~50% of wild-type capacity). Hits that still had an effect in the double mutant were considered to be working tissue autonomously in the intestine, whereas those that no longer had an effect in the presence of the *ppw-1(-)* mutation were considered to be working tissue-nonautonomously in the germline.

For hits from the Screen for Positive Effectors, we knew that the clones could be working in any tissue except the germline, as this tissue is absent in *glp-1(ts)* single mutants (at

the growth temperatures we used). To test the contribution of the intestine, we performed the same analyses in *rrf-1(-); glp-1(ts)* double mutants, which will only perform RNAi in the intestine, at ~50% of wild-type capacity, when raised at the restrictive temperature. Hits that still had an effect in the double mutant were considered to be working tissue autonomously in the intestine, whereas those that no longer had an effect in the presence of the *rrf-1(-)* mutation were considered to be likely working tissue non-autonomously in another part of the worm. However, it is important to note that these latter hits may actually still be working in the intestine, but are not reaching their critical threshold for knockdown due to the decreased RNAi strength in *rrf-1(-)* mutants.

Analysis of Gene Ontology (GO) Enrichment:

The lists of hits from both screens were independently subjected to analysis for GO term enrichment. This was performed using the freely available Gene Ontology enRICHment anaLYsis and visualIZAtion tool (GORilla) [<http://cbl-gorilla.cs.technion.ac.il>] (69-70). Specifically, each list of screen hits was compared as an unranked target list against an unranked background list of the 19000+ genes covered in the Aringer Library. All three types of ontology terms (process, function and component) were included in the analysis. The visualization functions of this program were not especially pertinent to our study, and were not used. GO term trimming was then performed on the output from GORilla, using the freely available REduce and VIualize Gene Ontology tool (REVIGO) [<http://revigo.irb.hr>] (71). A stringency of C= 0.5 was used to produce a “small” list of semantically diverse terms.

Quantification of Fluorescent Markers:

For certain markers and RNAi clones of interest, we further characterized their interactions through fluorescence quantification. For these analyses, worms were grown on solid culture RNAi, as described above, with five 6cm plates of worms being raised for each strain on each RNAi clone. At the border between Day's 1 and 2 of adulthood, 15-20 worms from each plate were picked at random onto new 3.5cm NG plates, each containing a 25uL drop of 10mM levamisole (dissolved in M9 buffer). The worms were allowed to soak in the levamisole for 15 minutes, before 10 worms per plate were randomly selected to be packed together, such that all worms in a pack were oriented in the same direction.

These packs of 10 worms were then imaged on the Leica MZ16F fluorescent stereomicroscope using the Leica Suite Application version 2.0. Each pack was imaged at 65X total magnification, first under regular transmitted white light, and then using a short pass GFP filter. The settings used were: exposure = 203.4ms, gain = 4.0x, gamma = 1.01, and full spectrum pass. Images were then analyzed using the ImageJ application as follows: the transmitted light and fluorescent images were put into a stack, the pack of 10 worms was then outlined in the transmitted light image, this outline was then transferred to the fluorescent image and the pixel intensity and area were measured, and then the outline was inverted and the background pixel intensity and area were measured.

This data was then exported to Microsoft Excel, where the average fluorescence of the background was subtracted from the average fluorescence of the worms. The differences obtained from all five plates were then averaged, and standard deviations were determined. These averages were then graphed in Excel as a Column Chart, using the standard deviations as

error bars. Students T-tests were performed to statistically compare between control and experimental RNAi conditions (most often using one-tailed tests, as our hypothesis was always that the RNAi clones decrease the marker's expression). The results of these statistical analyses were also reflected on the graphed results, using a horizontal bar above two columns to denote the comparison, and the following values above that bar to denote significance: N.S. = $p > 0.05$, * = $p < 0.05$, ** = $p < 0.01$.

Lifespans:

Lifespan analysis was performed on worms using either solid culture RNAi, as described above, or solid culture with OP50. In either case, bleached L1 arrested worms were spotted onto five plates per condition, and were grown at either 20°C or 25°C (depending on the need for genetic germline ablation) until the W-stage of L4. Then 25 worms were randomly chosen to transfer onto fresh plates, and then placed at 20°C for the remainder of their lifespan. These worms were transferred every other day onto new fresh plates through day 10 or 12 of adulthood, and then were transferred once more onto fresh plates at day 20 or 22, respectively. Each plate was scored for the number of dead worms every other day. A worm was considered dead if it did not move 1) independently, 2) in response to light touch on the tail, 3) in response to light touch on the head, or 4) in response to strong touch on the head. Worms were censored from analysis if they bagged (internal hatching of progeny), exploded (intestinal protrusion through the vulva), or were missing (crawled off the plate).

Lifespans were graphed using Kaplan-Meyer death curves, and analyzed for their mean lifespans. The difference in mean lifespan between control and experimental conditions were determined and reported.

Co-Immunoprecipitations:

Preparation of worm samples

For each round of KRI-1 Co-IPs, 600,000 worms per condition were grown up on 10cm plates containing 20X concentrated OP50 (and ~4000 worms per plate). These worms were spotted onto the plates as arrested L1's, and grown at 25°C for 40 hours (venting the plates near a flame at the 24hour mark). These now W-stage L4 worms were vented again and moved to 20°C for 24 more hours. Worms were then harvested from the plates using M9 buffer, gravity settled to remove the majority of eggs (if present), washed twice with M9 buffer, washed twice with KRI-1 Co-IP lysis buffer minus detergent, transferred to a 1.5mL Eppendorf tube and snap frozen using liquid nitrogen. These vials were stored at -80oC.

KRI-1 pulldowns

Lysis buffer without detergent containing 5X protease and phosphatase inhibitors was added to each tube at approximately 1/5th the volume of the worm pellet (Roche's cOmplete Protease Inhibitor Cocktail Tablets and PhosSTOP Phosphatase Inhibitor Cocktail Tablets). The pellets were then thawed at room temperature using a thermomixer at max speed. **All further Co-IP steps were done on ice or at 4°C.** For each strain, 1.5mL of worm pellets were pooled into 7mL screw cap vials containing 1.5mL of 0.7mm zirconia beads, and then 3mL of lysis buffer without detergent containing 2x inhibitors was added. To lyse the cells, the tubes were

subjected to four rounds of bead-beating, 20 seconds each, with a 20 second break in between each round. The detergent NP-40 was then added to 0.5%, and the samples were rocked for 15 minutes to allow full lysis and organelle disruption.

Afterwards, the tubes were briefly spun down in a clinical centrifuge to settle the beads, and the supernatant was then transferred to several 1.5mL tubes. These tubes were spun at 14,000rpm for 15 minutes, and the clearest portions of this supernatant were transferred to fresh 1.5mL tubes. The cloudy portions (right below the obvious lipid layer), were transferred to new 1.5mL tubes as well, and the insoluble pellets and lipid layer were discarded. These tubes were then spun again as before, and the twice cleared portions were transferred to a 5mL collection tube. The less clear portions were again transferred to new 1.5mL tubes, and the process was repeated until all clear portions had been obtained and transfer to the collection tube. 200uL of pre-washed, unconjugated, magnetic agarose beads were then added, and the tubes were rocked to pre-clear the samples. After 15 minutes, the beads were sequestered using Life Technology's DynaMag-5 magnet system, and the supernatant was transferred to a new tube. This pre-clearing procedure was also repeated a second time. The protein concentration in each tube was then determined using the Pierce BCA Assay kit, and the samples from each strain were divided into two tubes each, standardizing the amount of protein across all tubes (based on the strain sample that had the lower amount of protein). Equal volumes across the tubes was achieved by adding extra lysis buffer where needed. A small volume from each tube was kept for Western Blotting.

For the Co-IPs, two types of antibody-coupled magnetic agarose beads were used: Sigma's M2 anti-FLAG (mouse IgG1) for the experimental sample and MBL's anti-HA (mouse

IgG1) for the control sample. These beads were washed once with lysis buffer, resuspended in 1mL of Pierce's Protein Free Blocking Reagent, and rocked for 30 minutes. The beads were then sequestered using the magnet and washed once with lysis buffer. 50uL of beads was added to each sample tube, and these were rocked for 2 hours. The beads were then washed 4X with lysis buffer and twice with low salt buffer (10mM Tris, 100mM NaCl, pH7.4), using the magnet at each step to ensure little to no loss. The beads from each condition were separated into two tubes each, with 25% being dedicate to Western Blotting and 75% being dedicated to mass spec. The bound proteins were then eluted using 2X LDS sample buffer, boiling at 95°C for 10 minutes (20uL of LDF for the WB sample, and 40uL of LDS for the mass spec sample).

Mass spectrometry was performed at the University of Dundee's Fingerprints Proteomics Facility. This service included in-gel trypsin digestion, peptide extraction, mass spectrometry analysis using an nLC-MS/MS System (RSLCnano UHPLC coupled to LTQ Orbitrap Velos Pro). Data analysis was performed via Proteome Discoverer, using Mascot as the search engine. We then analysed the lists of proteins and peptide spectral counts ourselves. We removed proteins from our list of experimental interactors if they were also present in the control IP (unless they were significantly enriched in the experimental condition).

Western Blotting

For each condition, samples of the total worm lysates (0.25-0.5% of input) and eluted proteins (25%) were subjected to Western Blotting. The proteins were run out on a 4-12% Bis-Tris gel (Invitrogen's pre-cast NuPage system) alongside Bio-Rad's Precision Plus Protein Standard. The samples were then transferred to Millipore's Immobilon-P PVDF membrane using a wet transfer protocol with MOPS buffer (NuPage system). The membrane was rocked in

blocking buffer (5% milk in TBST), for 1 hour at room temperature. Primary antibodies were then added to the same blocking buffer and incubated with the membrane overnight at 4°C with gentle agitation (Cell Signaling's rabbit anti-DYKDDDDK [2386] at 1:1000 and AbCam's mouse anti-actin [AB3280] at 1:2000). The membrane was then washed 4X with TBST for 5 minutes each. Secondary antibodies were then added to blocking buffer and incubated with the membrane for 1 hour at room temperature (Cell Signaling's goat anti-mouse DyLight 680 [5470] and goat anti-Rabbit DyLight800 [5151], both at 1:2000). The membrane was then washed 4X with TBST, 5 minutes each time. Visualization of the membrane was performed on a LICOR Odyssey scanner, reading both the 700nm and 800nm channels simultaneously.

SCIENTIFIC CONTRIBUTORS

Thank you to Cynthia Kenyon, and the entire Kenyon Lab, for all of the ideas, suggestions and experimental support. Also thank you to Hao Li, and the entire Li Lab, for adopting me and giving me a place to finish my research. Special thanks to Hildegard Mack, who was my collaborator for all of the biochemistry experiments performed here. Thank you to Peter Chisnell for injecting the FLAG-tagged KRI-1 constructs and thank you to Nina Riehs for maintaining a shared strain, plasmid, bacteria and reagent library with me. Thank you to Howard Baylis for sending me RNAi bacteria against *itr-1* and all of the PLCs, as well as for his advice on this signaling pathway. Multiple strains were provided by the Caenorhabditis Genetics Consortium at the University of Michigan. Wormbase was an invaluable resource used for aligning all sequencing data, gathering information regarding genes and proteins found in my screens, and obtaining genetic information for mutant alleles. Funding was provided by an NIH training grant to the UCSF MSTP.

CITATIONS

- 1) Durieux, J., Wolff, S., and Dillion, A. (2011) The Cell-Non-Autonomous Nature of Electron Transport Chain-Mediated Longevity. *Cell*, 144: 79-91.
- 2) Bishop, N.A., and Guarente, L. (2007) Two neurons mediate diet-restriction-induced longevity in *C. elegans*. *Nature*, 447: 545-549.
- 3) Hwangbo, D.S., Gersham, B., Tu, M-P., Palmer, M., and Tatar, M. (2004) Drosophila dFOXO controls lifespan and regulates insulin signaling in brain and fat body. *Nature*, 429: 562-566.
- 4) Kappeler, L., De Magalhaes Filho, C., Dupont, J., Leneuve, P., Périn, L., Loudes, C., Blaise, A., Klein, R., Epelbaum, J., Le Bouc, Y., and Holzenberger, M. (2008) Brain IGF-1 receptors control mammalian growth and lifespan through a neuroendocrine mechanism. *PLoS Biol.* 6(10):e254
- 5) Hsin, H., and Kenyon, C. (1999) Signals from the reproductive system regulate the lifespan of *C. elegans*. *Nature*, 399: 362-366.
- 6) Patel, M.N., Knight, C.G., Karageorgi, C., and Leroi, A.M. (2002) Evolution of germ-line signals that regulate growth and aging in nematodes. *Proc. Natl. Acad. Sci.* 99: 769-774.
- 7) Wang, M.C., O'Rourke, E.J., and Ruvkun, G. (2008) Fat metabolism links germline stem cells and longevity in *C. elegans*. *Science*, 322: 957-60.
- 8) Yamawaki, T.M., Arantes-Oliveira, N., Berman, J.R., Zhang, P., and Kenyon, C. (2008) Distinct activities of the germline and somatic reproductive tissues in the regulation of *Caenorhabditis elegans*' lifespan. *Genetics*, 178: 513-26.
- 9) Flatt, T. Min, K.J., D'Alterio, C., Villa-Cuesta, E., Cumbers, J. Lehmann, R., Jones, D.L., and Tatar, M. (2008) Drosophila germ-line modulation of insulin signaling and lifespan. *Proc. Natl. Acad. Sci.* 105: 6368-73.
- 10) Hatle, J.D., Paterson, C.S., Jawaid, I., Lentz, C., Wells, S.M., and Fronstin, R.B. (2008). Protein accumulation underlying lifespan extension via ovariectomy in grasshoppers is consistent with the disposable soma hypothesis but is not due to dietary restriction. *Exp Gerontol.* 43: 900-8.
- 11) Drori, D., and Folman, Y. (1976) Environmental effects on longevity in the male rat: Exercise, mating, castration and restricted feeding. *Exp Gerontol.* 11: 25-32.
- 12) Min, K-J., Lee, C-K., Park, H-N. (2012) The lifespan of Korean eunuchs. *Curr Biol.* 22: R792-3.
- 13) Kenyon, C.J., Chang, Gensch, E., Rudner, J., and Tabtiang, R. (1993) A *C. elegans* mutant that lives twice as long as wild type. *Nature* 366: 461-464.
- 14) Arantes-Oliveira, N. Apfeld, J., Dillin, A., and Kenyon, C. (2001) Regulation of lifespan by germline stem cells in *Caenorhabditis elegans*. *Science*, 295: 502-505.
- 15) Lapierre, L.R., Gelino, S., Meléndez, A., and Hansen, M. (2012) Autophagy and lipid metabolism coordinately modulate life span in germline-less *C. elegans*. *Curr Biol.* 21: 1507-14.
- 16) Goudeau, J, Bellemin, S, Toselli-Mollereau, E, Shamalnasab, M, Chen, Y, and Aguilaniu H. (2011) Fatty acid desaturation links germ cell loss to longevity through NHR-80/HNF4 in *C. elegans*. *PLoS Biol.* 9: e1000599

- 17) Shen, Y, Wollam, J, Magner, D, Karalay, O, Antebi, A. (2012) A steroid receptor-microRNA switch regulates life span in response to signals from the gonad. *Science*, 338: 1472-6.
- 18) Boulas, K., and Horvitz, H.R. (2012) The *C. elegans* microRNA *mir-71* acts in neurons to promote germline-mediated longevity through regulation of DAF-16/FOXO. *Cell Metab.* 15: 439-50.
- 19) Yamawaki, TM, Berman, JR, Suchanek-Kavipurapu, M, McCormick, M, Gaglia, MM, Lee, SJ, and Kenyon, C. (2010) The somatic reproductive tissues of *C. elegans* promote longevity through steroid hormone signaling. *PLoS Biol.* 10.1371/journal.pbio.1000468.
- 20) Ghazi, A., Henis-Korenblit, S., and Kenyon, C. (2009) A transcription elongation factor that links signals from the reproductive system to lifespan extension in *Caenorhabditis elegans*. *PLoS Genet.* 5: e1000639.
- 21) Berman, J.R., and Kenyon, C. (2006) Germ-cell loss extends *C. elegans* life span through regulation of DAF-16 by *kri-1* and lipophilic-hormone signaling. *Cell*, 124:1055-68.
- 22) Kumsta, C., and Hansen, M. (2012) *C. elegans rrf-1* mutations maintain RNAi efficiency in the soma in addition to the germline. *PLoS One* 7: e35428
- 23) Van Voorhies, W.A. (1992) Production of sperm reduces nematode lifespan. *Nature*, 360: 456-458.
- 24) Gems, D., and Riddle, D.L. (1996) Longevity in *Caenorhabditis elegans* reduced by mating but not gamete production. *Nature*, 379: 723-725.
- 25) Johnson T.E., Cypser J., de Castro E., de Castro S., Henderson S., Murakami S., Rikke B., Tedesco P., Link C. (2000) Gerontogenes mediate health and longevity in nematodes through increasing resistance to environmental toxins and stressors. *Exp Gerontol*, 35(6-7): 687-694.
- 26) Cypser, J.R., and Johnson, T.E. (1999) The *spe-10* mutant has longer life and increased stress resistance. *Neurobiol Aging*, 5: 503-12.
- 27) DePina A.S., Iser W.B., Park S.S., Maudsley S., Wilson M.A., Wolkow C.A. (2011) Regulation of *Caenorhabditis elegans* vitellogenesis by DAF-2/IIS through separable transcriptional and posttranscriptional mechanisms. *BMC Physiol*, 11:11.
- 28) Fisher A.L., Lithgow G.J. (2006) The nuclear hormone receptor DAF-12 has opposing effects on *Caenorhabditis elegans* lifespan and regulates genes repressed in multiple long-lived worms. *Aging Cell*, 5(2):127-38.
- 29) Riedel C.G., Downen R.H., Lourenco G.F., Kirienko N.V., Heimbucher T., West J.A., Bowman S.K., Kingston R.E., Dillin A., Asara J.M., Ruvkun G. (2013) DAF-16 employs the chromatin remodeller SWI/SNF to promote stress resistance and longevity. *Nat Cell Biol*, 15(5): 491-501.
- 30) Lin K., Hsin H., Libina N., Kenyon C. (2001) Regulation of the *Caenorhabditis elegans* longevity protein DAF-16 by insulin/IGF-1 and germline signaling. *Nat Genet.* 28(2): 139-45.
- 31) Lapierre L.R., De Magalhaes Filho D., McQuary P.R., Chu C., Visvikis O., Chang J.T., Gelino S., Ong B., Davis A.E., Irazoqui J.E., Dillin A., Hansen M. (2013) The TFEB orthologue HLH-30 regulates autophagy and modulates longevity in *Caenorhabditis elegans*.

- 32) Ratnappan R., Amrit F.R.G., Chen S., Gill H., Holden K., Ward J., Yamamoto K.R., Olsen C.P., Ghazi A. (2014) Germline signals deploy NHR-49 to modulate fatty-acid B-oxidation and desaturation in somatic tissues of *C. elegans*. *PLoS Genet.* 10(12): 1-20.
- 33) Steinbaugh M.J., Narasimhan S.D., Robida-Stubbes S., Mazzeo L.E.M., Dreyfuss J.M., Hourihan J.M., Raghavan P., Operaña T.N., Esmailie R., Blackwell T.K. (2015) Lipid-mediated regulation of SKN-1/Nrf in response to germ cell absence. *eLife*, 10.7554/eLife.07836.
- 34) Riedel C.G., Downen R.H., Lourenco G.F., Kirienko N.V., Heimbucher T., West J.A., Bowman S.K., Kingston R.E., Dillin A., Asara J.M., Ruvkun G. (2013) DAF-16 employs the chromatin remodeller SWI/SNF to promote stress resistance and longevity. *Nat Cell Bio.* 15(5):491-501.
- 35) Heimbucher T., Liu Z., Bossard C., McCloskey R., Carrano A.C., Riedel C.G., Tanasa B., Klammt C., Fonslow B.R., Riera C.E., Lillemeier B.F., Kempfues K., Yates III J.R., O'Shea C., Hunter T., Dillin A. (2015) The Deubiquitylase MATH-33 Controls DAF-16 Stability and Function in Metabolism and Longevity. *Cell Metab.* 22: 151-163.
- 36) Amrit F.R.G., Steenkiste E.M., Ratnappan R., Chen S., McClendon T.B., Kostka D., Yanowitz J., Olsen C.P., Ghazi A. (2016) DAF-16 and TCER-1 Facilitate Adaptation to Germline Loss by Restoring Lipid Homeostasis and Repressing Reproductive Physiology in *C. elegans*. *PLoS Genet.* 12(2): e1005788.
- 37) Li T., Liu W., Lu S., Zhang Y., Jia L., Chen J., Li X., Lei X., Dong M. (2015) No Significant Increase in the D4- and D7-Dafachronic Acid Concentration in the Long-Lived *glp-1* Mutant, nor in the Mutants Defective in Dauer Formation. *G3*, 5: 1473-1479.
- 38) Baylis H.A., Vázquez-Manrique R.P. (2012) Genetic analysis of IP3 and calcium signaling pathways in *C. elegans*. *Biochim et Biophys Acta*, 1820: 1253-1268.
- 39) Walker D.S., Gower N.J.D., Ly S., Bradley G.L., Baylis H.A. (2002) Regulated disruption of inositol 1,4,5-triphosphate signaling in *Caenorhabditis elegans* reveals new functions in feeding and embryogenesis. *Mol Bio of Cell*, 13: 1329-1337.
- 40) Gower, N.J., Walker D.S., Baylis, H.A. (2005) Inositol 1,4,5-triphosphate signaling regulates mating behavior in *Caenorhabditis elegans* males. *Mol Bio of Cell*, 16: 3978-3986.
- 41) Walker D.S., Ly S., Gower N.J.D., Baylis H.A. (2004) IRI-1, a LIN-15B Homologue, Interacts with Inositol- 1,4,5-Triphosphate Receptors and Regulates Gonadogenesis, Defecation, and Pharyngeal Pumping in *Caenorhabditis elegans*. *Mol Bio of Cell*, 15: 3073-3082.
- 42) Walker, D.S., Vázquez-Manrique R.P., Gower, N.J.D., Gregory E., Schafer W.R., Baylis H.A. (2009) Inositol 1,4,5-triphosphate signaling regulates the avoidance response to nose touch in *Caenorhabditis elegans*. *PLoS Genet.* 5(9): e1000636.
- 43) Silva M.C., Amaral M.D., Morimoto R.I. (2013) Neuronal reprogramming of protein homeostasis by calcium-dependent regulation of the heat shock response. *PLoS Genet.* 9(8): e1003711.
- 44) Xu K., Tavernarakis N., Driscoll M. (2001) Necrotic Cell Death in *C. elegans* Requires the Function of Calreticulin and Regulators of Ca²⁺ Release from the Endoplasmic Reticulum. *Neuron*, 31: 957-971.
- 45) Cobrun C., Allman E., Mahanti P., Benedetto A., Cabreiro F., Pincus Z., Matthijsse F., Araiz C., Mandel A., Vlachos M., Edwards S., Fischer G., Davidson A., Pryor R.E., Stevens A., Slack F.J., Tavernarakis N., Braeckman B.P., Schroeder F.C., Nehrke K., Gems D. (2013)

- Anthranilate Fluorescence Marks a Calcium-Propagated Necrotic Wave That Promotes Organismal Death in *C. elegans*. PLoS Bio, 11(7): e1001613
- 46) Nagy A.I., Vázquez-Manrique R.P., Lopez M., Christov C.P., Sequedo M.D., Herzog M., Herlihy A.E., Bodak M., Gatsi R., Baylis H.A. (2015) IP3 signaling regulates exogenous RNAi in *Caenorhabditis elegans*. EMBO reports, 16(3): 341-350.
 - 47) Xing J., Yan X., Estevez A., Strange K. (2008) Highly Ca²⁺-selective TRPM Channels regulate IP3-dependent oscillatory Ca²⁺ signaling in the *C. elegans* Intestine. J Gen Physiol. 131(3): 245-255.
 - 48) Nehrke N., Denton J., Mowrey W. (2007) Intestinal Ca²⁺ wave dynamics in freely moving *C. elegans* coordinate execution of a rhythmic motor program. Am J Physiol Cell Physiol, 294: C333-C344.
 - 49) Espelt M.V., Estevez A.Y., Yin X., Strange K. (2005) Oscillatory Ca²⁺ Signaling in the Isolated *Caenorhabditis elegans* Intestine: Role of the Inositol-1,4,5-trisphosphate Receptor and Phospholipases C B and γ . J Gen Physiol. 126(4) 379-392.
 - 50) Kwan, C.S.M., Vázquez-Manrique R.P., Ly S., Goyal K., Baylis H.A. (2008) TRPM channels are required for rhythmicity in the ultradian defecation rhythm of *C. elegans*. BMC Physiol. 8:11.
 - 51) Iwasaki K., Teramoto T. (2006) Intestinal calcium waves coordinate a behavioral motor program in *C. elegans*. Cell Calcium, 40: 319-327.
 - 52) Gower N.J.D., Temple G.R., Schein J.E., Marra M., Walker D.S., Baylis H.A. (2001) Dissection of the Promoter Region of the Inositol 1,4,5-trisphosphate Receptor Gene, *itr-1*, in *C. elegans*: A Molecular Basis for Cell-specific Expression of IP3R Isoforms. J Mol Biol. 306: 145-157.
 - 53) Walker D.S., Ly S., Lockwood K.C., Baylis H.A. (2002) A Direct Interaction between IP3 Receptors and Myosin II Regulates IP3 Signaling in *C. elegans*. Curr Biol. 12: 951-956.
 - 54) Iwasa H., Yu S., Xue J., Driscoll M. (2010) Novel EGF pathway regulators modulate *C. elegans* healthspan and lifespan via EGF receptor, PLC- γ and IP3R activation. Aging Cell, 9: 490-505.
 - 55) Ito S., Greiss S., Gartner A., Derry W.B. (2010) Cell-nonautonomous regulation of *C. elegans* germ cell death by *kri-1*. Curr Biol. 20(4): 333-338.
 - 56) Morthorst T.H., Olsen, A. (2013) Cell-nonautonomous inhibition of radiation-induced apoptosis by dynein light chain 1 in *Caenorhabditis elegans*. Cell Death and Disease, 4: e799.
 - 57) Tao L., Xie Q., Ding Y., Li S., Peng S., Zhang Y., Tan D., Yuan Z., Dong M. (2013) CAMKII and Calcineurin regulate the lifespan of *Caenorhabditis elegans* through the FOXO transcription factor DAF-16. eLife, 10.7754/eLife.00518.
 - 58) Zhu H., Shen H., Sewell A.K., Kniazeva M., Han M. (2013) A novel sphingolipid-TORC1 pathway critically promotes post-embryonic development in *Caenorhabditis elegans*. eLife, 10.7554/eLife.00429.
 - 59) Schieber M., Chandel N.S. (2014) TOR signaling couples oxygen sensing to lifespan in *C. elegans*. Cell Reports, 9: 9-15.
 - 60) Timmons L., Court D.L., Fire A. (2001) Ingestion of bacterially expressed dsRNAs can produce specific and potent genetic interference in *Caenorhabditis elegans*. Gene, 263: 103-112.

- 61) Choe K.P., Przybsz A.J., Strange K. (2009) The WD40 repeat protein WDR-23 functions with the CUL4/DDB1 ubiquitin ligase to regulate nuclear abundance and activity of SKN-1 in *Caenorhabditis elegans*. *Mol Cell Biol.* 29(10): 2704-15.
- 62) Wang J., Robida-Stubbes S., Tullet J.M., Rual J.F., Vidal M., Blackwell T.K. (2010) RNAi screening implicates a SKN-1-dependent transcriptional response in stress resistance and longevity deriving from translation inhibition. *PLoS Genet.* 6(8): e1001048.
- 63) Crook-McMahon H.M., Oláhová M., Button E.L., Winter J.J., Veal E.A. (2014) Genome-wide screening identifies new genes required for stress-induced phase 2 detoxification gene expression in animals. *BMC Biol.* 12: 64.
- 64) Runkel E.D., Liu S., Baumeister R., Schulze E. (2013) Surveillance-activated defenses block the ROS-induced mitochondrial unfolded protein response. *PLoS Genet.* 9(3): e1003346.
- 65) Bennett C.F., Vander Wende H., Simko M., Klum S., Barfield S. Choi H., Pineda V.V., Kaeberlein M. (2014) Activation of the mitochondrial unfolded protein response does not predict longevity in *Caenorhabditis elegans*. *Nat Commun.* 5: 3483.
- 66) Liu W., Draheim K.M., Zhang R., Calderwood D.A., Boggon T.J. (2013) Mechanism for KRIT1 release of ICAP1-mediated suppression of integrin activation. *Mol Cell*, 49(4): 719-729.
- 67) Burnett C., Valentini S., Cabreiro F., Goss M., Somogyvári M., Piper M.D., Hoddinott M., Sutphin G.L., Leko V., McElwee J.J., Vazquez-Manrique R.P., Orfila A.M., Ackerman D., Au C., Vinti G., Riesen M., Howard K., Neri C., Bedalov A., Kaeberlein M., Soti C., Partridge L., Gems D. (2011) Absence of effects of Sir2 overexpression on lifespan in *C. elegans* and *Drosophila*. *Nature*, 477(7365): 482-485.
- 68) van Haaften G., Vastenhouw N.L., Nollen E.A., Plasterk R.H., Tijsterman M. (2004) Gene interactions in the DNA damage-response pathway identified by genome-wide RNA-interference analysis of synthetic lethality. *PNAS*, 101(35): 12992-12996.
- 69) Eden E., Navon R., Steinfeld I., Lipson D., Yakhini Z. (2009) Gorilla: a tool for the discovery and visualization of enriched GO terms in ranked gene lists. *BMC Bioinform.* 10: 48.
- 70) Eden E., Lipson D., Yagev S. Yakhini Z. (2007) Discovering motifs in ranked lists of DNA sequences. *PLoS Comp Biol.* 3(3) e39.
- 71) Supek F., Bošnjak M., Škunca N., Šmuc T. (2011) REVIGO summarizes and visualizes long lists of gene ontology terms. *PLoS ONE* 6(7): e21800

TABLES

Negative Effecters		Positive Effecters
371	Preliminary Hits	339
234	Validated Hits	170
210	Sequenced Hits (Unique)	149

Table 1. Dual whole-genome RNAi screens unveil many DAF-16 regulators. Both screens initially had a very large number of preliminary hits, yet upon multiple rounds of validation almost half proved to be false positives. Those hits that did pass through three rounds of validation were sequenced. This sequencing revealed that many of the RNAi clones were either duplicates or target the same gene. The number of unique genes identified per screen is reported in the bottom row.

Gene	Function
C23G10.8	Uncharacterized
C37C3.2	translation initiation factor 5 (eIF5)
dlst-1	dihydrolipoamide S-succinyltransferase (E2 component of 2-oxo-glutarate complex)
dyci-1	dynein intermediate chain
dyn-1	dynamin GTPase
emb-5	Spt6 family of RNA polymerase II transcription elongation factors
his-2	H3 histone
ima-3	importin alpha nuclear transport factor
let-526	component of the SWI/SNF complex
let-70	class I E2 ubiquitin conjugating enzyme
let-92	PP2AC, the catalytic subunit of protein phosphatase 2A (PP2A)
mog-5	DEAH helicase
nsf-1	N-ethylmaleimide-sensitive factor
ogdh-1	Oxoglutarate dehydrogenase (E1 component of 2-oxo-glutarate complex)
paa-1	structural subunit of protein phosphatase 2A (PP2A)
pap-1	poly (A) polymerase
rnr-1	large subunit of ribonucleotide reductase
rpb-3	RNA Polymerase II (B) subunit
spg-7	nuclear-encoded mitochondria metalloprotease
spt-5	SPT transcription elongation factor
symk-1	SYMpleKin cleavage and polyadenylation factor
T13H5.4	Splicing factor 3A subunit 3
tars-1	Threonyl Amino-acyl tRNA Synthetase
tbb-2	Beta-tubulin
xrn-2	5'-3' exoribonuclease, required for degradation of levels of mature miRNAs

Table 2. Identity and function of the 25 genes that were found in both genetic screens. These overlapping genes have a diverse set of functions. Interestingly, two members of the 2-oxo-glutarate complex (*dlst-1* and *ogdh-1*) appear in this list, as well as two members of the protein phosphatase 2A complex (*let-92* and *paa-1*).

Top 20 GO Terms for Negative Effectors		log10 p-value
reproduction		-84.94
embryo development		-67.40
developmental process		-56.66
multicellular organismal process		-50.04
→ single organism reproductive process		-31.44
→ endocytosis		-30.69
→ single-organism process		-30.13
→ vesicle-mediated transport		-26.84
reproductive process		-25.88
cellular process		-22.28
single-organism cellular process		-18.17
→ apoptotic process		-17.81
cellular component organization or biogen.		-17.58
→ death		-17.08
establishment of localization		-17.02
translation		-16.60
RNA processing		-13.74
cell migration		-13.72
cellular metabolic process		-13.62
locomotion		-13.4685

Top 20 GO Terms for Positive Effectors		log10 p-value
nematode larval development		-49.25
reproduction		-48.67
developmental process		-42.43
multicellular organismal process		-38.00
locomotion		-32.05
single-organism process		-24.04
→ endocytosis		-17.66
→ reproductive structure development		-16.05
→ vesicle-mediated transport		-15.26
reproductive process		-14.85
localization		-11.76
→ apoptotic process		-10.54
→ cell migration		-10.39
→ death		-10.30
positive regulation of biological process		-9.64
nucleus organization		-9.52
establishment of localization		-9.52
single-organism cellular process		-8.68
cellular component movement		-8.53
cellular process		-8.51

Table 3. Significant overlap in enriched GO Terms between the two screens. GO terms related to reproduction and development are at the top of both lists, though these are pretty broad categories. More interesting are the two term doublets “endocytosis” & “vesicle-mediated transport” and “apoptotic process” & “death”, both of which show up at approximately the same place in each list. Though not shown here, it is also worth noting that “determination of adult lifespan” was also enriched in both the negative regulator screen (log10 P-value = -7.5575), as well as the positive regulator screen (log10 P-value = -3.6904).

Table 4. Characterization of sequence-verified hits from the screen for **negative effectors** of DAF-16 activity. All metrics were analyzed at least three times, each time assigning a qualitative score from 0 to 3, with zero meaning no change and 3 meaning total change from control RNAi. These scores were averaged and are reported below. Note that all strains are in the *rrf-1(-)* background, which only performs RNAi in the germline and intestine.

Main Gene	Fertility	<i>sod-3</i> :: <i>gfp</i>	<i>sod-3</i> in <i>daf-16(-)</i>	<i>sod-3</i> in <i>ppw(-)</i>	<i>gst-4</i> :: <i>gfp</i>	<i>hsp-6</i> :: <i>gfp</i>
E04A4.5	3.00	1.75	0.67	0.00	0.00	1.67
T09B4.9	3.00	1.75	1.00	0.00	0.33	2.33
C16A3.5	3.00	1.50	0.33	0.00	1.00	2.67
F30A10.9	3.00	1.50	1.33	0.00	1.00	0.00
hrp-1	3.00	1.25	0.67	0.00	0.33	0.00
T02H6.11	3.00	1.00	0.00	0.00	0.00	1.67
srpa-68	3.00	1.00	0.00	0.00	0.33	0.00
prp-4	3.00	1.00	0.33	0.00	0.33	0.00
rha-2	3.00	1.00	0.33	0.00	0.67	0.00
nuo-3	3.00	1.00	0.67	0.00	0.67	1.67
dlst-1	3.00	1.00	0.67	0.00	0.67	1.00
nsf-1	3.00	1.00	1.00	0.00	0.00	0.00
cdc-37	3.00	0.75	0.00	0.00	0.00	0.00
rsp-7	3.00	0.75	0.00	0.00	0.00	0.00
pdcd-2	3.00	0.75	0.00	0.00	0.33	0.00
ZK686.2	3.00	0.75	0.00	0.00	0.67	0.00
rpac-19	3.00	0.75	0.00	0.00	0.33	0.00
lpd-6	3.00	0.75	0.00	0.00	0.67	0.33
yars-1	3.00	0.75	0.00	0.00	0.67	1.00
Y67D8A.2	3.00	0.75	0.00	0.00	0.00	0.00
syx-5	3.00	0.75	0.00	0.00	1.00	0.00
syx-5	3.00	0.75	0.00	0.00	0.67	0.00
W07E6.2	3.00	0.75	0.33	0.00	1.00	0.00
snr-4	3.00	0.75	0.33	0.00	0.00	0.00
asg-1	3.00	0.75	0.67	0.00	1.33	0.00
Y82E9BR.3	3.00	0.75	0.67	0.00	0.33	0.00
zfh-2	3.00	0.50	0.00	0.00	0.00	0.00
him-10	3.00	0.50	0.00	0.00	0.00	0.00
F21C10.1	3.00	0.50	0.00	0.00	0.00	0.00
pap-1	3.00	0.50	0.00	0.00	0.33	0.00
C14C10.4	3.00	0.50	0.00	0.00	1.33	1.00
ZK265.6	3.00	0.50	0.33	0.00	0.33	0.00
acr-14	3.00	0.50	0.33	0.00	0.00	0.00
Y82E9BR.3	3.00	0.50	0.33	0.00	0.00	1.00
sym-2	3.00	0.50	0.33	0.00	0.00	0.67
Y82E9BR.3	3.00	0.50	0.67	0.00	0.33	0.00
K08A2.2	3.00	0.25	0.00	0.00	0.00	0.00
C53A5.16	3.00	0.25	0.00	0.00	0.00	0.00
srx-44	3.00	0.25	0.00	0.00	0.00	0.00

M04C3.2	3.00	0.25	0.00	0.00	0.00	0.00
clcc-259	3.00	0.25	0.00	0.00	0.00	0.00
hpk-1	3.00	0.25	0.00	0.00	0.00	0.00
unc-97	3.00	0.25	0.00	0.00	0.00	0.00
R07E3.2	3.00	0.25	0.00	0.00	0.00	0.00
C34E11.2	3.00	0.25	0.00	0.00	0.00	0.00
Y62H9A.5	3.00	0.25	0.00	0.00	0.00	0.00
T08D10.5	3.00	0.25	0.00	0.00	0.00	0.00
srd-41	3.00	0.25	0.00	0.00	0.00	0.00
pat-9	3.00	0.25	0.00	0.00	0.00	0.00
Y66H1A.4	3.00	0.25	0.67	0.00	0.00	0.00
ogdh-1	3.00	0.25	0.67	0.00	0.33	0.67
unc-45	2.75	1.50	0.00	0.00	1.00	0.33
gtbp-1	2.75	1.50	0.33	0.00	1.67	0.00
ran-3	2.75	1.00	0.00	0.00	0.33	0.00
ppp-1	2.75	0.75	0.33	0.25	0.33	0.00
srd-60	2.75	0.50	0.00	0.00	0.00	0.00
wars-1	2.50	1.75	0.33	0.00	1.33	0.00
tag-151	2.50	1.50	0.67	0.25	0.33	0.00
snr-5	2.50	1.25	0.00	0.00	0.67	0.00
W01D2.1	2.50	1.25	0.33	0.00	1.00	0.00
W01D2.1	2.50	1.25	0.67	0.00	0.33	0.00
nsf-1	2.50	1.25	1.00	0.00	0.33	0.00
rpl-43	2.50	1.00	0.33	0.00	0.33	0.00
cpf-2	2.50	1.00	0.33	0.00	1.00	0.00
xrn-2	2.50	0.75	0.00	0.00	0.33	0.00
C23G10.8	2.50	0.75	0.00	0.00	1.00	0.00
vha-2	2.50	0.75	0.67	0.00	0.33	0.00
his-2	2.50	0.50	0.00	0.00	0.00	0.00
C47E12.7	2.50	0.50	0.67	0.00	0.33	0.00
nol-1	2.25	1.75	0.67	0.00	1.00	0.00
C16A3.6	2.25	1.75	1.00	0.25	0.67	0.00
F10C2.4	2.25	1.50	0.67	0.00	1.00	0.33
sas-5	2.25	1.00	0.00	0.00	0.67	0.00
hcp-3	2.25	0.75	0.00	0.00	0.33	0.00
ima-3	2.25	0.75	0.00	0.00	0.00	0.00
dic-1	2.25	0.75	0.33	0.00	0.00	0.00
sptl-3	2.25	0.50	0.00	0.00	0.00	0.00
let-526	2.25	0.50	0.33	0.00	0.00	0.00
ncam-1	2.25	0.25	0.00	0.00	0.00	0.00
sca-1	2.00	2.50	1.67	0.00	0.67	0.00
aap-1	2.00	2.25	0.33	0.00	1.33	2.00
nuo-4	2.00	2.25	0.33	0.25	1.33	3.00
mcm-5	2.00	2.25	1.00	0.00	1.00	0.00
pri-1	2.00	1.75	0.00	0.00	0.67	0.00
F10C2.4	2.00	1.75	0.33	0.00	0.67	0.00
T26G10.1	2.00	1.75	0.67	0.00	1.33	0.00
atp-5	2.00	1.75	0.67	0.00	0.67	2.67

rpl-37	2.00	1.75	1.00	0.00	0.67	0.00
lin-5	2.00	1.50	0.00	0.00	0.33	0.00
T06E6.2	2.00	1.50	0.33	0.00	0.33	0.00
snr-6	2.00	1.50	0.67	0.00	0.33	0.00
T25G3.3	2.00	1.50	1.00	0.00	1.33	0.00
toe-1	2.00	1.50	1.33	0.00	1.00	0.00
cin-4	2.00	1.50	1.33	0.00	0.67	0.00
tba-1	2.00	1.25	0.00	0.00	0.33	0.00
tars-1	2.00	1.25	0.00	0.00	1.00	0.00
tbb-2	2.00	1.25	0.00	0.00	0.67	0.00
tlk-1	2.00	1.25	0.00	0.00	0.67	0.00
dyci-1	2.00	1.25	0.00	0.00	0.33	0.00
rars-1	2.00	1.25	0.33	0.00	0.33	0.00
imb-3	2.00	1.25	0.67	0.25	0.33	0.00
F33H2.5	2.00	1.00	0.33	0.00	0.67	0.67
let-767	2.00	1.00	0.33	0.00	0.00	0.33
F23B12.7	2.00	1.00	0.33	0.50	1.00	0.00
asb-2	2.00	0.75	0.00	0.00	0.00	3.00
dnc-1	2.00	0.50	0.00	0.00	0.00	0.00
ubl-1	1.75	2.25	1.33	0.25	1.33	0.00
lars-1	1.75	2.00	0.00	0.25	0.67	0.00
cdl-1	1.75	2.00	0.33	0.00	1.67	0.00
let-716	1.75	2.00	0.67	0.00	1.00	0.00
rps-29	1.75	1.75	0.33	0.00	1.00	0.00
let-858	1.75	1.75	1.00	0.00	0.33	0.00
F59C6.5	1.75	1.50	0.67	0.00	1.67	2.67
rpoa-2	1.75	1.50	1.00	0.00	1.33	0.00
F55F8.2	1.75	1.25	0.00	0.00	0.67	0.00
cacn-1	1.75	1.25	0.00	0.00	1.33	0.00
mog-5	1.75	1.25	0.33	0.00	1.33	0.00
T13H5.4	1.75	1.25	0.33	0.00	1.00	0.00
C55A6.9	1.75	1.25	0.33	0.00	0.67	0.00
hda-1	1.75	1.25	0.33	0.50	1.33	0.67
F43D9.3	1.75	1.00	0.00	0.00	0.00	0.00
emb-27	1.75	0.75	0.00	0.00	1.33	0.00
nuo-1	1.50	3.00	1.00	0.00	2.00	3.00
ucr-1	1.50	2.75	0.67	0.25	0.67	3.00
spg-7	1.50	2.75	1.67	0.00	0.33	3.00
B0491.5	1.50	2.50	0.33	0.00	1.00	2.67
hcp-4	1.50	2.25	1.33	0.00	1.67	0.33
byn-1	1.50	2.25	1.67	0.00	1.33	0.00
dld-1	1.50	2.00	0.33	0.00	1.67	1.67
mrps-30	1.50	2.00	1.33	0.00	2.33	2.00
ril-2	1.50	1.75	0.33	0.00	1.33	2.00
Y45F10D.7	1.50	1.50	0.33	0.25	1.33	1.00
T23D8.3	1.50	1.50	0.67	0.00	1.00	0.00
daz-1	1.50	1.50	1.33	0.25	1.33	0.00
smc-4	1.50	1.50	1.33	0.00	1.67	0.00

rnr-1	1.50	1.25	0.00	0.75	1.33	0.00
T04A8.6	1.50	1.25	0.33	0.00	0.33	0.00
act-2	1.50	1.25	0.33	0.75	1.67	0.00
C23G10.8	1.50	1.00	0.33	0.00	1.33	0.00
rps-13	1.25	2.50	1.67	0.25	1.33	0.00
ngp-1	1.25	2.00	1.33	1.00	1.00	0.00
Y39G10AR.8	1.25	1.75	1.00	1.00	0.67	0.00
fos-1	1.25	1.75	1.00	0.50	1.33	0.00
rpl-39	1.25	1.75	1.00	0.00	0.67	0.00
C37C3.2	1.25	1.75	1.00	0.25	1.67	0.00
ant-1.1	1.25	1.50	0.00	0.25	0.67	0.33
snr-1	1.25	1.50	0.33	0.00	0.33	0.00
emb-5	1.25	1.00	0.00	0.00	0.00	0.00
dyn-1	1.25	0.75	0.33	0.00	0.33	0.00
plk-1	1.00	2.50	1.00	0.75	1.67	0.00
lig-1	1.00	2.50	1.33	0.00	2.33	0.00
F11A3.2	1.00	2.25	0.33	0.00	0.33	0.00
let-70	1.00	2.25	0.67	0.00	0.67	0.00
F26E4.4	1.00	2.25	1.00	0.00	2.00	0.00
rps-7	1.00	2.25	1.00	0.75	1.00	0.00
F22B5.2	1.00	2.00	0.33	0.75	0.67	0.00
Y61A9LA.10	1.00	2.00	0.33	0.00	1.33	0.00
spd-5	1.00	2.00	0.67	0.00	1.33	0.00
C55E6.9	1.00	2.00	1.00	0.00	1.67	0.00
scc-3	1.00	1.75	0.00	0.00	1.00	0.00
lin-41	1.00	1.75	1.00	0.00	2.00	0.33
rps-21	1.00	1.75	1.00	0.00	0.33	0.00
sap-49	1.00	1.75	1.33	0.00	1.00	0.00
M28.5	1.00	1.50	0.33	0.00	1.00	0.00
F43D9.3	1.00	1.25	0.33	0.00	0.33	0.00
mix-1	0.75	2.75	1.67	0.00	1.67	0.00
kle-2	0.75	2.50	1.00	0.00	1.67	0.00
D2013.7	0.75	2.25	0.00	0.75	1.00	0.00
D2013.7	0.75	2.25	0.67	0.25	0.00	0.00
fib-1	0.75	2.25	1.00	1.25	0.33	0.00
cdc-25.1	0.75	2.00	1.00	0.00	2.00	0.00
ubl-1	0.75	2.00	1.00	0.75	1.33	0.00
rps-22	0.75	2.00	1.33	0.25	1.00	0.00
tba-2	0.75	2.00	1.67	0.75	1.67	0.33
symk-1	0.75	1.75	0.33	0.00	0.67	0.00
rpl-41	0.75	1.75	1.00	0.00	0.67	0.00
nars-1	0.75	1.50	1.00	0.00	1.33	0.33
atad-3	0.50	2.75	1.33	0.75	0.33	2.67
B0511.6	0.50	2.50	1.67	1.75	1.33	0.00
Y48B6A.1	0.50	2.25	0.67	0.25	1.33	0.00
paa-1	0.50	2.25	1.67	0.00	2.33	0.00
rpc-2	0.50	2.25	1.67	0.25	1.67	0.00
mcm-6	0.50	2.25	1.67	0.75	1.67	0.00

gld-2	0.50	1.75	0.67	0.00	2.00	0.33
let-92	0.50	1.75	1.00	0.00	1.67	0.00
vha-1	0.50	1.75	1.33	0.00	0.33	0.00
rpl-22	0.50	1.50	1.00	0.50	0.33	0.33
phb-2	0.25	3.00	0.67	1.75	0.33	3.00
hsp-6	0.25	3.00	1.00	2.25	0.00	2.33
ctps-1	0.25	2.50	0.33	0.00	2.67	0.00
T08A11.2	0.25	2.25	0.33	0.75	0.33	0.00
R53.4	0.25	2.25	0.67	1.25	0.67	3.00
B0511.10	0.25	2.25	1.33	1.00	0.67	0.00
prp-21	0.25	2.00	0.67	0.00	1.00	0.00
rpl-20	0.25	2.00	0.67	0.50	0.67	1.00
cdk-1	0.25	2.00	1.00	1.00	2.00	0.00
teg-4	0.25	2.00	1.33	0.50	0.67	0.00
rps-19	0.25	2.00	1.67	0.50	0.33	0.00
rpb-3	0.25	1.75	0.67	0.50	1.00	0.00
cdt-1	0.25	1.50	0.33	0.00	1.00	0.00
act-2	0.25	1.50	0.67	1.00	2.00	0.00
rpl-7	0.25	1.50	1.00	0.75	0.00	0.00
cyc-1	0.00	3.00	1.00	1.00	0.67	3.00
atp-2	0.00	2.75	0.67	2.50	0.67	2.67
mcm-7	0.00	2.75	1.33	1.75	1.67	0.00
ril-1	0.00	2.50	0.33	0.50	1.00	3.00
K07C5.4	0.00	2.50	1.00	1.00	0.67	0.33
cyb-3	0.00	2.50	1.33	0.00	2.67	0.00
uaf-2	0.00	2.25	0.67	0.00	0.67	0.00
rpa-1	0.00	2.25	1.00	1.25	1.00	0.33
K07C5.4	0.00	2.25	1.00	1.50	1.00	0.33
cyb-3	0.00	2.25	1.00	0.00	2.33	0.00
toe-1	0.00	2.25	1.33	1.50	1.00	0.00
ZK1127.5	0.00	2.25	1.33	1.00	2.33	0.33
rps-14	0.00	2.25	1.33	1.00	0.33	0.00
rps-5	0.00	2.25	1.33	2.00	0.00	0.00
rps-3	0.00	2.00	0.67	0.75	0.00	0.00
rab-1	0.00	1.75	0.33	0.00	0.00	0.00
spt-5	0.00	1.75	0.67	0.00	1.33	0.00
T13H5.4	0.00	1.75	1.00	0.75	1.33	0.00
Y54E2A.11	0.00	1.75	1.33	2.50	0.00	0.00
T08A11.2	0.00	1.50	0.33	1.00	0.67	0.00
vha-13	0.00	1.50	0.33	0.00	0.00	0.00
imb-3	0.00	1.50	0.67	1.25	0.00	0.00
act-1	0.00	1.50	0.67	0.75	1.67	0.00
act-2	0.00	1.50	0.67	0.75	2.33	0.00
rpl-33	0.00	1.50	1.00	0.75	0.00	0.33
rps-9	0.00	1.50	1.33	2.00	0.00	0.00
act-3	0.00	1.25	0.33	0.75	1.67	0.00

Table 5. Characterization of sequence-verified hits from the screen for **positive effectors** of DAF-16 activity. All metrics were analyzed at least three times, each time assigning a qualitative score from 0 to 3, with zero meaning no change and 3 meaning total change from control RNAi. These scores were averaged and are reported below. Note that all strains are in the *glp-1(ts)* background, which genetically ablates the germline.

Main Gene	sod-3::gfp	Health	sod-3 in <i>rrf-1(-)</i>	<i>gst-4::gfp</i>	<i>hsp-6::gfp</i>
erfa-3	3.00	2.00	2.33	2.33	2.67
eef-1B.1	3.00	2.00	0.00	2.67	1.67
erfa-3	3.00	1.67	2.00	2.67	3.00
eef-1G	3.00	1.67	0.33	2.33	1.67
sptl-1	3.00	1.33	0.00	3.00	1.67
let-70	3.00	1.33	0.00	2.67	3.00
lpin-1	3.00	1.33	0.00	2.67	2.33
hars-1	2.67	3.00	0.00	1.00	1.33
Y47D3A.29	2.67	2.33	0.33	2.00	0.67
tars-1	2.67	2.33	0.00	2.33	2.00
cct-1	2.67	1.67	1.33	1.00	2.00
hmgs-1	2.67	1.67	0.00	2.67	1.67
mdt-15	2.67	1.00	0.00	3.00	2.33
dyn-1	2.67	1.00	0.00	3.00	2.67
elt-2	2.67	0.67	1.00	3.00	1.67
dve-1	2.33	3.00	0.33	0.67	1.00
cct-2	2.33	2.00	1.67	1.00	1.33
nxt-1	2.33	2.00	0.00	1.67	2.33
npp-6	2.33	2.00	0.00	2.00	1.67
snr-3	2.33	1.67	0.00	2.33	2.00
osm-11	2.33	1.67	0.00	0.67	2.67
arx-2	2.33	1.33	1.00	3.00	2.33
tba-4	2.33	1.33	0.00	2.67	1.33
elo-5	2.33	0.67	0.00	3.00	2.67
C23G10.8	2.00	3.00	0.00	1.33	1.67
peb-1	2.00	3.00	0.00	0.00	1.33
nipi-3	2.00	3.00	0.00	1.33	1.00
rbpl-1	2.00	2.67	0.00	1.33	1.67
C23G10.8	2.00	2.67	0.00	1.33	1.67
symk-1	2.00	2.67	0.00	2.00	1.00
W04A4.5	2.00	2.33	0.00	1.67	2.33
itr-1	2.00	2.00	1.67	2.33	2.67
itr-1	2.00	2.00	1.33	2.33	2.67
cct-5	2.00	2.00	1.00	1.33	1.33
epn-1	2.00	2.00	0.00	2.00	1.33
spt-5	2.00	1.67	0.67	2.33	2.67
Mixed	2.00	1.67	0.00	2.33	2.00
fat-6	2.00	1.67	0.00	2.00	1.33
plrg-1	2.00	1.67	0.00	2.33	1.67

nsf-1	2.00	1.33	0.00	3.00	3.00
mog-5	2.00	1.33	0.00	2.67	2.33
cct-8	2.00	1.33	0.00	1.00	1.67
skp-1	2.00	1.00	0.33	2.33	2.67
npp-10	2.00	0.67	1.00	3.00	3.00
his-73	1.67	3.00	0.00	1.00	0.00
rheb-1	1.67	2.67	0.00	1.00	0.33
cct-8	1.67	2.67	0.00	0.67	0.67
dlst-1	1.67	2.67	0.00	1.00	0.33
ruvb-1	1.67	2.67	0.00	1.33	0.67
cpsf-2	1.67	2.33	0.67	2.00	1.67
elf-3.E	1.67	2.33	0.00	1.67	2.00
iff-2	1.67	2.33	0.00	2.00	1.33
ogdh-1	1.67	2.33	0.00	0.67	0.33
his-63	1.67	2.33	0.00	1.67	1.33
T08B1.1	1.67	2.33	0.00	2.00	1.00
cct-4	1.67	2.00	1.00	0.33	1.00
emb-5	1.67	2.00	0.33	1.67	2.33
let-526	1.67	2.00	0.00	2.33	0.33
ima-3	1.67	2.00	0.00	2.00	2.00
rack-1	1.67	2.00	0.00	1.33	0.00
his-38	1.67	2.00	0.00	2.33	1.33
his-38	1.67	2.00	0.00	2.33	1.33
cct-7	1.67	1.67	1.00	1.33	1.67
paa-1	1.67	1.67	0.00	1.33	2.00
his-38	1.67	1.67	0.00	2.33	1.33
cct-6	1.67	1.33	0.67	2.00	2.00
C37C3.2	1.67	1.33	0.00	1.67	3.00
his-38	1.67	1.33	0.00	2.33	1.67
tbb-2	1.67	1.00	0.00	2.33	1.67
apl-1	1.67	1.00	0.00	2.67	3.00
elo-5	1.67	0.67	0.00	3.00	2.67
daf-16	1.33	3.00	1.67	0.33	0.00
fars-1	1.33	3.00	0.00	1.33	1.00
pri-2	1.33	3.00	0.00	1.00	1.00
cgt-3	1.33	3.00	0.00	1.00	0.33
prp-19	1.33	3.00	0.00	1.67	1.67
thoc-2	1.33	3.00	0.00	1.00	2.00
rheb-1	1.33	3.00	0.00	1.00	0.67
pap-1	1.33	3.00	0.00	0.67	0.33
pas-3	1.33	2.67	0.67	0.67	0.00
arx-7	1.33	2.67	0.00	1.00	0.67
rpb-3	1.33	2.67	0.00	1.33	1.33
cyl-1	1.33	2.67	0.00	1.33	1.33
C15C7.5	1.33	2.67	0.00	2.00	1.00
xpo-2	1.33	2.33	0.00	1.67	2.33
xpo-2	1.33	2.33	0.00	1.67	1.67
xpo-2	1.33	2.33	0.00	1.67	1.67

F52C6.2	1.33	2.33	0.00	0.33	1.00
his-9	1.33	2.33	0.00	1.67	0.67
xrn-2	1.33	2.33	0.00	2.00	1.33
npp-6	1.33	2.33	0.00	1.33	1.00
npp-3	1.33	2.00	1.00	2.33	2.00
unc-32	1.33	2.00	0.33	1.00	1.33
cct-8	1.33	2.00	0.33	1.00	1.00
nekl-2	1.33	2.00	0.00	0.33	1.33
his-14	1.33	2.00	0.00	1.33	0.67
mua-6	1.33	2.00	0.00	1.00	0.67
his-13	1.33	1.67	1.00	1.33	1.00
nsf-1	1.33	1.67	0.00	2.33	2.00
his-26	1.33	1.67	0.00	2.33	1.00
his-48	1.33	1.00	0.00	2.33	1.33
npp-8	1.33	1.00	0.00	2.00	1.33
eat-6	1.33	1.00	0.00	1.00	1.67
rnr-1	1.00	3.00	0.33	0.67	0.33
pabp-2	1.00	3.00	0.00	1.33	1.33
his-67	1.00	3.00	0.00	0.00	0.33
ntl-2	1.00	3.00	0.00	1.00	0.00
mdt-26	1.00	3.00	0.00	1.67	1.33
hmg-4	1.00	3.00	0.00	1.00	1.00
icl-1	1.00	3.00	0.00	1.00	0.67
his-65	1.00	3.00	0.00	0.67	0.00
qars-1	1.00	3.00	0.00	1.33	0.67
his-2	1.00	3.00	0.00	1.33	0.00
his-71	1.00	3.00	0.00	1.00	0.67
C30F12.1	1.00	2.67	0.67	1.67	1.33
icd-2	1.00	2.67	0.00	2.00	0.00
npp-9	1.00	2.67	0.00	0.67	0.67
dpy-9	1.00	2.67	0.00	0.33	1.33
his-61	1.00	2.67	0.00	0.67	0.33
pyp-1	1.00	2.67	0.00	1.67	0.00
his-8	1.00	2.67	0.00	1.00	1.00
his-10	1.00	2.33	0.33	1.33	0.67
dpy-10	1.00	2.33	0.00	0.00	1.33
F19F10.9	1.00	2.33	0.00	1.33	0.67
prp-31	1.00	2.00	0.33	2.33	1.67
cct-3	1.00	2.00	0.00	1.00	0.67
sos-1	1.00	2.00	0.00	1.33	1.00
his-62	1.00	2.00	0.00	1.00	0.33
sams-1	1.00	2.00	0.00	2.33	0.33
drl-1	1.00	1.67	0.00	2.67	1.00
T13H5.4	1.00	1.67	0.00	2.00	1.00
hsp-4	1.00	1.33	0.00	2.33	2.67
his-15	1.00	1.33	0.00	1.67	1.00
npp-8	1.00	1.33	0.00	2.00	1.67
mfap-1	0.67	3.00	0.00	1.33	1.00

mag-1	0.67	3.00	0.00	0.00	0.67
C34F11.3	0.67	3.00	0.00	1.00	0.67
lpd-7	0.67	3.00	0.00	0.67	1.00
thoc-2	0.67	3.00	0.00	1.00	0.67
C01B10.11	0.67	3.00	0.00	0.33	0.00
F08B4.7	0.67	3.00	0.00	1.00	0.33
his-57	0.67	3.00	0.00	1.00	0.00
his-66	0.67	3.00	0.00	0.33	0.00
his-64	0.67	3.00	0.00	0.33	0.00
eps-8	0.67	3.00	0.00	1.33	1.00
fat-7	0.67	3.00	0.00	1.00	0.67
his-41	0.67	3.00	0.00	0.33	0.33
his-37	0.67	3.00	0.00	0.67	0.00
pmt-1	0.67	2.67	0.00	1.67	0.00
col-101	0.67	2.33	0.00	1.67	0.33
F19F10.9	0.67	2.33	0.00	1.00	1.00
spg-7	0.67	2.00	0.00	2.00	0.33
his-4	0.67	2.00	0.00	1.00	1.00
flr-1	0.67	2.00	0.00	2.33	1.33
let-92	0.67	1.33	0.33	1.33	1.00
mca-3	0.67	1.00	0.00	0.67	2.67
cmd-1	0.67	0.67	0.00	3.00	2.67
daf-16	0.33	3.00	1.00	0.33	0.00
mag-1	0.33	3.00	0.00	0.00	1.00
his-42	0.33	3.00	0.00	0.00	0.00
C01B10.11	0.33	3.00	0.00	0.00	0.00
his-5	0.33	3.00	0.00	1.00	0.00
his-74	0.33	3.00	0.00	1.00	0.33
his-11	0.33	2.67	0.00	0.33	0.67
glf-1	0.33	2.67	0.00	0.00	0.00
dyci-1	0.33	2.67	0.00	1.33	0.33
rskn-1	0.00	3.00	0.33	0.00	0.00
gcy-15	0.00	3.00	0.33	0.67	0.00
his-46	0.00	3.00	0.00	1.00	0.00
pab-2	0.00	3.00	0.00	1.00	1.00

Table 6. List of all high-confidence KRI-1 interacting proteins identified from the Co-IPs. The proteins are separated based on which germline state they preferentially interact with KRI-1 in, or if they appear to interact constitutively.

preferentially interacts in germline(+)	constitutive interactor	preferentially interacts in germline(-)
aco-2	aldo-2	F37C4.5
act-1	atp-2	
alh-9	cah-3	
cct-1	cct-5	
cct-2	cdc-48.1	
cct-4	eef-2	
cct-6	egl-45	
cct-8	enol-1	
eef-1B.2	ers-1	
eef-1G	F46H5.3	
gta-1	F47B10.1	
hsp-6	F54D5.7	
hsp-60	gpd-2	
kat-1	his-24	
pas-5	idhb-1	
pcca-1	lec-8	
pde-6	mdh-2	
smg-2	mrs-1	
tbb-2	nmt-1	
unc-54	ola-1	
vha-12	pas-3	
vha-13	pas-6	
	pas-7	
	ran-3	
	rpn-2	
	rpn-3	
	rpt-1	
	rpt-2	
	rpt-3	
	rpt-4	
	rrbs-1	
	rsp-4	
	sams-4	
	sax-1	
	sdha-1	
	sip-1	
	snr-4	
	ttr-15	
	ufd-1	
	unc-112	
	unc-15	
	Y73F4A.1	

FIGURES

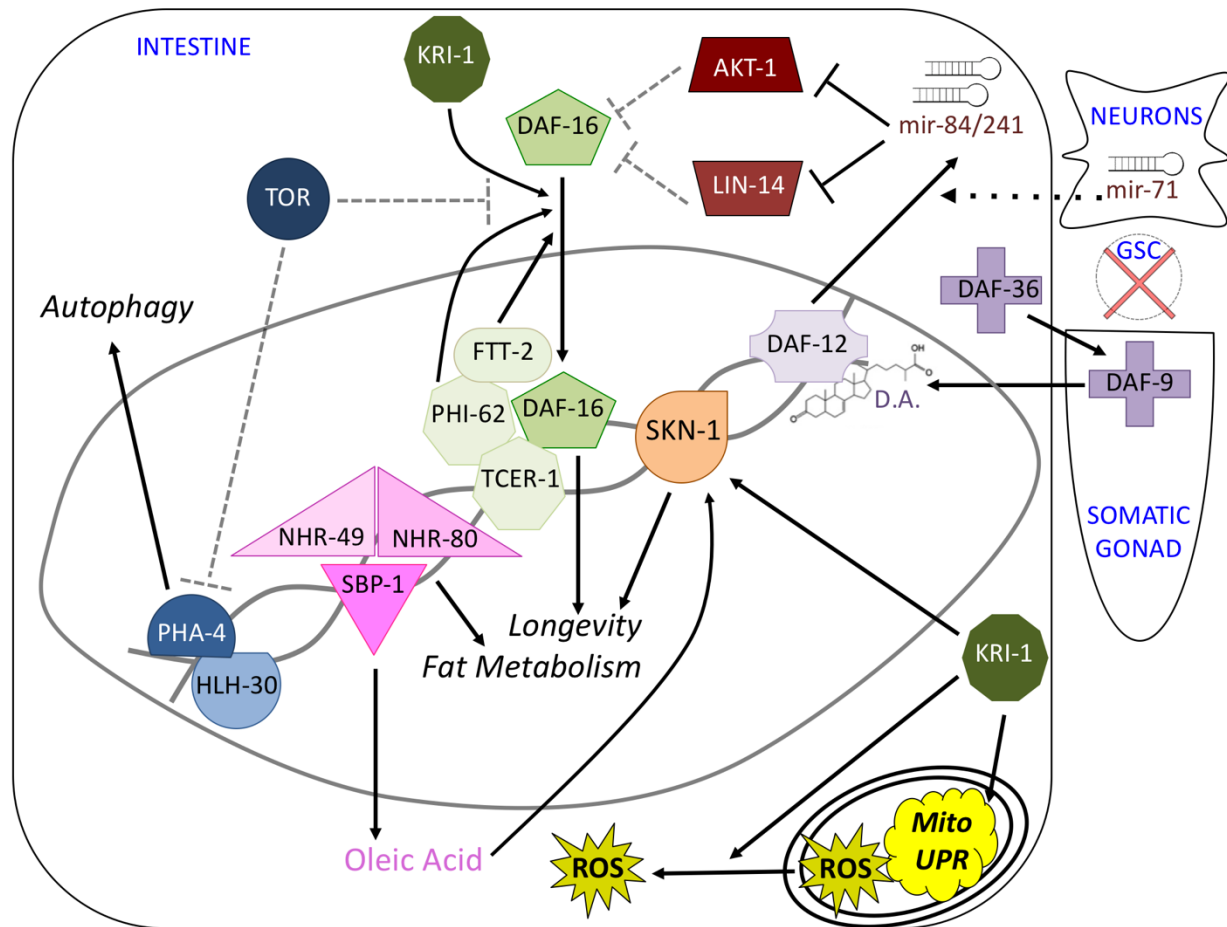


Figure 1. Molecular activity in the absence of the germline. Note that multiple tissues and pathways are involved in the coordinated longevity of germline-less *C. elegans*. This includes DAF-16 activity (green), steroid hormone signaling from the somatic gonad (purple), microRNA signaling (red), decreased TOR and increased autophagy (blue), nuclear hormone receptor control of fat metabolism and oleic acid synthesis (pink), mitochondrial and cytosolic ROS production and the mitoUPR (yellow), and SKN-1 activity (orange). D.A. = dafachronic acid. ROS = reactive oxygen species. Dashed gray lines represent potential actions that are not occurring. Dotted black lines represent theoretical actions.

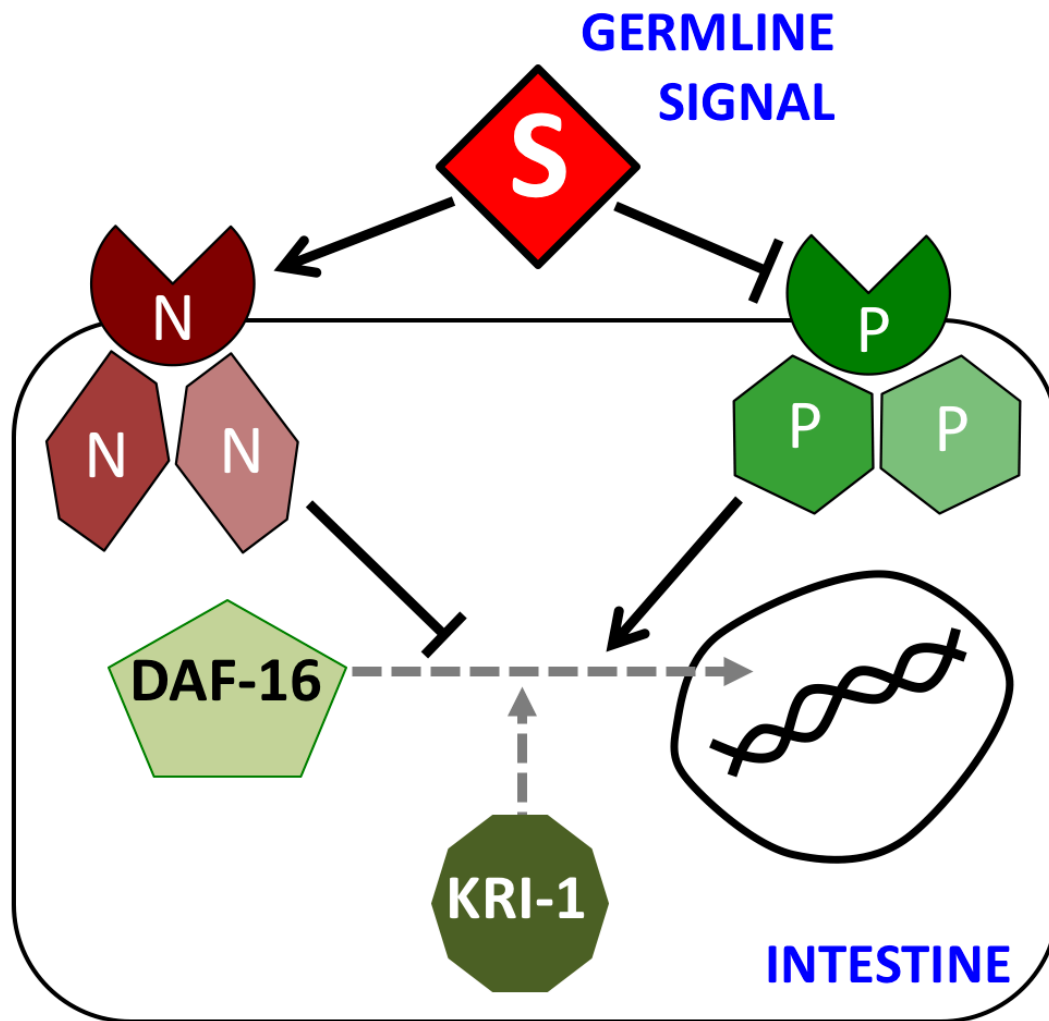
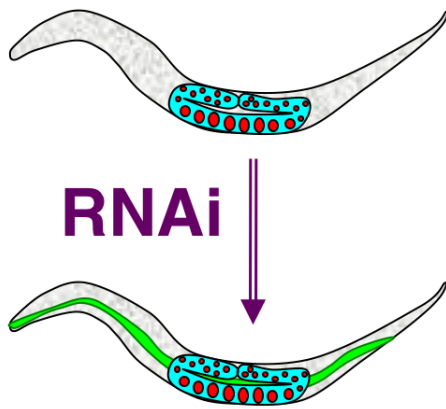


Figure 2. Two potential models for germline inhibition of KRI-1-mediated DAF-16 nuclear localization. The first model (left), proposes that the germline signal activates a series of negative effectors that inhibit DAF-16 translocation and function. The second model (right), proposes that the germline inhibits a series of positive effectors that would otherwise be able to promote DAF-16 translocation and function. S = theoretical germline signal, N = negative effector of DAF-16, P = positive effector of DAF-16.

Negative Effector Screen:



Positive Effector Screen:

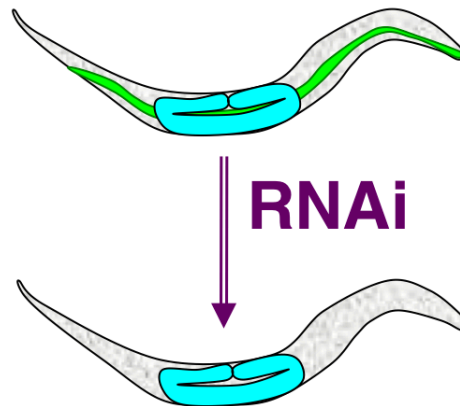


Figure 3. Dual whole genome-wide RNAi screens to find DAF-16 regulators. The first screen was designed to find negative effectors of DAF-16 activity by looking for RNAi clones that could turn on the *Psod-3::gfp* reporter in the intestine of germline(+) worms. In other words, RNAi clones that could mimic germline-ablation in worms that should be germline-intact. The second screen was designed to find positive effectors of DAF-16 activity by looking for RNAi clones that could turn off the *Psod-3::gfp* reporter in the intestine of germline(-) worms. In other words, RNAi clones that could mimic the germline-intact state in germline-ablated worms.

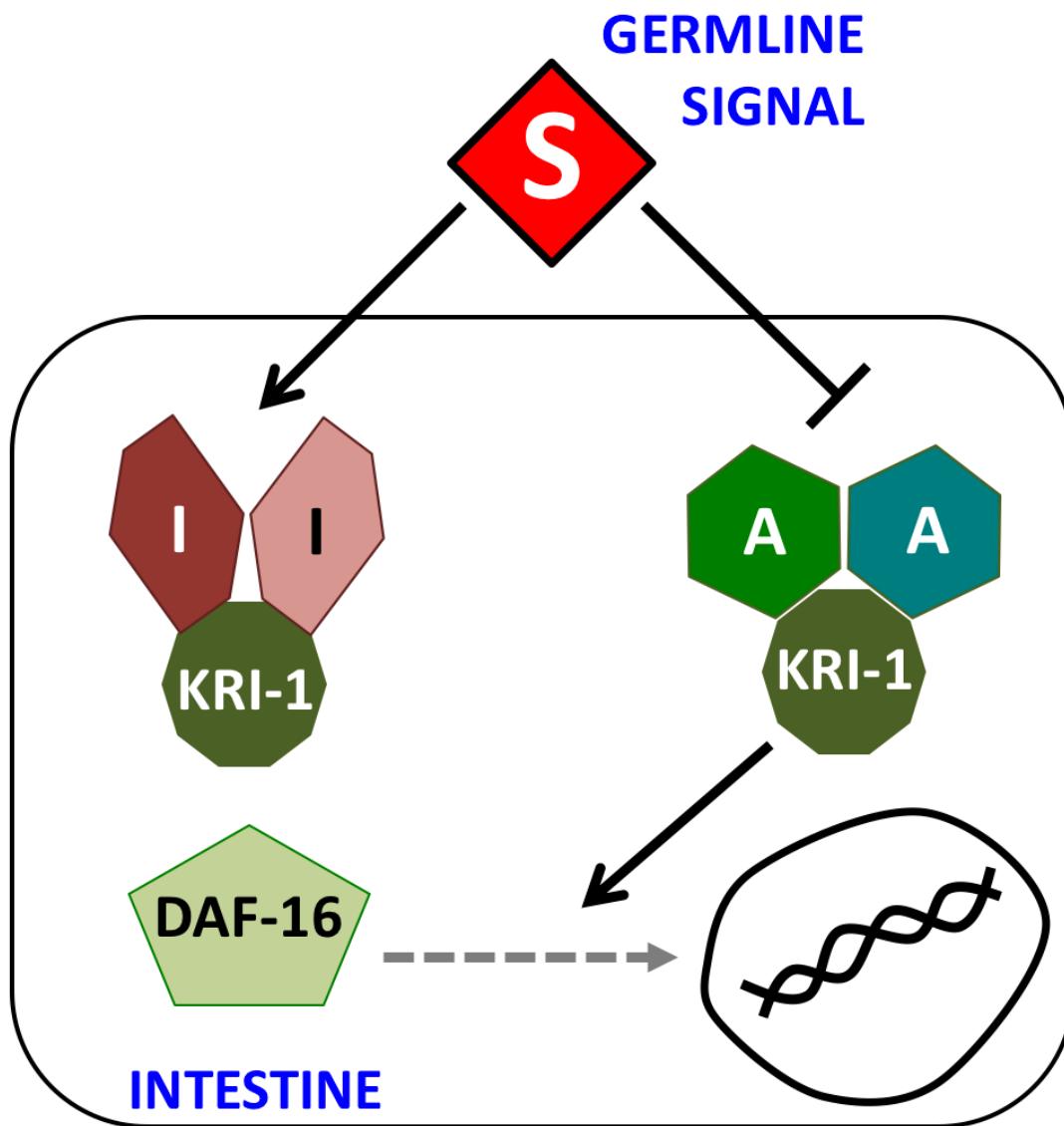
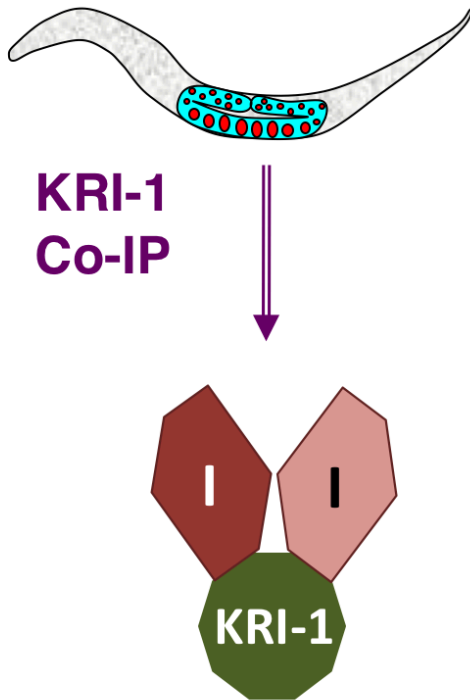


Figure 4. Two protein complex based models for germline inhibition of KRI-1-mediated DAF-16 translocation. The first model (left) proposes that the germline signal promotes the formation of an inhibitory complex, which sequesters KRI-1 in a non-functional state. The second model (right) proposes that the germline signal inhibits the formation of an activating complex that would otherwise promote KRI-1 function. S = theoretical germline signal, I = inhibitory complex member, A = activating complex member.

Inhibitory Complex Co-IP:



Activating Complex Co-IP:

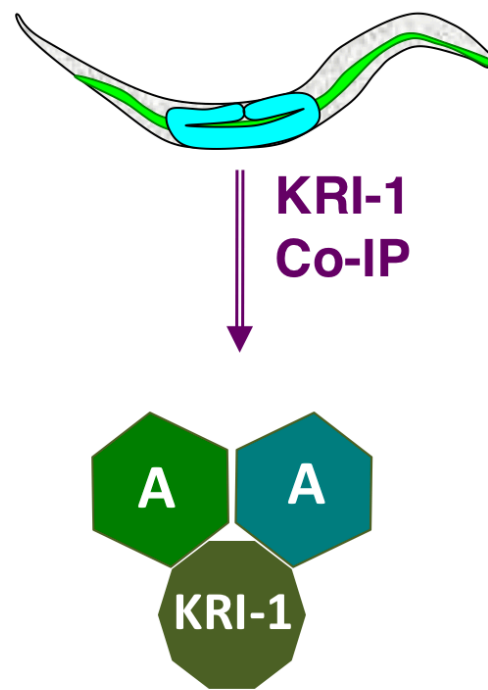


Figure 5. Dual biochemical screens to find KRI-1 binding partners. The first screen was designed to find potential inhibitory complex members by looking for proteins that Co-IP with KRI-1 in germline-intact worms. The second screen was designed to find potential activating complex members by looking for proteins that Co-IP with KRI-1 in germline-ablated worms. I = inhibitory complex member, A = activating complex member.

	Dilute	Grow 2hrs	Add IPTG	Induce 2hrs	Kanamycin
A	-	-	-	-	-
B	10X	-	-	-	-
C	10X	-	+	-	-
D	10X	-	+	+	-
E	10X	+	-	-	-
F	10X	+	+	-	-
G	10X	+	+	+	-
H	10X	+	+	+	+

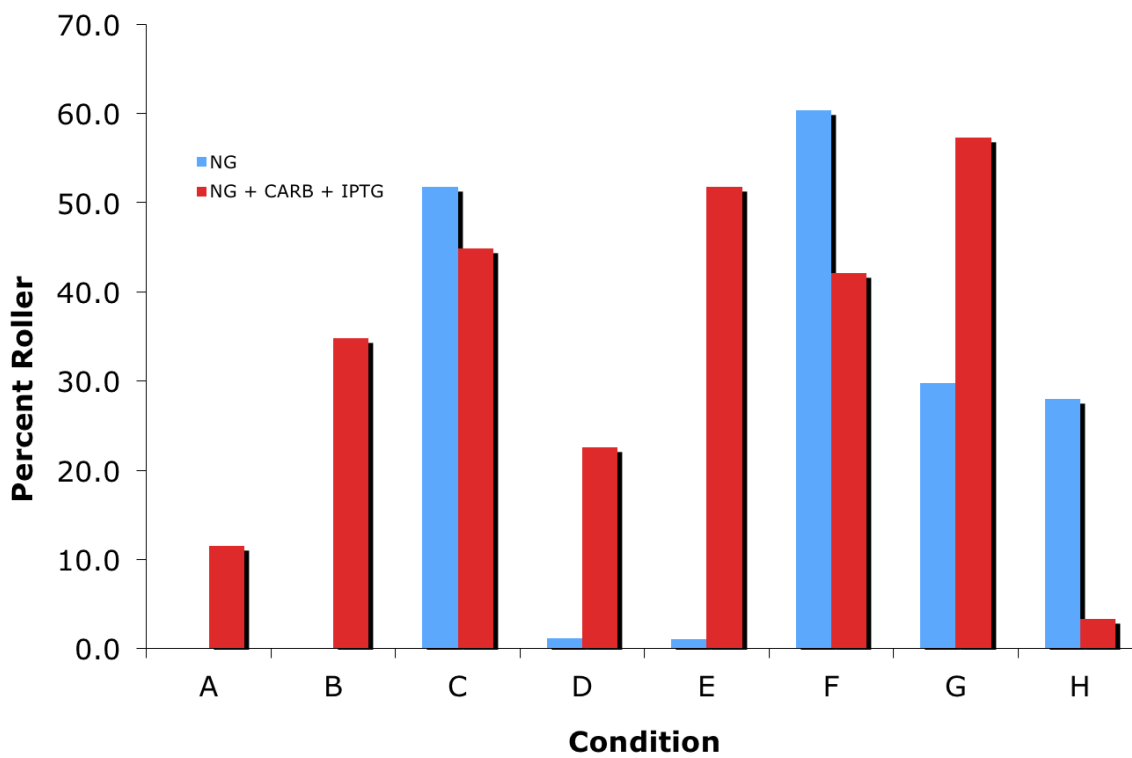


Figure 6. Initial optimization of solid agar RNAi protocol. Effectiveness of different strategies (A-H) were compared using *rol-5(RNAi)*, which causes a roller phenotype. The effectiveness of all of these strategies were compared on both plain NG plates as well as NG + CARB + IPTG plates (blue versus red bars, respectively).

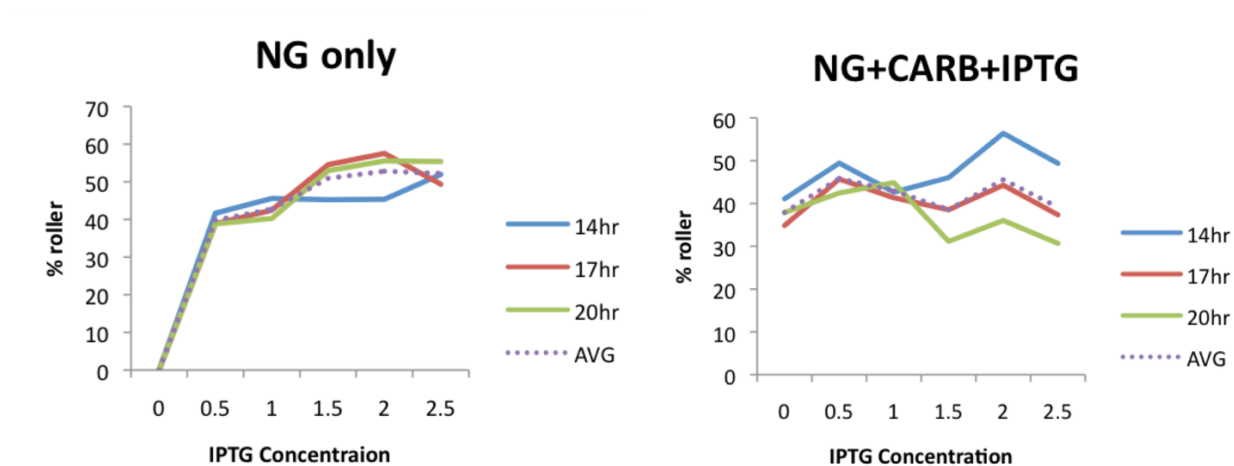


Figure 7. Further optimization of solid agar RNAi protocol. After choosing strategy F from Figure 8 (dilute O/N culture 10-fold, grow for 2 hours, add IPTG then spot on plates), we optimized it further by determining the ideal concentration of IPTG to add (shown along the X-axis in uM) and the ideal amount of drying time before adding the worms (shown by comparing the different colored lines). The effectiveness of these strategies were compared on both plain NG plates as well as NG + CARB + IPTG plates.

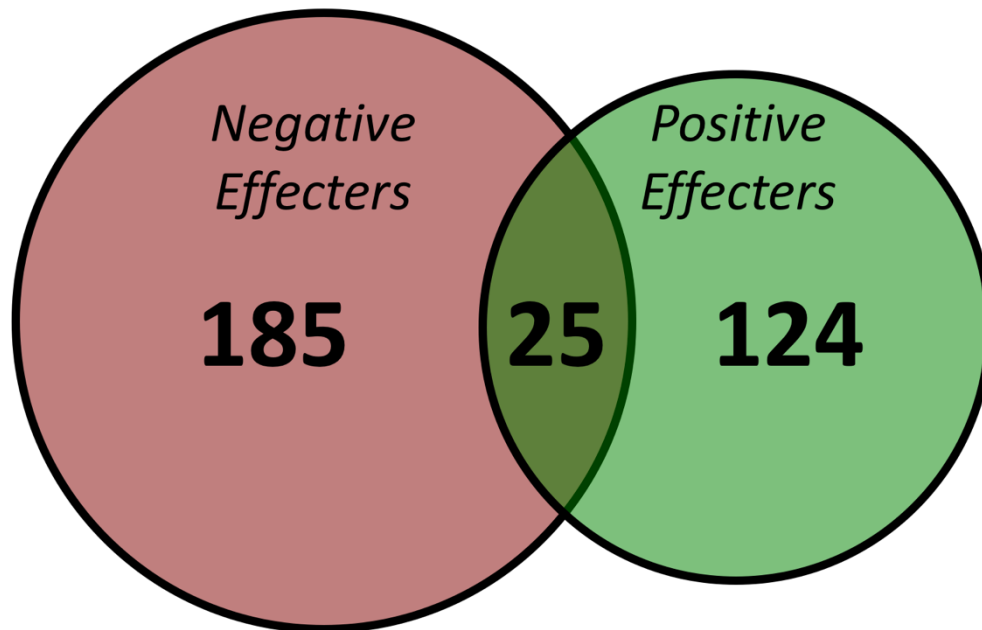


Figure 8. Significant overlap between the two genetic screens. 25 genes were independently found in both screens, a somewhat surprising finding considering that the screens were designed to find genes with opposite effects on DAF-16 activity.

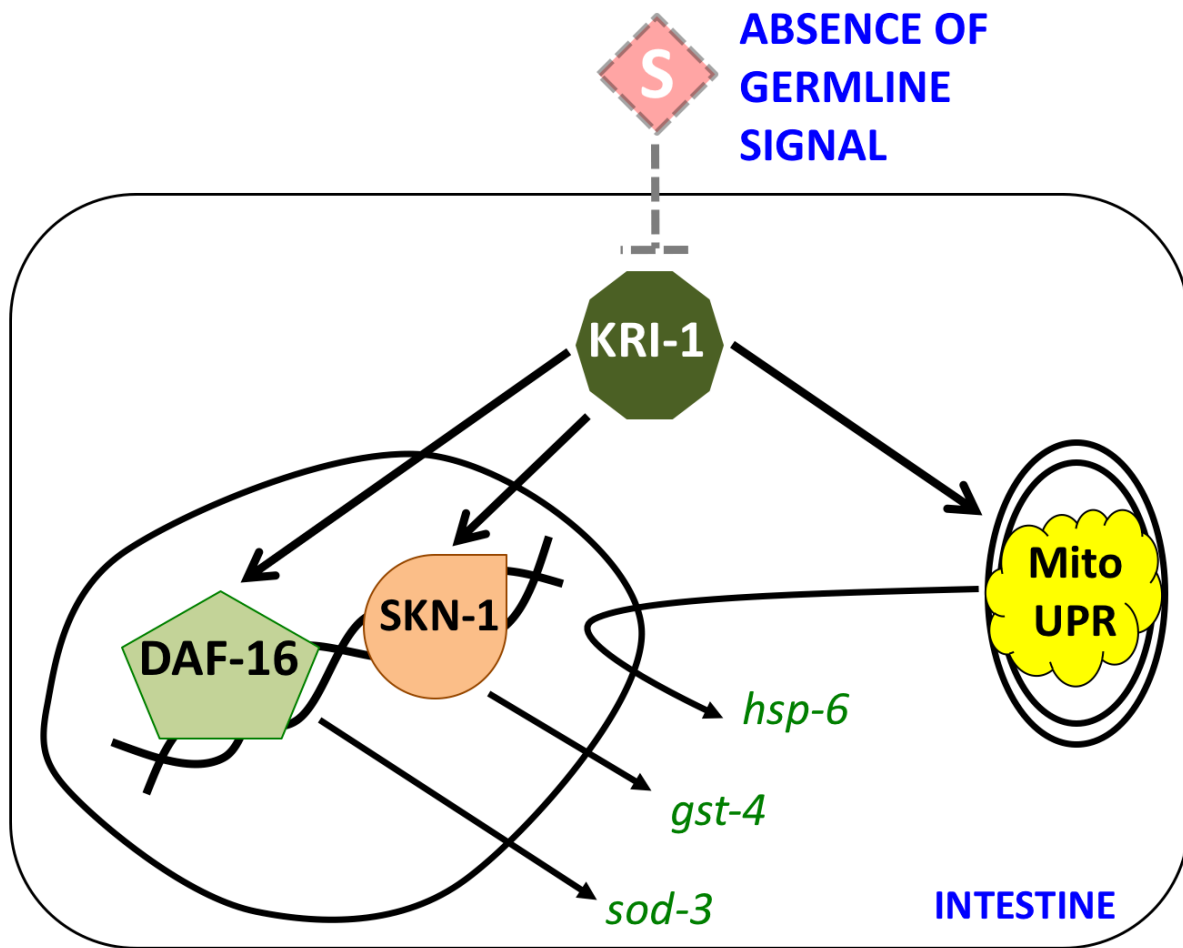
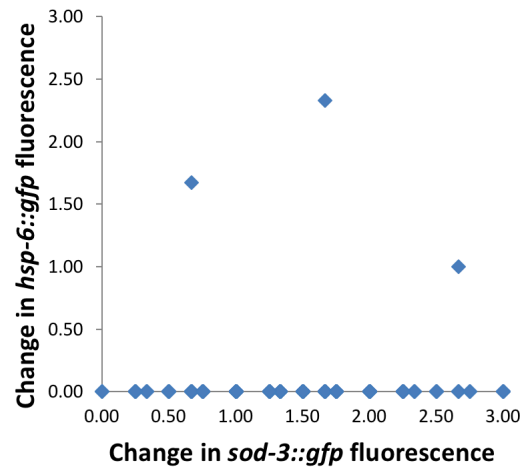
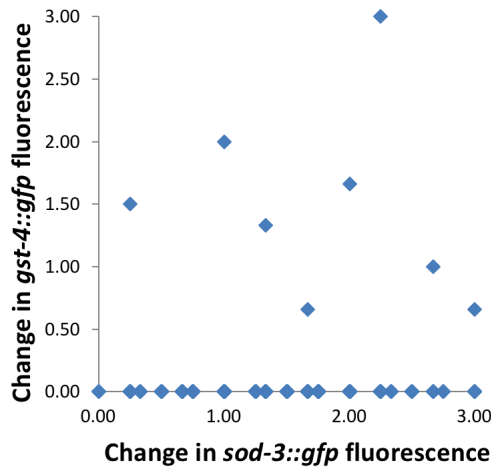


Figure 9. KRI-1 promotes the activation of multiple components of the germline-less longevity pathway. Yuehua Wei, a post-doc in our lab, discovered that germline-ablation activates SKN-1 (initially discovered by Sivan Henis-Korenblit, a former postdoc, and now independently by the Blackwell lab) and the MitoUPR, and that this activation is KRI-1 dependent. SKN-1 activity can be assessed using the *Pgst-4::gfp* reporter, and MitoUPR activity can be assessed using the *Phsp-6::gfp* reporter.

Predicted results of screen hits tested for their effect on other markers



Actual results of screen hits tested for their effect on other markers

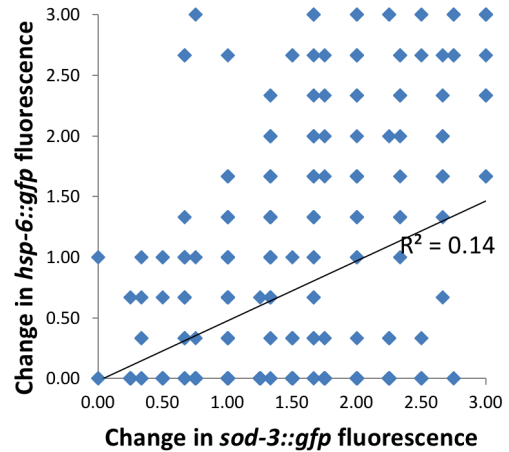
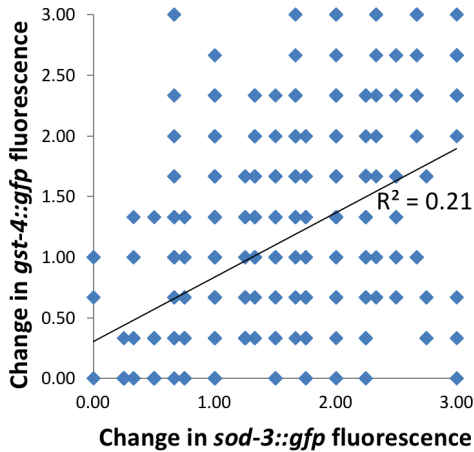


Figure 10. The list of DAF-16 effectors found in both genetic screens is enriched for modulators of SKN-1 and MitoUPR activity. All hits from both screens were assessed for their abilities to alter expression of the SKN-1 reporter *Pgst-4::gfp* and the MitoUPR reporter *Phsp-6::gfp*. The top two graphs show predicted results based on the hit rates of previously published genome-wide screens for SKN-1 and MitoUPR reporters: assuming a 2.2% hit rate, 8 out of the 398 hits should also impact *Pgst-4::gfp* expression; and assuming a 0.83% hit rate, 3 out of the 398 hits should also impact *Phsp-6::gfp* expression. The bottom two graphs show the actual results: 339 out of the 398 hits also impacted *gst-4::gfp* expression, representing an 85% hit rate; and 196 out of the 398 hits also impacted *hsp-6::gfp* expression, representing a 49% hit rate.

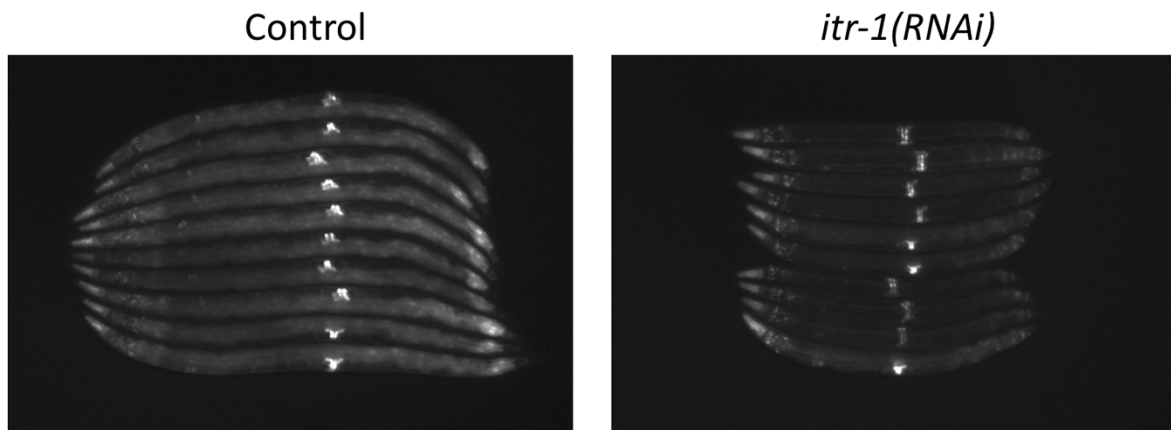


Figure 11. *itr-1 RNAi* inhibits DAF-16 activity in germline-ablated worms. All worms represented here are germline(-) and carry the *Psod-3::gfp* reporter. Control treated worms have bright GFP fluorescence throughout the intestine of the animal, whereas *itr-1 RNAi* treated worms do not. Background expression of this marker in the pharynx and vulva does not appear to be effected. From these images, it is also apparent that *itr-1 RNAi* makes the worms smaller (both pictures are at 65X total magnification).

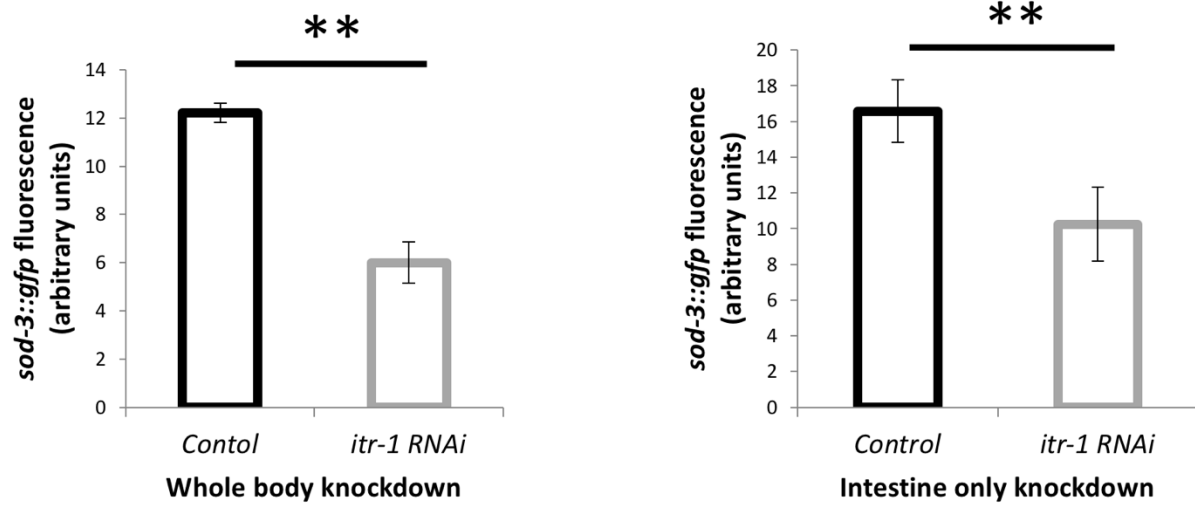


Figure 12. *itr-1* RNAi tissue-autonomously inhibits intestinal DAF-16 activity in germline-ablated worms. *Psod-3::gfp* reporter fluorescence upon *itr-1* RNAi was similarly effected in germline-less worms that perform whole body knockdown or intestine-only knockdown. Intestine-only RNAi was achieved using an *rrf-1*(-) background.

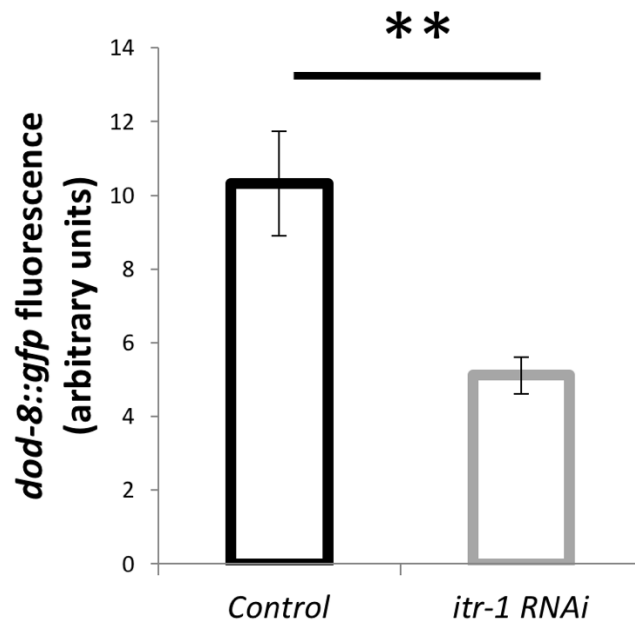


Figure 13. Expression of *dod-8*, a TCER-1 co-regulated DAF-16 target gene, is also reduced by *itr-1 RNAi*. In germline-less worms, DAF-16 interacts with the transcriptional co-regulator TCER-1 to regulate expression of a specific set of genes; one of these targets is *dod-8*. Fluorescence of the *Pdod-8::gfp* reporter is significantly decreased in germline(-) worms by treatment with *itr-1 RNAi*.

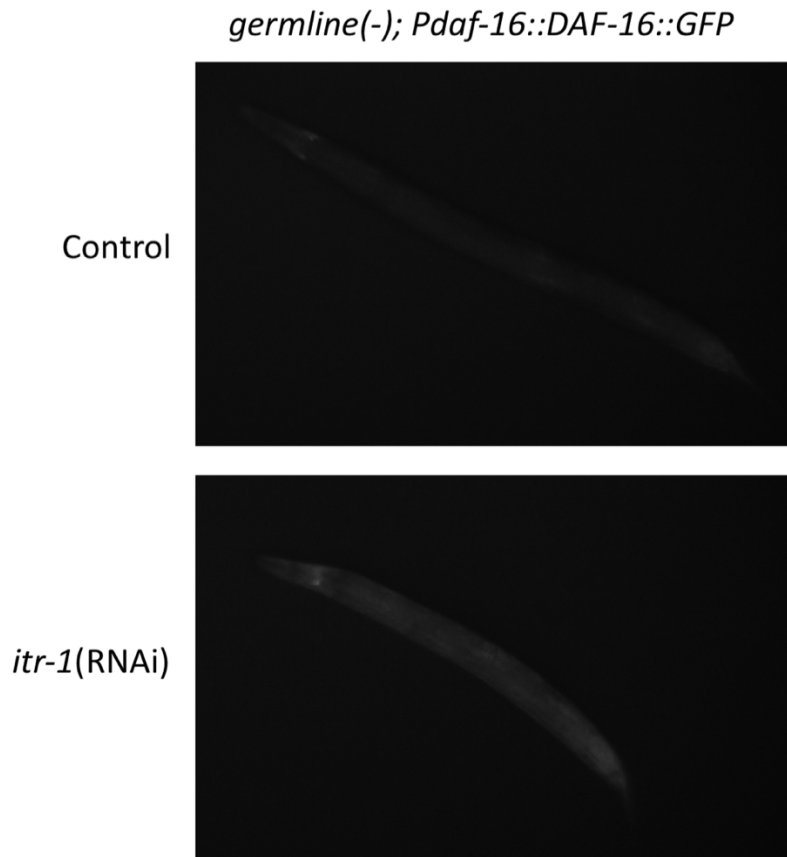


Figure 14. Germline-ablated worms treated with *itr-1 RNAi* do not display a pattern of nuclear localized DAF-16. The DAF-16::GFP fusion protein normally localizes to the nucleus of intestinal cells in *germline(-)* worms. As seen above, no nuclear puncta are visible in the *germline(-)* worms treated with *itr-1 RNAi*, even though substantial cytosolic DAF-16::GFP can be visualized. However, expression of the transgene is very much decreased in the control treated worms, making identification of nuclear puncta impossible, and thus results from this experiment are suggestive at best. Jen Berman, a previous graduate student in the Kenyon lab, found that RNAi bacteria (HT115) decreases lifespan of germline-less worms by 30% compared to worms grown on OP50. Perhaps the reason for this decrease is the large repression of DAF-16 expression seen on RNAi bacteria that is shown above.

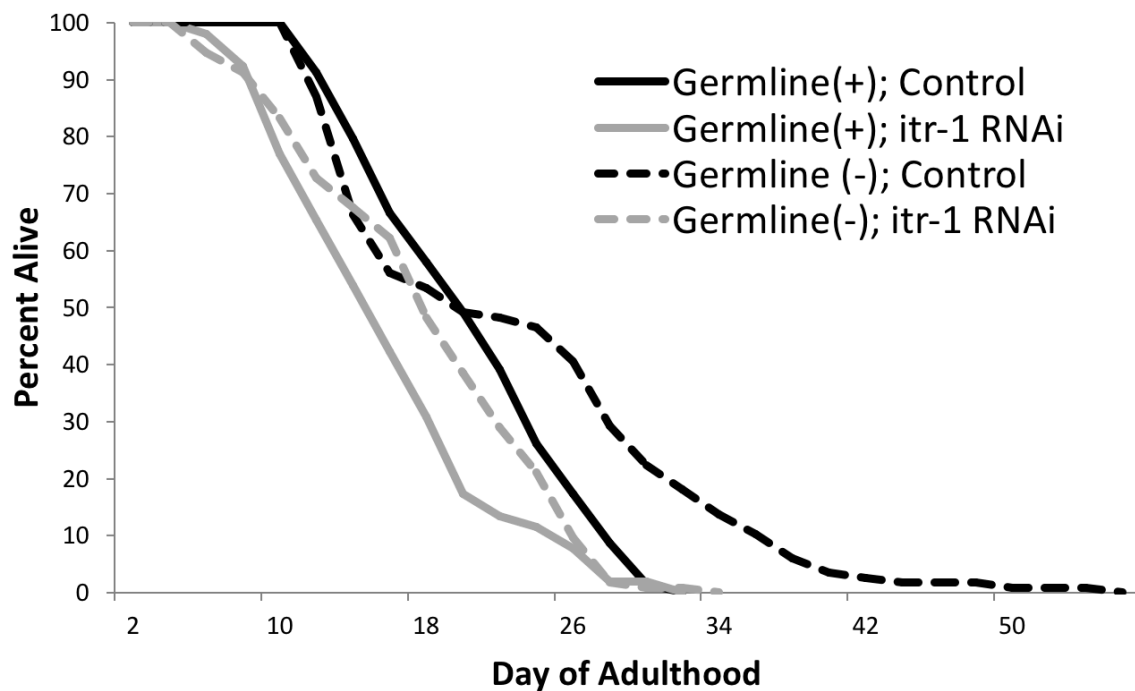


Figure 15. *itr-1 RNAi* inhibits longevity of germline(+) and germline(-) worms. As shown above, knocking down *itr-1* in germline-ablated worms (grey dashed line) inhibits the longevity seen in control worms (black dashed line). However, knocking down *itr-1* in germline-intact worms (grey solid line) also caused a decrease in lifespan as compared to controls (black solid line). Both germline(+) and germline(-) worms had a significant 21% decrease in mean lifespan in response to *itr-1 RNAi*. All worms were raised at 25°C until W-stage of L4 and then switched to 20°C for the rest of their life.

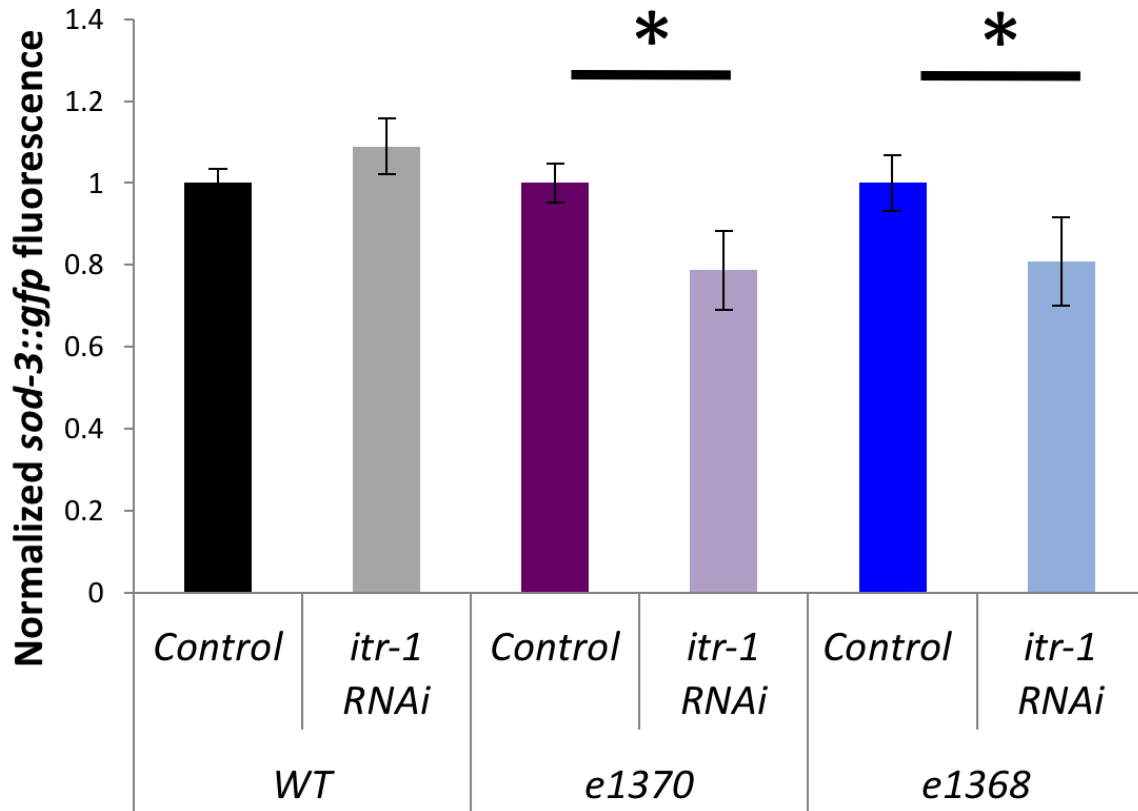


Figure 16. Knocking down *itr-1* lowers DAF-16 activity in insulin signaling mutants. Two *daf-2* mutants (*e1370* and *e1368*) display significant ~20% decreases in *Psod-3::gfp* expression when treated with *itr-1 RNAi* as compared to controls. No significant decrease was seen in otherwise wild-type worms, which normally have very low DAF-16 activity to begin with. It is interesting to note that the majority of the decrease in fluorescence observed in the *daf-2* mutants appears to occur in the intestine (data not shown).

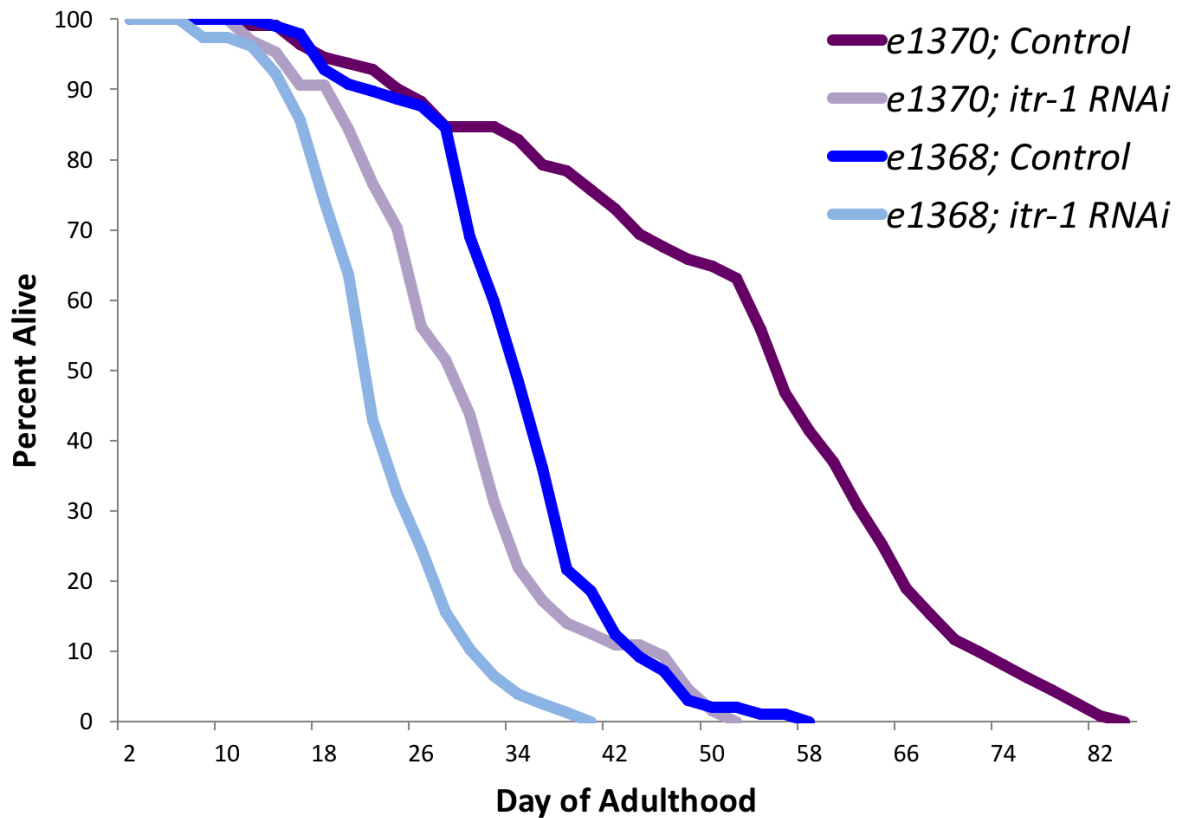


Figure 17. The longevity of insulin signaling mutants is partially ITR-1 dependent. Two *daf-2* mutants (*e1370* and *e1368*) display profound and significant decreases in lifespan on *itr-1 RNAi* (light colored lines) as compared to control treated worms (dark colored lines). The decrease in mean lifespan for *e1370* and *e1368* was 44% and 33%, respectively. Worms were always kept at 20°C throughout their entire lives.

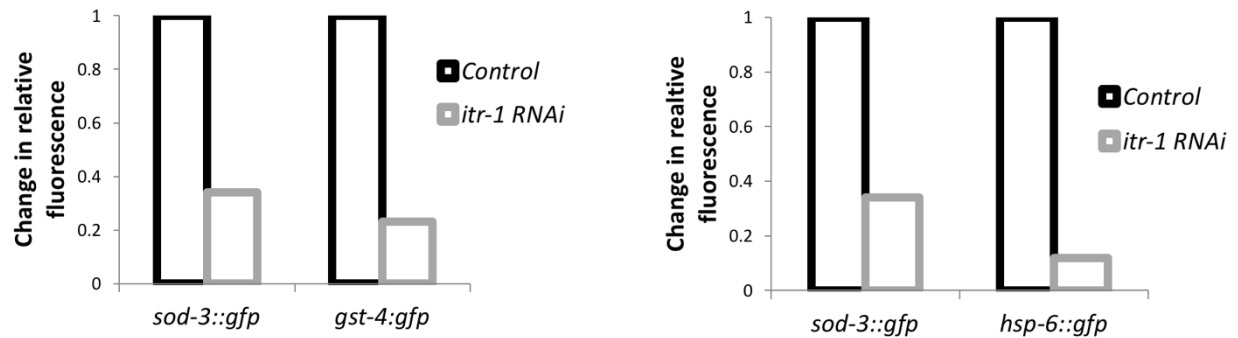


Figure 18. The increased SKN-1 and MitoUPR activity seen in germline-ablated worms is ITR-1 dependent. As shown above, *itr-1(RNAi)* inhibits the expression of the SKN-1 reporter *Pgst-4::gfp* and the MitoUPR reporter *Phsp-6::gfp*, in germline-less animals. The effect of *itr-1* knockdown on these components of the germline-less longevity pathway is comparable in strength to its effect on DAF-16 activity. As DAF-16, SKN-1 and MitoUPR activity are all KRI-1-dependent in germline(-) worms, these results place ITR-1 at the genetic pathway level of KRI-1.

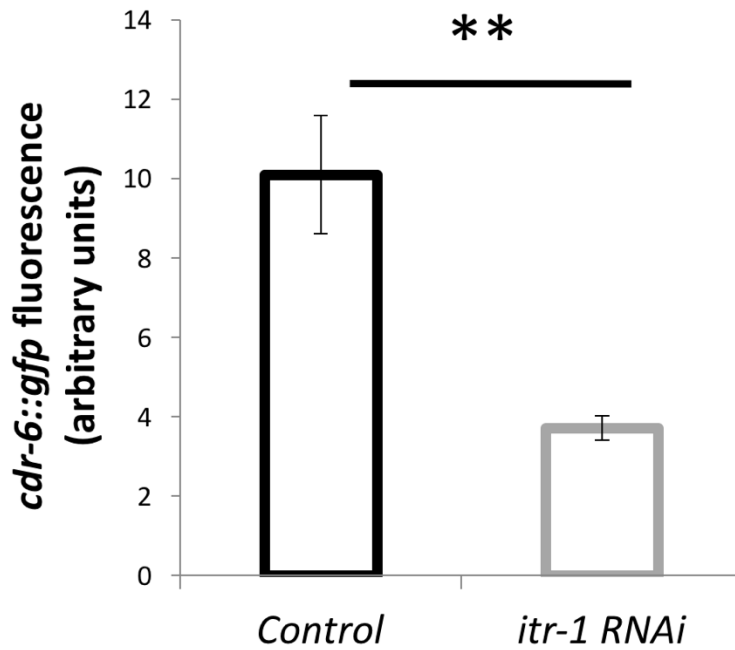


Figure 19. ITR-1 also regulates DAF-12 action in germline-ablated *C. elegans*. The reporter *P_{cdr-6}::gfp* is normally turned on by ligand bound DAF-12, in germline-less worms. As shown above, *itr-1 RNAi* significantly blunts this expression. It is unclear from these results whether *itr-1 RNAi* is preventing synthesis of the ligand (dafachronic acid), or preventing activity of the nuclear hormone receptor (DAF-12).

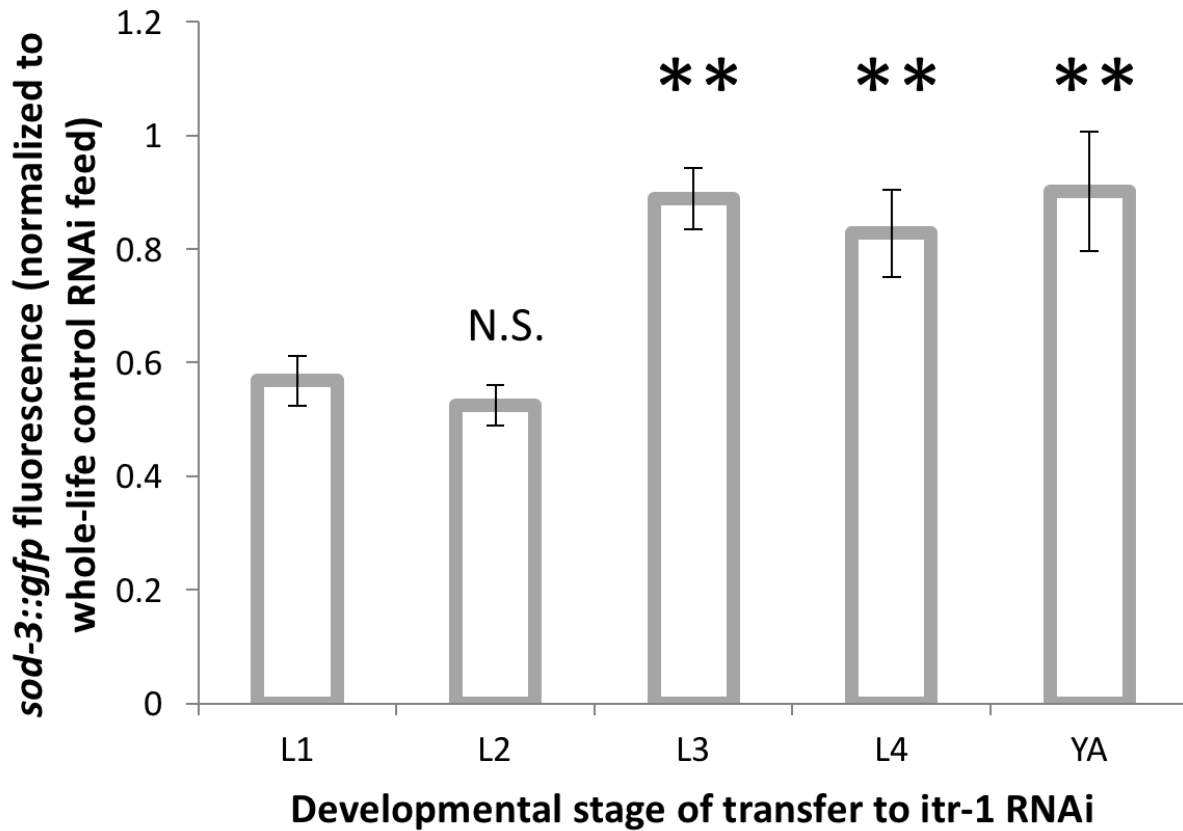


Figure 20. Initiation of *itr-1 RNAi* after L2 is insufficient to inhibit DAF-16 activity. Germline-ablated worms were placed on control RNAi plates at L1 arrest, and were then moved to *itr-1 RNAi* plates at various developmental stages. Compared to worms kept on control RNAi plates their whole lives, those moved to *itr-1 RNAi* at L1 had much lower expression of the DAF-16 reporter *Psod-3::gfp*, as shown before. Worms placed on *itr-1 RNAi* at L2 had no significant difference in *Psod-3::gfp* expression as compared to those moved at L1. However, those moved to *itr-1 RNAi* at L3 or beyond had significantly higher *Psod-3::gfp* expression compared to those moved at L1, meaning DAF-16 activity was not inhibited in these worms. All worms were grown at 25°C until W-stage of L4, and then transferred to 20°C.

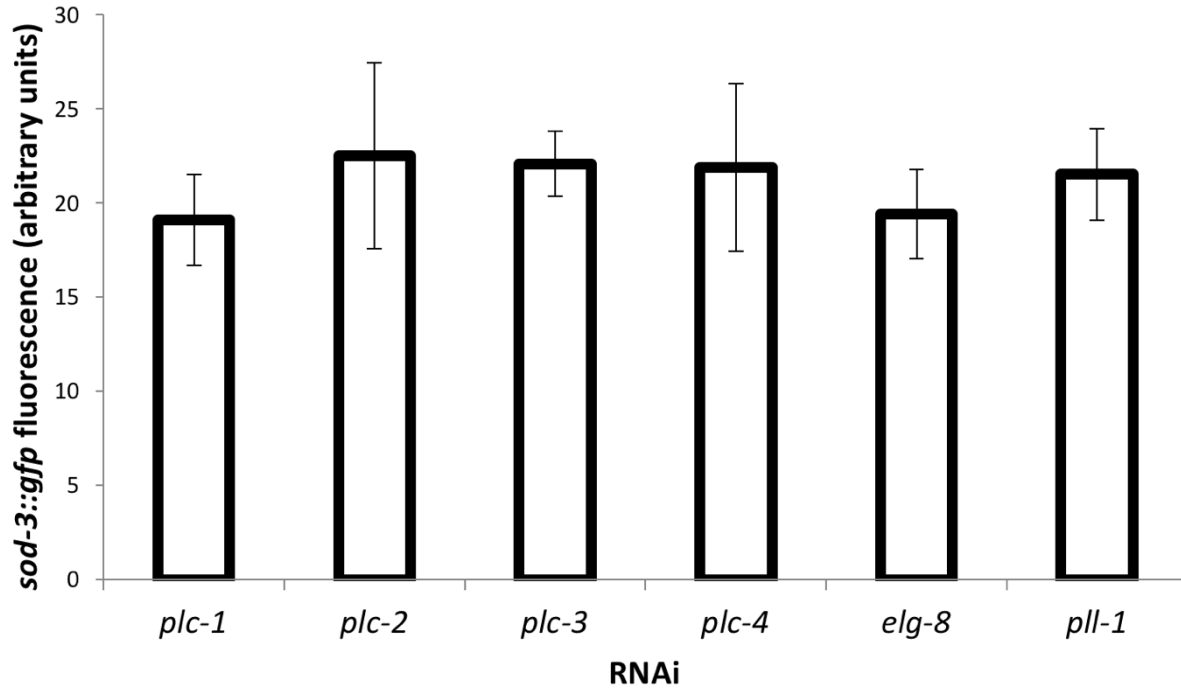


Figure 21. Individual knockdown of the five worm phospholipase C enzymes fails to phenocopy *itr-1 RNAi*. We know that one (or more) of the PLC enzymes must be acting upstream of ITR-1, since ITR-1 must be activated through IP₃ production. However, knocking down each PLC individually was unable to lower expression of the DAF-16 reporter *Psod-3::gfp*, as compared to control RNAi (targeting the catalytically dead PLC-like enzyme *pll-1*).

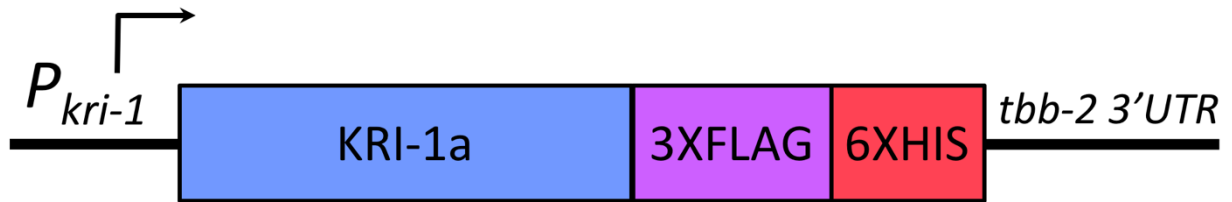


Figure 22. Schematic of the C-terminally FLAG-tagged KRI-1 construct. The transgene was driven by the endogenous KRI-1 reporter, which expresses only in the pharynx and intestine. cDNA of the KRI-1a isoform was fused to a triple FLAG tag, followed by a 6X Histamine tag. The *tbb-2* 3'UTR was used for permissive expression. Not shown is that the construct also had an *unc-119(+)* rescuing cassette, and the extrachromosomal array also contained a *Podr-1::rfp* marker.

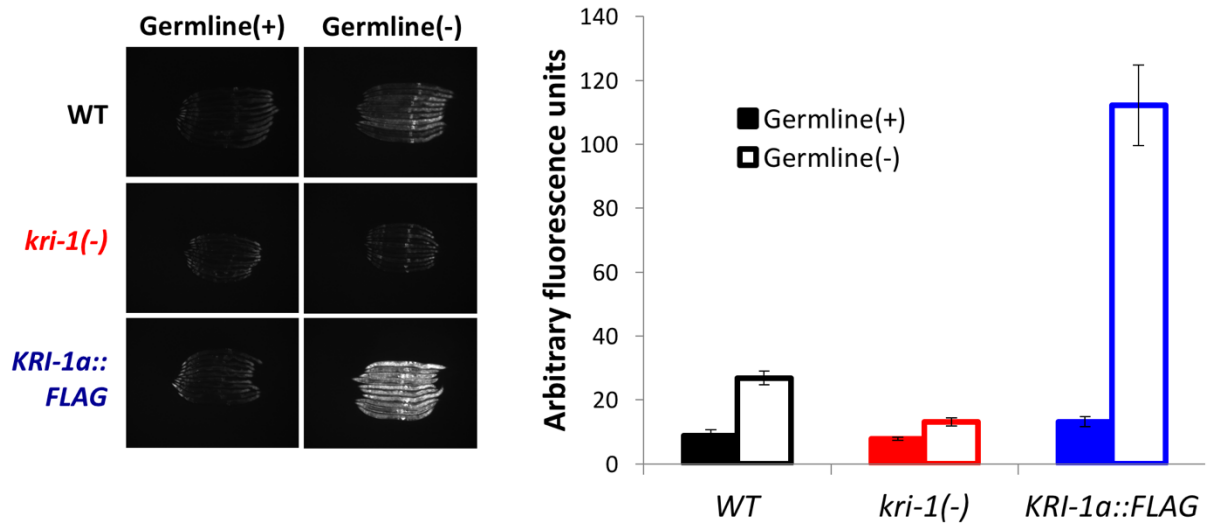


Figure 23. The C-terminally FLAG-tagged KRI-1 construct rescues DAF-16 activity in *kri-1(null)* worms. As can be seen in the photos, *Psod-3::gfp* expression increases in otherwise WT germline(-) worms, as compared to germline(+) controls. This increase in DAF-16 reporter activity is almost fully blunted in *kri-1(-)*, but can be rescued via expression of the tagged-KRI-1 transgene. In fact, this overexpression construct actually causes a dramatic increase in *Psod-3::gfp* levels, but only in the the germline-ablated state. This suggests that increased KRI-1 activity can also lead to increased DAF-16 localization, but only in the permissive context of germline-ablation.

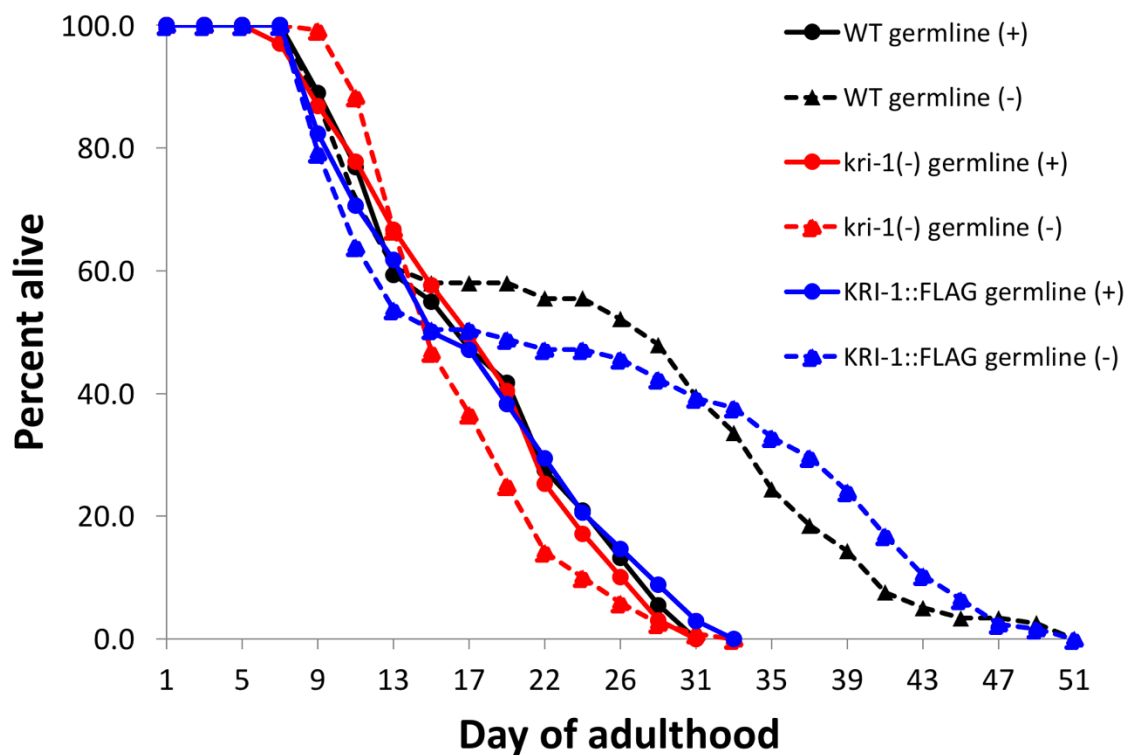


Figure 24. The C-terminally FLAG-tagged KRI-1 construct rescues germline-less longevity in *kri-1(null)* worms. As compared to germline-intact WT worms (black solid line), there is a large lifespan increase upon germline-ablation (black dashed line). This lifespan increase is fully inhibited in *kri-1(-)* mutants (red lines). Expression of the KRI-1a::FLAG construct in a *kri-1(-)* background was able to fully rescue the germline-less longevity phenotype. It's worth noting that even though KRI-1 is overexpressed in this construct (which interestingly leads to dramatic induction of *Psod-3::gfp* upon germline-ablation), there is no added lifespan benefit seen in these worms, as compared to WT.

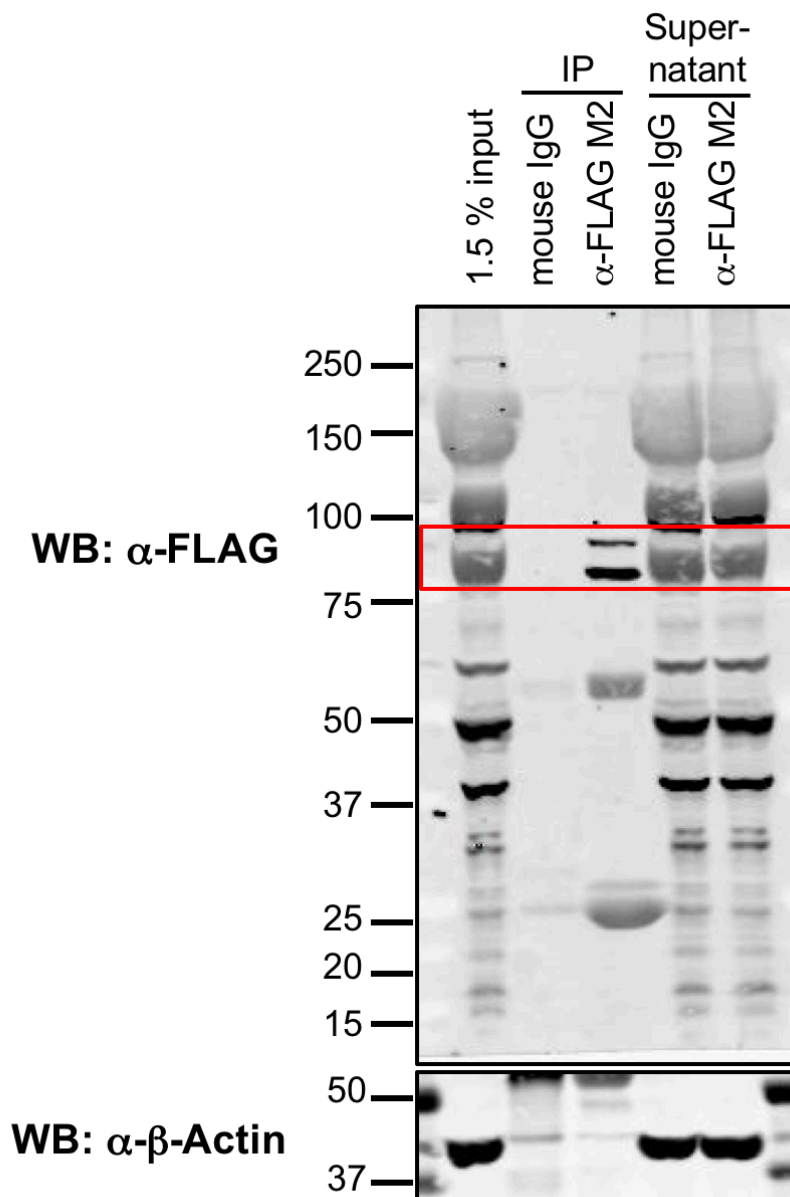


Figure 25. Western blot of pilot KRI-1a::FLAG pulldown. An ~80KD band, corresponding to the size of tagged-KRI-1 and reacting to an anti-FLAG antibody, can be seen in the IP:a-FLAG-M2 lane, but not the control IP:mouse-IgG lane. This protein band cannot be seen in the lane for total worm lysate (1.5% input), or the lanes for the IP supernatants, suggesting that we've significantly concentrated and enriched KRI-1a::FLAG via pulldown.

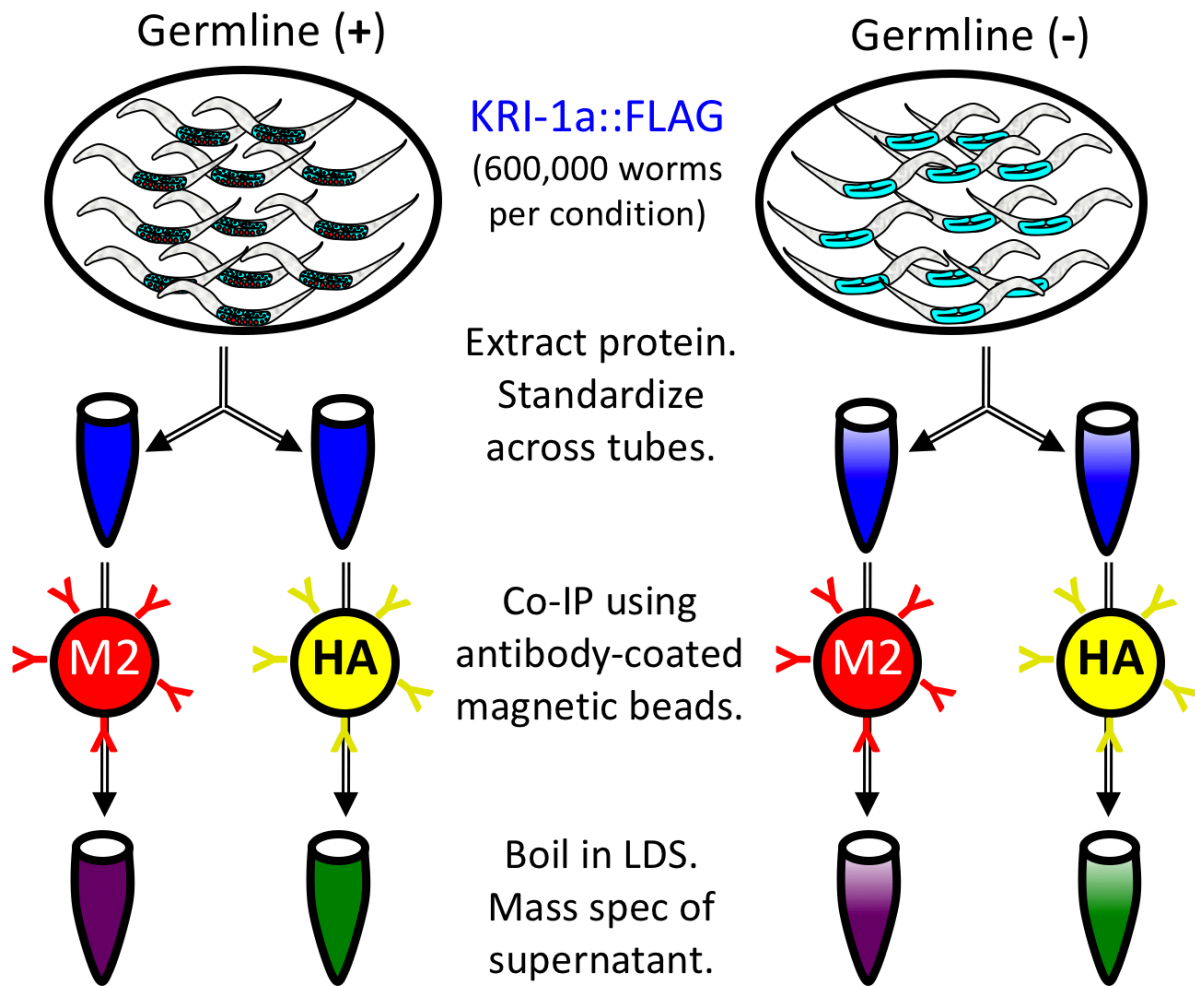


Figure 26. Schematic of both KRI-1 Co-IP experiments. Both germline(+) and germline(-) worms carrying the KRI-1a::FLAG transgene were raised on solid agar plates with OP50, washed off at late Day 1 of adulthood, and snap frozen using liquid nitrogen. Protein was extracted via bead-beating, quantified, standardized between conditions, and split into two tubes per condition. Co-immunoprecipitation was performed using magnetic-agarose beads coated with either experimental M2 antibodies (anti-FLAG) or control HA antibodies. The beads were washed several times and then boiled in LDS to remove the bound proteins. Samples were frozen and sent for mass spec analysis.

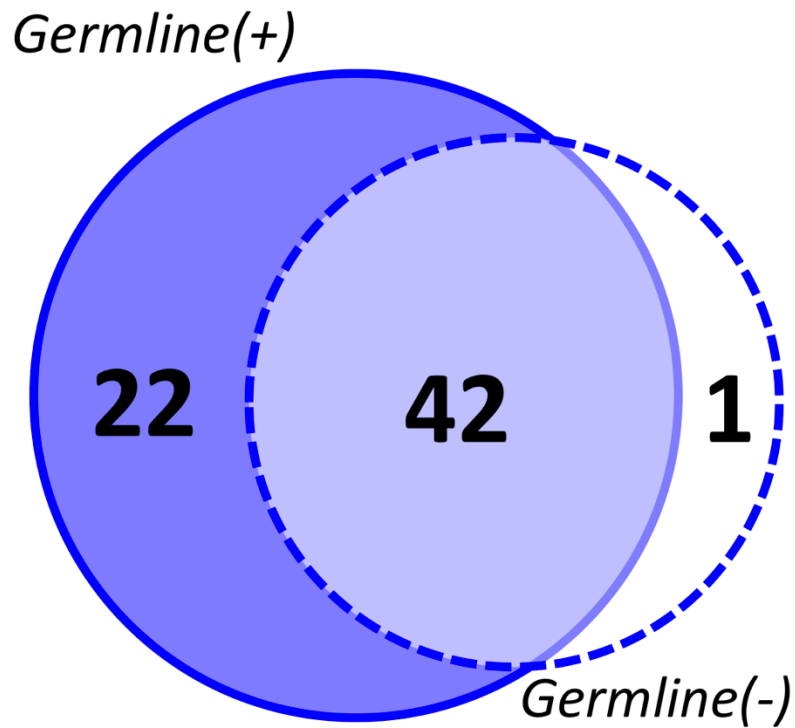


Figure 27. KRI-1 is preferentially bound in the germline(+) state. Only one protein, F37C4.5, was found to be preferentially bound to KRI-1 in the Co-IP of germline(-) worms. The majority of KRI-1 binding partners (40) appear to interact constitutively, in relation to the germline. Still, there are a large number of proteins (22) that preferentially bind KRI-1 in germline-intact worms, and these may be members of an inhibitory complex that prevents KRI-1 function.

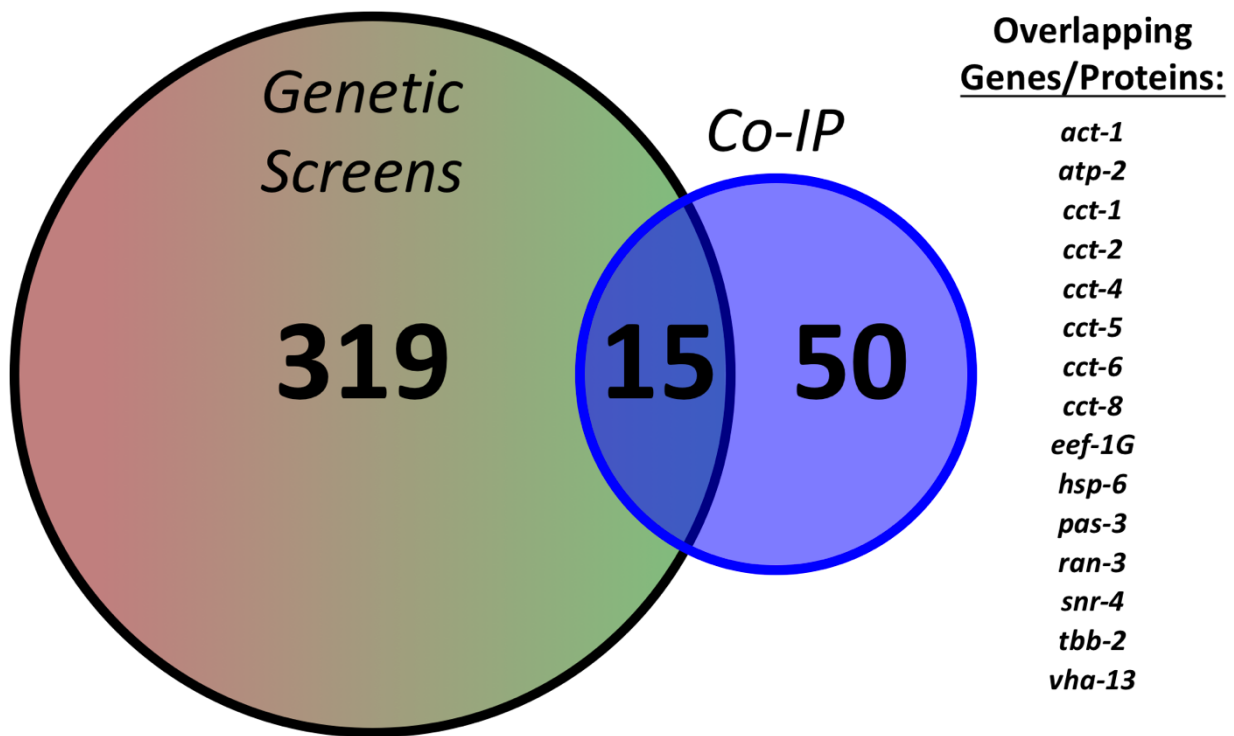


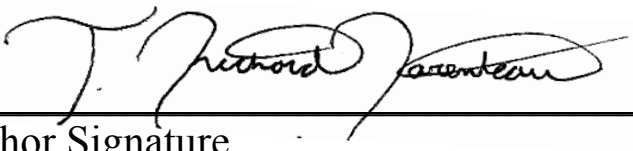
Figure 28. Significant overlap between genetic and biochemical screens. The combined 339 unique genes found in two genetic screens represent 1.7% of the genome, yet make-up 23% of the high-confidence interacting proteins found in the KRI-1 Co-IPs. This is a huge enrichment, and validates that both screening approaches appear to be interrogating the same set of pathways. The 15 overlapping genes/proteins are shown above. These are excellent targets for follow-up experiments, as they have been functionally validated to effect DAF-16 activity, and are known to physically interact with KRI-1.

Publishing Agreement

It is the policy of the University to encourage the distribution of all theses, dissertations, and manuscripts. Copies of all UCSF theses, dissertations, and manuscripts will be routed to the library via the Graduate Division. The library will make all theses, dissertations, and manuscripts accessible to the public and will preserve these to the best of their abilities, in perpetuity.

Please sign the following statement:

I hereby grant permission to the Graduate Division of the University of California, San Francisco to release copies of my thesis, dissertation, or manuscript to the Campus Library to provide access and preservation, in whole or in part, in perpetuity.



Author Signature

3/23/16

Date